TURUN YLIOPISTON JULKAISUJA
ANNALES UNIVERSITATIS TURKUENSIS

SARJA - SER. A I OSA - TOM. 477

ASTRONOMICA - CHEMICA - PHYSICA - MATHEMATICA

PHENOLICS OF THE INNER BARK OF SILVER BIRCH: CHARACTERIZATION AND INTRASPECIFIC VARIATION

by

Jaana Liimatainen

TURUN YLIOPISTO
UNIVERSITY OF TURKU
Turku 2013

From the Laboratory of Organic Chemistry and Chemical Biology, Department of Chemistry, University of Turku, Finland

Supervised by
Docent Dr Maarit Karonen
Department of Chemistry
University of Turku
Turku, Finland

Docent Dr Jari Sinkkonen
Department of Chemistry
University of Turku
Turku, Finland

Custos
Professor Dr Juha-Pekka Salminen
Department of Chemistry
University of Turku
Turku, Finland

Reviewed by
Professor Dr Irene Mueller-Harvey
School of Agriculture, Policy and Development
University of Reading
Reading, U.K.

Docent Dr Hannu Maaheimo
VTT Technical Research Centre of Finland
Helsinki, Finland

Opponent
Professor Dr Stefan Willför
Department of Chemical Engineering
Åbo Akademi University
Åbo, Finland

The originality of this thesis has been checked in accordance with the University of Turku quality assurance system using the Turnitin OriginalityCheck service.

ISBN 978-951-29-5589-3 (PRINT)
ISBN 978-951-29-5590-9 (PDF)
ISSN 0082-7002
Painosalama Oy – Turku, Finland 2013

TABLE OF CONTENTS

PREFACE

This work was carried out in the Laboratory of Organic Chemistry and Chemical Biology at the Department of Chemistry, University of Turku, since May 2006. The plant material was mainly collected from the Botanical Garden of the University of Turku.

First of all, I want to thank professors Kalevi Pihlaja and Juha-Pekka Salminen for providing the high-grade facilities to carry out this research. The former professor Kalevi Pihlaja first introduced me to the field of environmental chemistry and chemistry of natural products. I am grateful for his contacts, encouragement and long-lasting interest towards my results which have continued despite his retirement. The present professor Juha-Pekka Salminen was a big help in the early years of this Ph.D. work when our section was under changes. We had inspiring discussions about the analysis of phenolics and the world of science in general during the uncrowded coffee breaks. I admire his dedication to his work and I am grateful to him for his patience and allowing me to spend so many years with this topic.

My deepest gratitude goes equally to my supervisors Dr. Maarit Karonen and Dr. Jari Sinkkonen. They have encouraged and skillfully instructed me all these years. Maarit have taught me a lot about the analysis of phenolic compounds. She has helped me in the scientific writing and revised my manuscripts with an admirable perseverance. Jari is an amazing scientist, who has an exceptional ability to teach difficult things understandably. He has taught me the most of what I know about the NMR and computational methods. Maarit and Jari have a big heart and they are both full of new ideas. I could not have wished for better supervisors.

I want to thank Dr. Marjo Helander for letting me to use the birch clones she had planted on the Botanical Garden. In addition, she did the statistical analysis and helped whenever a perspective of a biologist was needed. I am grateful for Dr. Petri Tähtinen for his help on ECD spectroscopy and on stereochemistry in general. I also wish to thank Dr. Jeff Ahern for kindly reviewing the language of this thesis.

Great thanks belong to the personnel of the Instrument Centre, workshop, teaching lab, and office of Department of Chemistry. I am grateful for Dr. Petri Ingman, Dr. Henri Kivelä, Dr. Karel Klika, and Jaakko Hellman for lending a hand with the tricky NMR instruments whenever needed. I wish to thank Kirsti Wiinamäki and Dr. Olli Martiskainen for running the mass spectra and for the instrument support. Mauri Nauma and Kari Loikas deserve special thanks for keeping the business running by maintaining the instruments and

computers. I would also like to thank the personnel of the Botanical Garden for their help in the sampling. I warmly thank Essi Kangasaho for her assistance in the laboratory.

The support of other Ph.D. students has been invaluable. I wish to express my deep gratitude to Anu Tuominen, Johanna Moilanen, and Matti Vihakas for their friendship and company during conference trips, courses, and evening times at the department. I also want to thank other former and present workmates, especially Riitta Koivikko, Maria Lahtinen, Marica Engström, Nicolas Baert, Anne Koivuniemi, and Jorma Kim for pleasant working atmosphere.

I am highly thankful for the personal grants from the Finnish Cultural Foundation, the Palomaa−Erikoski Scholarship Fund, the Alfred Kordelin Foundation, the Emil Aaltonen Foundation, the Niemi Foundation, the Turku University Foundation, and the University of Turku, as well as for the travel grants from the Palomaa−Erikoski Scholarship Fund and the Graduate School of Organic Chemistry and Chemical Biology. I sincerely thank professors Kalevi Pihlaja, Juha-Pekka Salminen, Harri Lönnberg, and Dr. Jari Sinkkonen for my funding and job opportunities between grants.

Finally, I owe my dearest thanks to my family and friends. I wish to thank my mom for her continuous support and being there for me. I miss my dad, and I believe that he would be proud of me. I wish to thank my brother Janne for all the words of wisdom of a big brother. I know I can always trust him. I am grateful to all my friends who keep me rolling. And last, Kari, you are the delight of my life. Thank you for being by my side.

Turku, November 2013

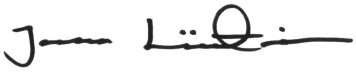

ABSTRACT

This thesis describes work related to the in-depth characterization of the phenolic compounds of silver birch (*Betula pendula*) inner bark. Phenolic compounds are the most ubiquitous class of plant secondary compounds. The unifying feature of this structurally diverse group is an aromatic ring containing at least one hydroxyl group. Due to the structural diversity, phenolics have various roles in the plant defense against biotic and abiotic stresses. In addition, they can confer several health-promoting properties to humans. Furthermore, the structural diversity of this class of compounds causes challenges for their analysis. The study species in the present work, silver birch, is economically the most important hard wood species in northern Europe. Its inner bark contains a high level of phenolic compounds and it has shown one of the strongest antioxidant activities among 92 Finnish plant materials.

The literature review surveys the diversity and organ specific distribution of phenolic compounds in silver birch as well as the proposed ecological functions of phenolic compounds in nature. In addition, the basis for the characterization of phenolics by mass spectrometry (MS), nuclear magnetic resonance spectroscopy (NMR), and circular dichroism spectroscopy (CD) are reviewed.

The objective of the experimental work was to extract, purify, characterize, and quantify the inner bark phenolic compounds. Overall 36 compounds were characterized by MS and ultraviolet spectroscopy (UV). 24 compounds were isolated and their structures confirmed by NMR and CD spectroscopy. Five novel natural compounds were identified. Special emphasis was placed on the establishment of a method for the characterization of proanthocyanidins (PAs). Hydrophilic interaction liquid chromatography (HILIC) was utilized because of its high resolution power and predictable elution order of oligomeric and polymeric PAs according to an increasing degree of polymerization. The combination of HILIC and high-resolution MS detection allowed the identification of procyanidin (PC) polymers up to the degree of polymerization of 22. In addition, a series of oligomeric and polymeric PC monoxylosides were observed for the first time in nature.

Season and genotype influenced the quantities of the main inner bark phenolics, yet qualitative differences were not observed. However, manual wounding of the inner bark induced the production of ellagitannins (ETs) in the wounded tissues, i.e. callus. Since ETs were not detected in the intact inner bark, this finding may reflect the capacity of silver birch to exploit ellagitannins in its defense.

LIST OF ORIGINAL PUBLICATIONS

The thesis is based on the following publications and on some unpublished results. The publications are referred to in the text by their Roman numerals.

I Liimatainen, J., Sinkkonen, J., Karonen, M., Pihlaja, K. 2008. Two new phenylbutanoids from inner bark of *Betula pendula*. *Magn. Reson. Chem*. 46:195–198.

II Liimatainen, J., Karonen, M., Sinkkonen, J., Helander, M., Salminen, J.-P. 2012. Characterization of phenolic compounds from inner bark of *Betula pendula*. *Holzforschung* 66:171–181.

III Liimatainen, J., Karonen, M., Sinkkonen, J., Helander, M., Salminen, J.-P. 2012. Phenolic compounds of the inner bark of *Betula pendula*: seasonal and genetic variation and induction by wounding. *J. Chem. Ecol.* 38:1410–1418.

IV Karonen, M., Liimatainen, J., Sinkkonen, J. 2011. Birch inner bark procyanidins can be resolved with enhanced sensitivity by hydrophilic interaction HPLC-MS. *J. Sep. Sci*. 34:3158–3165.

V Liimatainen, J., Karonen, M., Sinkkonen, J. 2012. Procyanidin xylosides from the bark of *Betula pendula*. *Phytochemistry* 76:178–183.

Article **I**, Copyright © 2007 John Wiley & Sons, Ltd. Article **II**, Copyright © 2012 Walter de Gruyter. Article **III**, Copyright © 2012 Springer Science + Business Media, reprinted with kind permission. Article **IV**, Copyright © 2011 WILEY-VCH Verlag GmbH & Co. KGaA, Article **V**, Copyright © 2012 Elsevier, reprinted with permission.

ABBREVIATIONS

APCI	atmospheric pressure chemical ionization
API	atmospheric pressure ionization
CD	circular dichroism
CE	Cotton effect
CID	collision induced dissociation
COSY	correlation spectroscopy
CT	condensed tannin (syn. proanthocyanidin)
DAD	diode array detector
DNA	deoxyribonucleic acid
DP	degree of polymerization
DPPH	1,1-diphenyl-2-picrylhydrazyl
DQF-COSY	double quantum filtered COSY
ECD	electronic circular dichroism
ESI	electrospray ionization
ET	ellagitannin
FAB	fast atom bombardment
GG	galloyl glucose
GT	gallotannin
HHDP	hexahydroxydiphenoyl
HILIC	hydrophilic interaction liquid chromatography
HMBC	heteronuclear multiple bond correlation
HPLC	high-performance liquid chromatography
HR	high-resolution
HRF	heterocyclic ring fission
HSQC	heteronuclear single quantum coherence
HT	hydrolysable tannin
i.d.	internal diameter
LC	liquid chromatography
m/z	mass-to-charge ratio
MS	mass spectrometry
NMR	nuclear magnetic resonance
NP	normal-phase
NOESY	nuclear Overhauser effect spectroscopy
PA	proanthocyanidin (syn. condensed tannin)
PC	procyanidin
PD	prodelphinidin

PGG	1,2,3,4,6-penta-*O*-galloyl-β-D-glucose
QM	quinone methide
RDA	retro-Diels−Alder
RNA	ribonucleic acid
ROESY	rotating-frame Overhauser effect spectroscopy
RP	reversed-phase
RSA	radical scavenging activity
Rt	retention time
r.t.	room temperature
TMS	tetramethylsilane
TOCSY	total correlation spectroscopy
TOF	time-of-flight
UV	ultraviolet

1. INTRODUCTION

The birches (*Betula* spp.) are comprised of 50 distinct species as well as several varieties and natural hybrids. Birches are distributed throughout the northern temperate climates and they have high morphological variability, ranging trees to shrubs (Atkinson 1992). The natural occurring birch species in Finland are silver birch (*Betula pendula* Roth), dwarf birch (*Betula nana* L.), and two subspecies of *Betula pubescens*: white birch (*Betula pubescens* ssp. *Pubescens* Ehrh.) and mountain birch (*Betula pubescens* ssp. *Czerepanovii* (Orlova) Hämet-Ahti) (Raulo 1981; Valkama et al. 2003).

Silver birch (*Betula pendula* Roth. synonym *Betula verrucosa* Ehrh.) is economically the most important hardwood species in northern Europe (Oksanen et al. 2009 and references therein). It has higher wood growing capacity than white birch and is therefore favored by the woodland owners (Raulo 1981). Its wood is mainly used in manufacturing short-fiber pulp, plywood, and furniture. Silver birch thrives in dry soils and it can grow up to 30 m tall. Its bark is smooth, silvery white, and often black and fissured at the base. Branches are brown, glabrous with pale warts. Leaves are ovate-deltate with an acuminate apex and the margins are double serrated (Atkinson 1992). Silver birch is easily confused with white birch because of their similar appearance. They can form natural hybrids, particularly in arctic conditions (Raulo 1981).

The phloem tissue consists of living cells that transport mainly sugars and amino acids from leaves to the rest of the plant for the utilization in growth and storage (Schulz and Thompson 2007). In contrast, the xylem transports water, mineral nutrients, and phytohormones from roots to other plant organs (Myburg and Sederoff 2007).

Phenolic compounds (or phenolics) are defined as compounds that possess at least one aromatic ring bearing one or more hydroxyl groups (Waterman and Mole 1994; Strack 1997). They are a large and heterogeneous group of compounds and the most abundant secondary metabolites in plants. Phenolics are formed through two different biogenetic routes in plants: the shikimate and acetate/malonate pathways (Strack 1997). In addition, the mevalonate pathway produces terpenes that may bear a phenolic function in their terpene core (Strack 1997). Phenolics may be etherified or esterified with sugars or other similar compounds. Most of the phenolics are stored in the vacuole or bound to the cell wall, but they can also be present in intercellular space or on the surfaces of plant organs (Hutzler et al. 1998; Grundhöfer et al. 2001; Valkama et al. 2003, 2004). Disruption of the

cell releases vacuolar phenolics where they can modify and/or be modified by other cell components such as enzymes and proteins (Chalker-Scott and Krahmer 1989).

The most abundant phenolic components in vascular plants are lignins. Lignins are branched polymers of phenylpropanoid units which are covalently bound to the polysaccharides of the cell wall. In this manner, they make cell walls thickened and impervious, providing mechanical support for the plant (Taiz and Zeiger 1998; Ralph et al. 2007).

Tannins are classically defined as water-soluble phenolic compounds that have molecular weights from 500 to 3000 Da that have the special ability to precipitate alkaloids and proteins (Swain and Bate-Smith 1962). At the present time tannins are known to have molecular weights as high as 55 000 Da (Guyot et al. 2001). Tannins can be divided into three subgroups: hydrolysable, condensed, and phlorotannins. Hydrolysable tannins (HTs) are built up from a polyol core which is esterified with gallic acid to form galloyl glucoses (GGs) and gallotannins (GTs). GGs may form hexahydroxydiphenoyl (HHDP) esters through oxidative couplings, forming ellagitannins (ETs) (Figure 1). The diversity of HTs is further enlarged through the oligomerization of ETs, opening of the polyol core, or oxidation or hydration reactions of HHDP groups (Porter 1989a; Haslam 2007). Condensed tannins (CTs) are also called proanthocyanidins (PAs), because when treated with acid in hot conditions they form anthocyanidins. PAs are oligomers and polymers of flavan-3-ol units. PAs differ from each other according to the degree of polymerization, hydroxylation pattern, configurations of the C2 and C3 of the flavan-3-ol units, and the location and configuration of interflavanoid bonds. The most common types of PAs are procyanidins (PCs) and prodelphinidins (PDs). PCs consist of catechin and/or its C2/C3 epimer, epicatechin, subunits, while PDs contain both gallocatechin/epigallocatechin and catechin/epicatechin units or merely gallocatechin/epigallocatechin units (Figure 1) (Hemingway 1989; Lazarus et al. 2003). Monomeric units are linked through C4−C8 or C4−C6 bonds (B-type PAs) or doubly linked with an additional C2−O−C7 or C2−O−C5 ether bond (A-type PAs). Phlorotannins consist of oligomers and polymers of phloroglucinol units (Figure 1). Phloroglucinol units are linked through aryl−aryl bonds and/or aryl−ether bonds. Phlorotannins are restricted phylogenetically, found only in brown algae (Porter 1989a; Koivikko 2008).

Flavonoids are a diverse group of compounds that include a C6-C3-C6 skeleton which is built up of two aromatic rings (A- and B-ring) joined together by a C3 unit (which may form a heterocyclic C-ring, Figure 1). Flavonoids can be divided into many subclasses, such as anthocyanins, isoflavonoids, chalcones, and flavonols according to the oxidation of

the C3 unit (Koes et al. 1994). Lignans are oligomers, mainly dimers, of cinnamic acid derivatives (Moss 2000), while cinnamic acids are classified as *trans*-phenyl-3-propenoic acids (Clifford 2003). Coumarins and chromones have a C6-C3 carbon framework which is cyclized to form chromen-2-one and chromen-4one structures (formerly named as benzopyran-2/4-ones), respectively. Stilbenes possess a structure of two aromatic rings linked by a C2 unit (Waterman and Mole 1994). Diarylheptanoids consist of two aryl groups held together by an aliphatic chain of seven carbon atoms (Keserü and Nógrádi 1995), while arylbutanoids are built up of one aromatic ring directly linked to a chain of four carbon atoms (Figure 1).

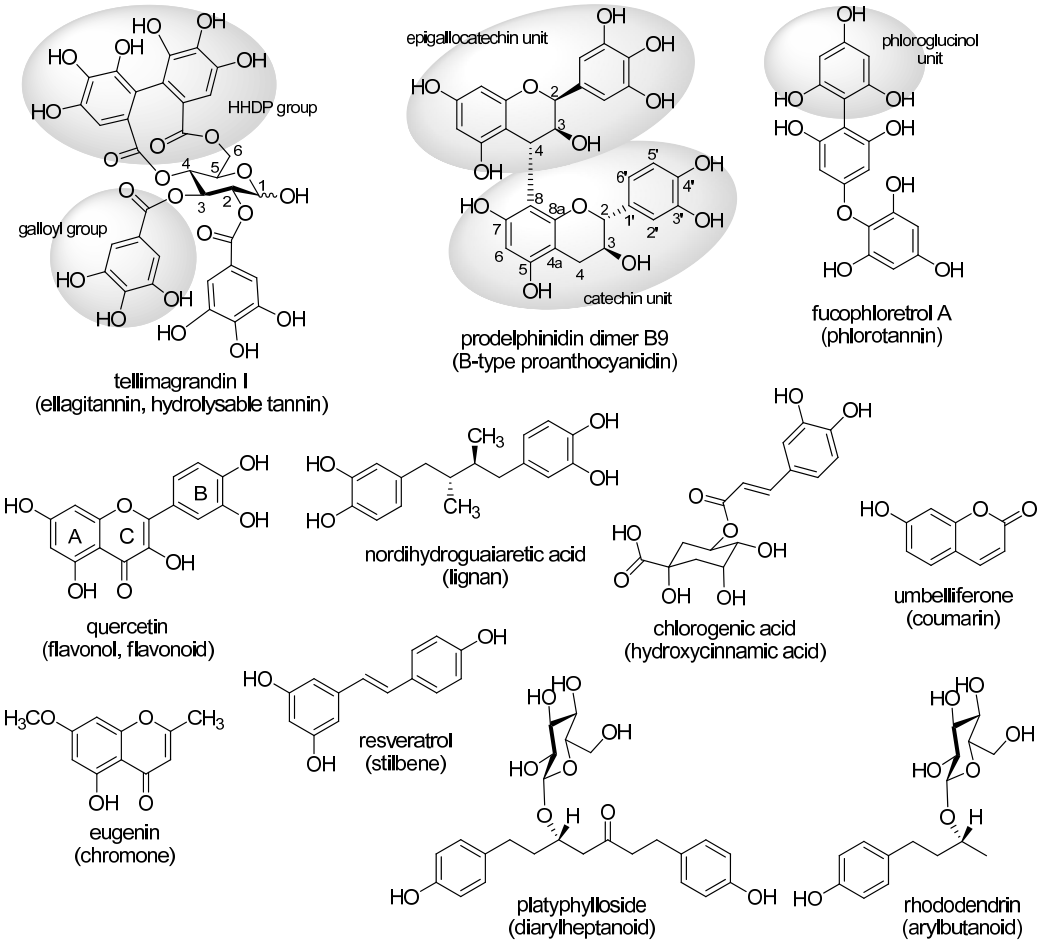

Figure 1. Example structures of the major classes of phenolic compounds.

In addition, there exist several other subgroups of phenolic compounds, such as phenolic acids, or mixed phenolic compounds containing characteristic features of two or more

phenolic or some other secondary compound subgroups. Further, the phenolic hydroxyl may be masked by an ether or ester bond such as seen in some glycosidic phenolics. However, these compounds are still regarded as phenolic compounds although they lack the free aromatic hydroxyl moieties (Waterman and Mole 1994).

It has been thought that phenolics have no intrinsic role in the physiological processes of the plant i.e. they are products of secondary metabolism (Waterman and Mole 1994). However, the existence of flavonoids in nuclei of certain plant species and the association of flavonoids with histone proteins suggest that they may have an influence on gene expression and cell development (Feucht et al. 2008, 2012). Further research is required to evaluate the potential role of phenolics as primary metabolites. As secondary metabolites, phenolics may have several protective effects which help increase plant survival in nature. For example, they offer protection against ultraviolet radiation, predators, and stress-created radical oxygen species (Chalker-Scott and Krahmer 1989). Furthermore, they possess structural roles in different supporting tissues, attract pollinators, and serve as signal molecules in the interactions between plants and their environment (Jaganath and Crozier 2010).

In addition to the protective effects of the phenolics on the plant itself, phenolics are thought to have several health-promoting properties for humans. For example, long-term intakes of phenolics may prevent or reduce the risk of cardiovascular diseases, diabetes, obesity, and cancer (Jaganath and Crozier 2010).

2. LITERATURE REVIEW

2.1. Phenolic compounds in the different plant organs of silver birch

While some of the known phenolic compounds are characteristic of only one or a limited number of plant species, many phenolics are broadly distributed (Waterman and Mole 1994). For example, PAs are found in high concentrations in most of woody plant species (Chalker-Scott and Krahmer 1989; Porter 1989b; Matthews et al. 1997). Different plant parts are also specialized in their production of phenolics. Silver birch is known to contain simple phenolics, phenolic acids, phenylpropanoids, arylbutanoids, diarylheptanoids, flavonoids, lignans, stilbenes, HTs, and PAs (Figure 2). Some organs of silver birch contain phenolics from almost all of these classes, but some are specialized to produce only one or very few types of compounds. In addition to extractable phenolics, birches contain polymeric compounds bound to the cell walls, such as lignin and suberin (Ekman 1983; Pinto et al. 2009). Furthermore, some of the extractable phenolics may be bound to cell walls, probably via covalent bonds (Hutzler et al. 1998 and references therein). These bound-phenolics cannot be extracted with common solvents. For example, the non-extractable PAs account 65 % of total PAs in birch bark (Matthews et al. 1997). Henceforth, this thesis covers only extractable phenolic compounds, unless otherwise stated.

In addition to the wide diversity of phenolic compounds in different organs of silver birch, the number and amount of phenolic compounds vary broadly between organs. The amounts given in the following subchapters are approximates. They cannot be compared with each other (except those values with the same reference) since they have been produced by different analytic methods, for example by Folin−Ciocalteu colorimetric method for total phenolics or by liquid chromatography (LC). In addition, phenolic compounds may have temporal changes in their contents (Salminen et al. 2002), while most of the quantitative studies are performed only once. Therefore, the contents given below may not be applicable to all seasons. Further, the phenolic profile of an organ may vary according to genetic (Laitinen et al. 2005a), climatic (Laitinen et al. 2005a), edaphic (Laitinen et al. 2005b), biotic (Agrawal et al. 2012), and ontogenetic (Valkama et al. 2004; Laitinen et al. 2005b) variation. Therefore, in order to generalize, discussion will be limited to fully developed birch organs. An exception to this is roots, which lack research data at the mature stage. Further information about the sampling days and habitat can be found in the cited references.

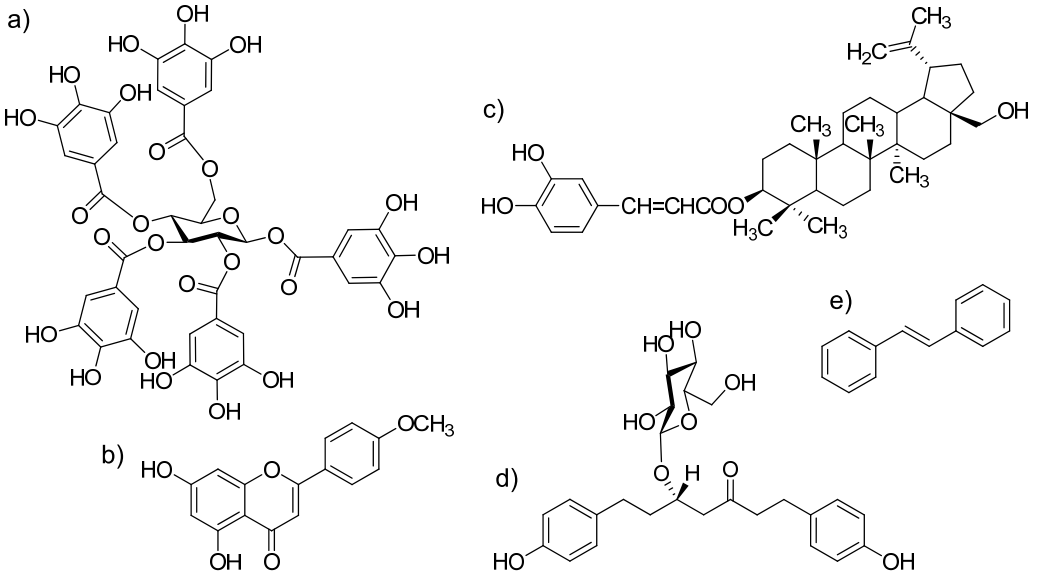

Figure 2. Example structures of the phenolics in the silver birch: a) a birch leaf hydrolysable tannin, 1,2,3,4,6-penta-*O*-galloyl-β-D-glucose, b) a leaf surface flavone, acacetin, c) an outer bark triterpene derivative, betulinol 3-caffeate, d) a diarylheptanoid, platyphylloside, in the wood and inner bark, and e) a backbone structure of stilbenes in the knot (e).

2.1.1. Leaves

The total content of phenolics in silver birch leaves is 27–38 mg/g of the dry weight (Ossipov et al. 1996; Keinänen and Julkunen-Tiitto 1998; Kähkönen et al. 1999). Several tens of compounds have been identified, i.e. flavonoid aglycones and glycosides, HTs, PAs, phenolic acids, and other simple phenolics (Ossipov et al. 1996; Keinänen and Julkunen-Tiitto 1998; Salminen et al. 2002; Karonen et al. 2006). Ca. 56% of the total low-molecular-mass phenolics in the leaves are flavonoids, consisting mainly of flavonoid glycosides (Ossipov et al. 1996).

2.1.2. Leaf surface

The phenolic content of a leaf surface is distinct from the rest of the leaf. The phenolic compounds detected on the leaf surface are flavonoid aglycones (Keinänen and Julkunen-Tiitto 1998; Valkama et al. 2003). These lipophilic compounds are localized on the surface of leaves instead of vacuoles. Silver birch leaves contain ca. 8 mg/g of epicuticular flavonoid aglycones. The main flavonoid is dihydroxy-dimethoxy-flavone (Valkama et al. 2003). The profiles of flavonoid aglycones of birch species differ from each other and they have been suggested to serve as chemotaxonomic markers. A high-performance liquid

chromatography (HPLC) method based on surface flavonoids has been developed for the preliminary taxonomic classification of birch species (Lahtinen et al. 2006).

2.1.3. Outer bark

The outer bark has a high content of extractives. However, the majority of this material is composed of triterpenes, and outer bark contains only 2 mg/g of phenolics (Kähkönen et al. 1999). Triterpenes account for about 30% of the dry weight of the outer bark, with betulinol as the main compound (Ekman 1983). The only phenolic compounds identified are esterified hydroxycinnamic acids. The dominant triterpene hydroxycinnamate, betulinol 3-caffeate comprises 0.5% of the acetone soluble extractives of the outer bark (Ekman and Sjöholm 1983, Figure 2c).

2.1.4. Inner bark

The inner bark of silver birch has a very high phenolic content, ca. 85 mg/g of the dry weight (Kähkönen et al. 1999). These phenolics consist of flavonoids, arylbutanoids, diarylheptanoids, lignans, phenylpropanoids, simple phenolics, and phenolic acids (Šmite et al. 1993, 1995). Furthermore, the bark of birch species, in general, contains PAs (Kolodziej 1989; Matthews et al. 1997) and this strongly suggests that inner bark of silver birch also contains PAs. The high amount of platyphylloside, the main diarylheptanoid in the inner bark (Figure 2d), can be exploited for species delineation between silver birch and white birch (Lundgren et al. 1995). The method is based on the formation of a precipitate when platyphylloside reacts with 2,4-dinitrophenylhydrazone. In this reaction, platyphylloside content over 5 mg/g yields a positive response. Although the inner bark of both silver and white birch contains platyphylloside, only the high concentration in silver birch leads to positive response (Lundgren et al. 1995).

2.1.5. Wood

The amount of known phenolics in the silver birch wood is rather low, ca. 1.5 mg/g comprising approximately 8% of the total methanol-soluble extractives (Hiltunen et al. 2006). However, the phenolic composition of wood is quite complex. Almost 30 individual phenolic compounds belonging to flavonoids, arylbutanoids, diarylheptanoids, lignans, phenylpropanoids, simple phenolics, and phenolic acids have been identified (Mämmelä 2001; Hiltunen et al. 2004, 2006). (+)-Catechin-7-*O*-β-D-xylopyranoside accounts for up to 1.0 mg/g in some individuals (Mononen et al. 2004).

2.1.6. Knotwood

Knots are branch stubs that are encased in the tree stem. Knots of many softwood and hardwood species contain several times more phenolic compounds than the corresponding stem wood (Willför et al. 2003a,b, 2004; Pietarinen et al. 2005, 2006). The phenolic composition in knots of the silver birch is very different from that in wood, notably containing stilbene-derived compounds. However, the exact structures of these stilbene-derived compounds are still to be determined (Willför et al. 2003c).

2.1.7. Roots of seedlings

The roots of silver birch seedlings have high levels of PAs. However, these PAs are detected mainly in the extraction residue by acid−butanol assay (ca. 130 mg/g), i.e. these PAs are non-extractable with methanol and therefore they are probably bound to the cell walls. In addition, roots contain extractable phenolic compounds, such as cinnamic acid derivatives, flavonoids, HTs, and PAs. (Sutela et al. 2009)

2.2. Functions of phenolics

Plants produce phenolic compounds as chemical defense and signaling compounds for a diverse variety of ecological and physiological purposes (Wink 2007; Lattanzio et al. 2012). The ecological functions cover roles such as herbivore deterrents and pollinator attractants (with colors and odors, Harborne 1982). As an example of physiological purposes, phenolics can improve plants physiological functioning by protecting against damage from ultraviolet (UV) radiation. It is common that the phenolic compounds, and other secondary metabolites as well, express multipurpose functions. Multiple functions enhance the probability that the compound is favored in natural selection (Wink 2007; Lattanzio et al. 2012).

2.2.1. Pollinator and seed disperser attractants

Plants attract pollinators and seed dispersers with flower and fruit pigments, volatiles, and floral structure (Harborne 2007). Different types of flavonoids comprise the majority of floral pigments found in plants. Anthocyanidins provide colors from orange to blue, while aurones, chalcones, and some flavonols give yellow, phlobaphenes reddish, and flavones and some flavonols white colors (Harborne 1982; Koes et al. 1994). Most of the anthocyanidins found in plants occur as glycosides (anthocyanins). Only 3-deoxyanthocyanidins are stable enough to occur as aglycones in nature (Wu and Prior 2005; Andersen 2007). Anthocyanins are the most common pigments in flowers and

widely distributed in berries and fruits. Glycosylation of an anthocyanidin enhances the structure and pigment stability but does not alter the flower color (Harborne 1982, 2007). Pelargonidin gives orange-red color, cyanidin magenta, and delphinidin mauve (Figure 3). Methylation of one or more of the free hydroxyl groups of the B-ring stabilizes the structure and it has a minor reddening effect on the color (Harborne 1982, Figure 3). Blue anthocyanin colors are formed by copigmentation with flavones or flavonols, through complexes with metals, or by acylation with aromatic or aliphatic acids to a sugar unit of an anthocyanin (Figueiredo et al. 1999; Harborne 2007). Other non-phenolic pigments in flowers are due to chlorophylls (green), carotenoids (yellow, orange, and red), and some alkaloids (e.g. betalain alkaloids giving yellow, red and purple colors).

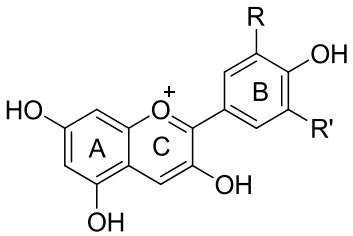

pelargonidin R = R' = H (510 nm, orange-red)
cyanidin R = OH, R' = H (525 nm, magenta)
delphinidin R = R' = OH (535 nm, mauve)
peonidin R = OCH_3, R' = H (523 nm, magenta)
petunidin R = OCH_3, R' = OH (534 nm, mauve)
malvidin R = R' = OCH_3 (532 nm, mauve)

Figure 3. Structures of the most common aglycones of anthocyanins. The visible wavelength maxima of each anthocyanidin in acidified methanol are presented in parentheses (Harborne 1982).

Different pollinators prefer distinct flower colors. For example, bees are attracted to intense yellow and blue colors. In addition, bees can observe differences in absorption in the UV region of the spectrum and are attracted to UV-absorbing flavones and flavonols (Harborne 1982). Beetles and bats have instead poor color sense. They are attracted to the plants by other types of signals, for example by flower scent (Harborne 1982). These volatiles are mainly mono- and sesquiterpenes, but for instance, phenolic vanillin is a known odor component in vanilla and orchids (Harborne 2007). Insects are sensitive to even small concentrations of volatiles. Attraction with volatiles is thought to be a more ancient phenomenon than attraction with a color, since some primitive flowers lack color components but have odors (Harborne 1982).

2.2.2. Herbivore and pathogen deterrents and inhibitors

A large number of different secondary metabolites inhibit the growth of pathogens and/or are toxic to herbivores. These substances include compounds from alkaloids, non-protein amino acids, cyanogenic glycosides, glucosinolates, terpenes, saponins, polyketides, and phenolics (Wink 2007). Many of these metabolites mimic the structure of endogenous hormones, neurotransmitters or other ligands. Other mechanisms consist of intercalation or

alkylation of DNA (deoxyribonucleic acid), inhibition of DNA and RNA (ribonucleic acid) related enzymes and protein biosynthesis, and disturbance of membrane stability (Wink 2007). As an example, isoflavonoids in red clover (*Trifolium pratense*) cause infertility to female sheep; *S*-equol, a metabolite of isoflavone formononetin was found to be the main component causing the estrogenic activity. Its structure mimics the structure of the natural steroidal female hormone, oestrogen (Harborne 1982; Mustonen et al. 2006).

In addition to toxins, a plant may produce a compound that is only unpleasant or distasteful, or reduce the nutritional value of the plant (Harborne 1982). For example, platyphylloside, a diarylheptanoid present in silver birch twigs, inner bark, and wood, has an inhibitory effect on ruminant digestibility *in vitro* (Sunnerheim et al. 1988). Platyphylloside is metabolized in rumen liquor to centrolobol (Sunnerheim-Sjöberg and Knutsson 1995) which is shown to be the active metabolite (Sunnerheim and Bratt 2004) responsible for almost five times slower digestion rate of hay than the hay without platyphylloside (Sunnerheim-Sjöberg and Knutsson 1995). In the case of insects, PAs in silver birch leaves correlated negatively with the relative growth rate and pupal mass of geometrid moth larvae (*Epirrita autumnata*) in fertilized and nonfertilized samplings while myricetin glycosides correlated negatively only with pupal mass in fertilized samplings (Mutikainen et al. 2000). However, not all PAs have antiherbivore activity; instead PAs confer only limited defense. The activity is dependent upon structural features of PAs (Clausen et al. 1990; Ayres et al. 1997) and physiology of the target insect or mammal (Robbins et al. 1991; Ayres et al. 1997). As a rough estimation, antiherbivore activity against insects is the greatest in PAs with a high molecular mass and a high ratio of gallocatechins as building blocks (Ayres et al. 1997). Further, the stereochemistry of PA structure has an impact on the activity (Zucker 1983; Clausen et al. 1990).

As a consequence of plant defensive chemistry, herbivores have adopted strategies for surviving with these deterrents. Some herbivores adopt a generalist strategy and feed on several plant species. By mixing diets they avoid acute intoxication from the defensive compounds in a single plant species. In contrast, specialist herbivores feed on only single or limited range of species, and– often have evolved enzymes to detoxify the noxious compounds of their host plant(s) (Wink 2007). Some mammalian herbivores have evolved into defend themselves against antinutritional effects of PAs by producing proline-rich salivary proteins with a high affinity to tannins (Hagerman and Butler 1981).

2.2.3. Nutrient cycling

Phenolics enter the soil as leachates from above- and belowground plant parts and from plant litter. In the soil, phenolics are known to affect nutrient cycling by inhibiting or

stimulating soil organisms and through physicochemical effects on the nutrients (Hättenschwiler and Vitousek 2000). Tannins may impact on the nitrogen cycling by forming complexes with proteins originating from plants or microorganisms. For example, in infertile and acidic coniferous soils, the tannin−protein complexes can be utilized as a nitrogen source mainly by some coniferous associated mycorrhizal fungi. Therefore, tannin−protein complexes are thought to constrain nitrogen availability of competing organisms and prevent nitrogen losses through leaching and denitrification (Northup et al. 1995 and references therein). In addition, phenolic compounds may be toxic to decomposing microorganisms (Scalbert 1991; Kraus et al. 2003) or they can directly inhibit or stimulate enzyme activities depending on tannin structures and enzymes (Triebwasser et al. 2012). The soil of the silver birch forest is known to contain PAs, hydroxybenzoic acids, and hydroxycinnamic acids (Suominen et al. 2003; Smolander et al. 2005; Kanerva et al. 2008).

2.2.4. Protection against UV radiation

Sunlight is essential for the photosynthesis of plants. However, the photosynthetically active radiation of the sun (400−700 nm) is accompanied by other types of radiation including UV radiation (100−400 nm). The shortest wavelengths of UV radiation, 100−280 nm (UV-C), are cut out by ozone and air and thus do not affect plants. However, longer wavelengths of UV radiation (UV-B and UV-A) are not blocked atmospherically and can damage plant tissues. UV-B radiation (280−315 nm) is very energetic and can damage DNA and affect photosynthesis, growth, and development of plants (A.-H.-Mackerness 2000; Newsham and Robinson 2009). Also UV-A radiation (315−400 nm) is harmful: it penetrates into leaves and produces active oxygen species. One of the protective mechanisms against UV radiation in plants is the accumulation of phenolic compounds with appropriate UV absorptive properties (Taiz and Zeiger 1998; Morales et al. 2010). The main groups of phenolic compounds that are considered as UV protective compounds are hydroxycinnamic acids and flavonoids, particularly flavonols and flavones. Hydroxycinnamic acids have absorption maxima in the ranges 310−332 nm, flavones in 250−270 nm (Band II) and 330−350 nm (Band I), and flavonols in 250−270 nm (Band II) and 350−390 nm (Band I) (Cerovic et al. 2002). These compounds absorb the UV radiation but do not impact photosynthetically active radiation.

Silver birch is a common model tree species for the studies of UV screening, because of its ecological importance and tolerance of relatively high levels of UV radiation (Morales et al. 2010). The biosynthesis of phenolic compounds in the silver birch is altered in response to different UV treatments. The concentration of some individual phenolic compounds, most often quercetin glycosides, is increased in the leaves of silver birch grown with

elevated UV-B radiation (Lavola et al. 1997; Wulff et al. 1999; de la Rosa et al. 2001; Kostina et al. 2001; Tegelberg et al. 2001). In contrast, exclusion of UV-B radiation from sunlight decreased the concentrations of six flavonoids in the birch leaves while the exclusion of UV-A radiation reduced the concentrations of only two flavonoids (Morales et al. 2010). In the bark of silver birch saplings, increased UV radiation had only minor effects on phenolic compounds (Tegelberg et al. 2002).

Since most of the flavonoids absorb UV light, it has been hypothesized that flavonoids have evolved in concert with the colonization of land by plants. This is because terrestrial plants are thought to have evolved from algae, but flavonoids have not been found in algae. Instead, flavonoids are present in the earliest land plants: mosses, liverworts, and ferns. The hypothesis has been questioned since the early flavonoid enzymes involved in the flavonoid biosynthesis were not as effective as enzymes nowadays and therefore, probably were not capable to produce enough UV screening flavonoids. (Rausher 2006)

2.2.5. Autumn colors

Autumn colors are an impressive phenomenon in temperate deciduous trees. The bright yellow and red colors are mainly due to two groups of secondary compounds, carotenoids (yellow-orange) and anthocyanins (red-purple) (Archetti et al. 2009). The green chlorophyll pigments in leaves degrade into colorless metabolites as a consequence of changes in the day length and temperature in the autumn (Hendry et al. 1987). The breakdown of chlorophyll reveals the yellow carotenoids which are present in the leaves throughout the whole season. Anthocyanins, instead, are produced *de novo* before the leaf fall. Although the meaning of autumnal leaf color change is not known, it is not a mere side effect of leaf senescence. Several hypotheses are debated. For instance, the photoprotection hypothesis proposes that anthocyanins protect leaves against photo-oxidative stress and therefore enhance the resorption of nutrients, while the coevolution hypothesis suggests that red anthocyanins function as a warning signal for insects that the tree is not a suitable host plant (Archetti et al. 2009). Red and yellow colored autumnal leaves are present in 12% and 16% of temperate tree species, respectively. Silver birch has a yellow autumn color (Archetti 2009) and there is significant genetic variation in leaf coloration (Sinkkonen et al. 2012).

2.3. Advanced characterization methods for the analysis of phenolics

A biological activity is usually a consequence of a certain structural feature of a compound or its metabolite. For example, structural features like conjugated double bonds affect the

UV absorption properties of some flavonoids. Alternatively, a certain activity may depend on the stereochemistry of the compound since target enzymes and biological systems in general are stereospecific. Therefore, the full characterization of the compound of interest is of paramount importance.

Prior to characterization, phenolic compounds need to be extracted and purified from the plant material. First, the metabolic activity of the plant is halted by flash freezing and lyophilization or by placing the plant material directly into acetone or ethanol. Phenolic compounds are usually extracted with alcohol or acetone or their water mixtures. Grinding the material prior or during the extraction enhances extraction yields as does sequential extraction. The crude extract may be purified by solvent extractions and the proper purification and isolation procedure is commonly achieved by sequential column chromatographic methods such as gel filtration over Sephadex LH-20 and reversed-phase (RP) chromatography. (Waterman and Mole 1994)

Identification of a specific compound is usually achieved by a combination of several physicochemical methods, such as ultraviolet spectroscopy (UV), circular dichroism spectroscopy (CD), optical rotation, nuclear magnetic resonance spectroscopy (NMR), mass spectrometry (MS), and X-ray crystallography. If the compound of interest is already known, it can be identified with less measurements by comparing its characteristic features with literature values or the data of standard compounds. In this thesis, NMR spectroscopy, MS, and CD spectroscopy, the main characterization methods in analysis of phenolic compounds, are discussed.

2.3.1. LC-MS

MS is a widely used characterization method in the analysis of phenolic compounds, especially after the development of atmospheric pressure ionization (API) interfaces, such as atmospheric pressure chemical ionization (APCI) and electrospray ionization (ESI) in the 1970's and 1980's (Thomson 1998). API interfaces enabled the easy connection of MS to HPLC due to the simultaneous solvent elimination and ionization step at atmospheric pressure (Brewer and Henion 1998). Both ESI and APCI are soft ionization techniques, i.e. the ions are produced as molecular ions without extensive fragmentation. An ESI source is a preferred interface in the LC-MS analysis of phenolic compounds because of its suitability for a wider range of compounds (Pérez-Magariño et al. 1999; Rauha et al. 2001, see the examples of ESI: Cádiz-Gurrea et al 2013; Ruiz et al. 2013; Simirgiotis et al. 2013). An APCI source is suitable for the ionization of small (MW < ~1000 Da) molecules with moderate or no polarity and for compounds that tolerate moderate thermal stress (Herderich et al. 1997). In addition, the ESI source generally provides a better sensitivity

and less background noise than the APCI source (Pérez-Magariño et al. 1999). APCI has been applied for the analysis of small phenolic molecules, such as flavonoids, hydroxycinnamic acids, anthocyanins, xanthones, and stilbenes (Li et al 2009; Zhu et al. 2009, 2010; Tibe et al. 2011). Other ionization techniques that have been used in conjunction with HPLC for the identification of phenolic compounds are continuous-flow liquid secondary ion mass spectrometry (Sumner et al. 1996) and thermospray ionization mass spectrometry (Wolfender et al. 1993). In general, phenolic compounds are better ionized in a negative ion mode in ESI (Swatsitang et al. 2000; Peng et al. 2011), with an exception for anthocyanidins, which are already positively charged in the form of flavylium cation at low pH (< 2) (Rivas-Gonzalo 2003; Touriño et al. 2008). However, the MS^1 spectra obtained by the positive ionization mode may contain more structural information in the fragmentation patterns than the spectra obtained by negative ionization mode (Swatsitang et al. 2000).

Accurate mass measurements revealing the isotopic patterns of ions are important in the structure elucidation in order to obtain molecular formula candidates. A mass deviation of 5 ppm is regarded as a limit of accurate mass definition. Ultrahigh mass accuracy (less than 1 ppm) and high resolving power can be achieved with Fourier transform ion cyclotron resonance (FT-ICR) and Orbitrap mass spectrometers. Mass deviations of 2−5 ppm are achievable with TOF instruments. At the present time, all of these mass analyzers are compatible with LC. However, FT-ICR-MS has low scan speeds, which is its main drawback (Allwood and Goodacre 2010) together with a high price. So far, only a few studies have exploited LC-Orbitrap-MS (Abreu et al. 2011; Peng et al. 2011; van der Hooft et al. 2012), or LC-FT-ICR-MS (Ren et al. 2013) in the analysis of phenolic compounds.

In ESI-MS, detailed structural information can be obtained through induced fragmentation either in a specific mass analyzer by colliding the ions with a target gas (collision induced dissociation, CID), or by adjusting the cone voltage above the typical acceleration voltage (in-source CID). Triple quadrupole and hybrid mass analyzers such as quadrupole-TOF are suitable for CID MS^2 experiments, while ion trapping instruments (and their hybrids) allow in addition multiple stage CID MS^n experiments. For example, linear triple quadrupole-Orbitrap, quadrupole-TOF, and ion trap-TOF instruments obtain accurate masses at least at the MS^2 level (Kind and Fiehn 2010) and they have been exploited in conjunction with LC in the characterization of phenolic compounds (Barnes et al. 2009; Abreu et al. 2011; Peng et al. 2011; Abu-Reidah et al. 2012; van der Hooft et al. 2012).

One of the most common fragments of phenolic glycosides obtained in first-order mass spectra is the aglycone ion which is formed after the cleavage of sugar or similar

compound. For example, flavonoids exist most often in the glycosylated form in nature. For flavonoid *O*-glycosides, low or medium fragmentation energy leads to the elimination of sugar residues, such as the loss of 162 Da (hexose), 146 Da (deoxyhexose) or 132 Da (pentose). Further fragmentation gives information about the aglycone structure. The formation of fragments is always dependent on the level of applied cone voltage or collision energy and the type of bonds. Therefore, low fragmentation energy does not fragment *C*-glycosidic flavonoids (Cuyckens and Clayes 2004; Vukics and Guttman 2010). Sometimes it is even possible to determine different substitution positions based on fragmentations. For example, it is possible to discriminate different chlorogenic acid regioisomers from each other based on their MS^2, MS^3, and MS^4 fragments (Clifford et al. 2003, 2005).

PA dimers have well-known MS^1 and MS^2 fragmentation patterns caused by established retro-Diels−Alder (RDA) mechanism, heterocyclic ring fission (HRF), and quinone methide (QM) cleavage (Gu et al. 2003). In dimers, the RDA cleaved group provides information about the hydroxylation pattern of the B-ring of the upper monomer unit (Figure 4). HRF occurs also in the upper monomer unit but this time the A-ring is cleaved as a phloroglucinol unit (Figure 4). The HRF pathway would be inhibited if the quinone formation is restricted, for example through the methylation of 4'-hydroxyl group. In higher oligomers, RDA and HRF fragmentations can occur in the middle units as well (Gu et al. 2003; Li and Deinzer 2007). QM leads to the cleavage of the interflavanoid bond. The upper unit forms a quinone and the lower unit stays as an intact monomer (Gu et al. 2003) (Figure 4). The connection sequences of heterogeneous PAs have been identified up to pentamers based on the product ions (Gu et al. 2003; Li and Deinzer 2007). Labeling experiments may aid the characterization of the fragments. For example, Sun and Miller (2003) used D_2O and H_2O solvents in direct infusion ESI-MS to study the fragments of a PA dimer through the mass shifts caused by H−D exchange.

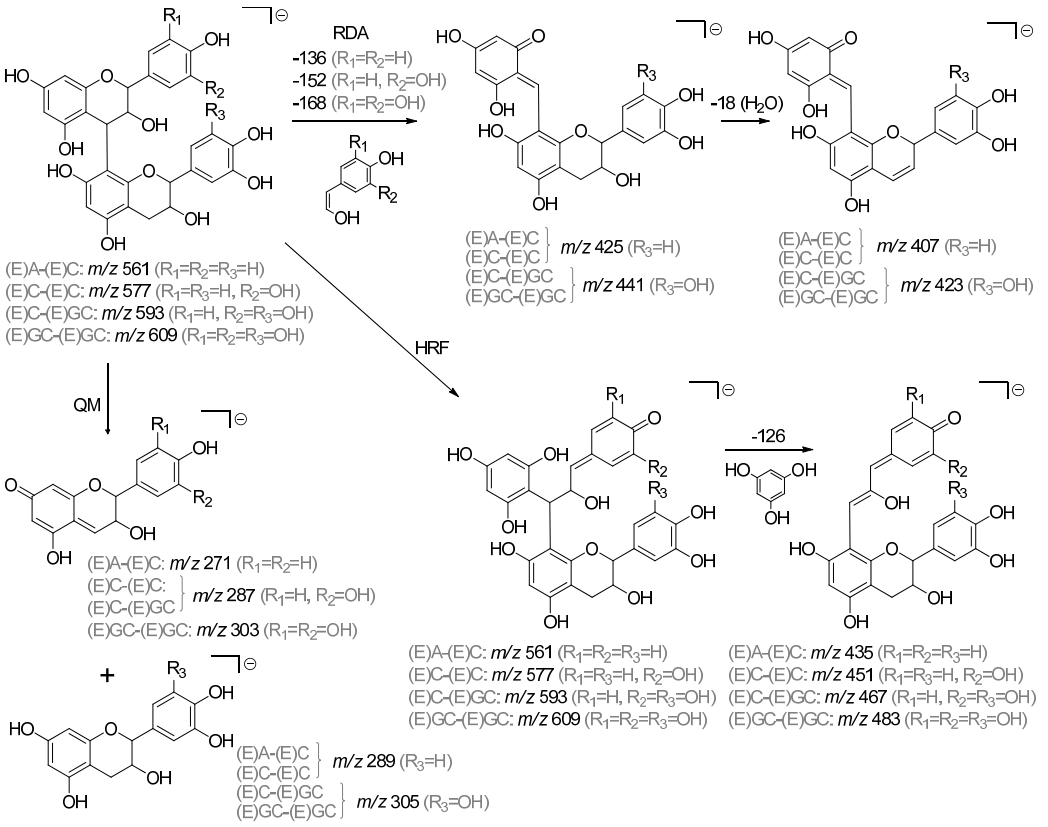

Figure 4. The fragmentation pathway of selected C4−C8 linked proanthocyanidin dimers according to Gu et al. (2003) and Jaiswal et al. (2012). The dimers consist of (epi)afzelechin ((E)A), (epi)catechin ((E)C), and (epi)gallocatechin ((E)GC) subunits.

2.3.2. NMR spectroscopy

"While no single form of spectroscopy is currently capable of resolving all structural problems, NMR spectroscopy is probably the technique of paramount importance" (Snyder et al. 1989). This statement was made by J. Snyder and coworkers back in 1989 and is still valid today. With NMR measurements, it is possible to obtain the constitution of a compound and sometimes even the configurational and conformational structure. The NMR phenomenon is based on the ability of certain atomic nuclei to receive electromagnetic energy at a characteristic frequency supplied by radio frequency pulses in a static magnetic field, and thereby attain a higher resonance state. The exact resonance frequency of each nucleus is dependent on the chemical environment of the nucleus. The difference in the resonance frequency of the nucleus and a standard (usually tetramethylsilane, TMS) is called chemical shift (δ/ppm). The nucleus will resonate at two slightly different frequencies, i.e. the resonance line will split, if the nuclear spin is coupled

to a magnetically non-equivalent nucleus via bonding electrons. This spin coupling is characterized by a coupling constant (*J*/Hz).

A set of one- and/or two-dimensional (1D, 2D) NMR experiments, such as heteronuclear single quantum coherence (HSQC), heteronuclear multiple bond correlation (HMBC), double quantum filtered correlation spectroscopy (DQF-COSY), total correlation spectroscopy (TOCSY), rotating-frame Overhauser effect spectroscopy (ROESY), and nuclear Overhauser effect spectroscopy (NOESY), in addition to ^{1}H and ^{13}C NMR measurements, is usually needed for the characterization of a novel compound. HSQC is a proton-detected experiment which identifies protons directly attached to a hetero atom (usually carbon, $^{1}J_{CH}$). The experiment allows the measurement of carbon atoms, except quaternary carbons, with higher sensitivity than direct ^{13}C NMR. An outcome of an HMBC experiment is rather similar to the HSQC experiment, but the coupling constants between carbons and protons are selected so that the connectivity over two or three bonds ($^{n}J_{CH}$, n = 2 or 3) is observed. In addition, correlation over four bonds ($^{4}J_{CH}$) may be observed through unsaturated bonds or in planar zigzag structures (*w*-coupling). Long-range coupling constants usually vary from 0 to 5 Hz for saturated bonds, and seldom exceed 25 Hz in any case (Table 1). In addition, the ^{3}J couplings display a Karplus-type relationship with the dihedral angle. The problem of the traditional HMBC experiment is that correlations over two or three bonds cannot be differentiated from each other or the correlation may be missing. The heteronuclear two bond correlation (H2BC) experiment can be applied to detect correlations exactly over two bonds. (Claridge 1999; Bross-Walch et al. 2005)

Table 1. Approximate long-range proton−carbon coupling constants (Claridge 1999)

Coupling	$^{2}J_{CH}$	Coupling	$^{3}J_{CH}$	Coupling	$^{4}J_{CH}$
H-C-**C**	≤ 5	**H**-C-C-**C**	≤ 5	**H**-C=C-C=**C**	≤ 1
H-C=**C**	≤ 10	**H**-C=C-**C** (trans)	≤ 15	**H**-C-C-C-**C** (*w*-configuration)	≤ 1
H-C≡**C**	40−60	**H**-C=C-**C** (cis)	< 10		
H-C(=O)-**C**	20−25	**H**-C≡C-**C**	≤ 5		

DQF-COSY is a homonuclear experiment that mainly yields the correlations of vicinal and geminal protons ($^{3}J_{HH}$ and $^{2}J_{HH}$, respectively). Correlations over four bonds ($^{4}J_{HH}$) can be observed in unsaturated or in *w*-geometry structures as in HMBC experiment. TOCSY experiment yields correlations between protons that lay within the same spin-system. The correlations of the continuous chain of spin-spin coupled protons are achieved through magnetization transfer. The TOCSY experiment resembles the COSY experiment, but it contains a mixing sequence known as a spin-lock sequence instead of a single mixing

pulse. The length of the spin-lock sequence determines the distance of transferred magnetization in the chain of spin coupled protons. Short spin-lock sequences, such as 20 ms, will cause only single-step transfer and correlations equivalent to those in COSY experiment are observed. The mixing time of 100−300 ms is usually sufficient to achieve correlations throughout the whole spin system. NOESY experiment identifies the correlations of protons by their magnetic interactions through space. Correlations can be observed for proton atoms with distances around 4 Å or less through space. The most important parameter in the NOESY experiment is mixing time, which should be around 1 s for small molecules and shorter for larger molecules (0.1−1 s). The problem of NOESY is that unwanted, residual COSY-like artifact correlations can be observed or the actual correlation may be missing. ROESY experiment is a modification of the NOESY technique. ROESY is suited for midsized molecules with masses of 1000−2000 Da, i.e. ROESY is suited for the compounds whose NOE is almost zero (Claridge 1999; Bross-Walch et al. 2005). The 2D homonuclear experiments have 1D versions, whose advantage is the better resolution compared with the corresponding 2D experiments.

The exact frequency at which a certain nucleus resonates, mainly results from the environment of the nucleus within the molecule. The electronegative surroundings of a proton cause its resonance to shift higher frequency compared with a proton in less electronegative surroundings. In addition, homonuclear and heteronuclear couplings provide information about the nearby nuclei. Therefore, based on merely ^{1}H and ^{13}C NMR data, a lot of structural information can be obtained for phenolics that contain mainly H, C, and O atoms.

The ^{1}H NMR spectra of phenolics contain resonances of aromatic protons at chemical shift (δ) ca. 6 to 9 ppm, unless the ring is fully substituted. Isolated olefinic protons resonate approximately at the same frequency. Different homonuclear coupling constants of ortho- (^{3}J ~ 8 Hz), meta- (^{4}J ~ 2 Hz), and para- (^{5}J < 1 Hz) coupled aromatic protons reveal the relationships of the protons. On an isolated olefinic system, *trans*-coupled protons (^{3}J =15−18 Hz) have larger coupling constants than *cis*-coupled protons (^{3}J = 8−12 Hz). Substituents in the aromatic ring can usually be assigned by HMBC or NOESY/ROESY correlations. In addition, the use of aprotic deuterated solvents may aid in assigning highly substituted aromatic rings by showing the exchanging aromatic hydroxyl signals (see e.g. Sinkkonen et al. 2005).

Glycosidic compounds show recognizable signals in their ^{13}C NMR spectra. The anomeric ^{13}C resonances of *O*-glycosides can be found in a well-separated area at ca. δ 90−110, and may allow the counting of *O*-linked sugar groups in the molecule, since other signals of the

sugars usually appear at δ 60−90 (Agrawal 1992). Some aromatic, unsubstituted carbons may also resonate at around δ 100. However, chemical shifts and coupling constants of protons directly attached to aromatic carbons (shown by HMBC correlations) may aid to distinguish anomeric resonances from aromatic resonances. The anomeric protons of *O*-glycosides usually resonate at δ 4.3−5.9. Glycosides that have a free anomeric hydroxyl group usually form a mixture of α- and β-anomers, and their anomeric carbon, as well as anomeric proton, signals appear at different δ values in a specific ratio (see e.g. Hatano et al. 1988a). Usually the anomeric signals of α-glycosides appear at a higher frequency position by 0.3−0.5 ppm compared with the corresponding resonances of β-glycosides (Agrawal 1992). However, it is recommended to determine the anomeric configuration with coupling constants. The anomeric resonances of *C*-glycosides appear at δ 70−80 (Agrawal 1992) and they cannot be distinguished as easily as *O*-glycosides.

HTs contain a polyol core, most often D-glucose, which is esterified with gallic acids. Although the hydroxyls of the polyol core are usually highly esterified, HTs show similar ^{13}C NMR resonances in the sugar area as monoglycosidic phenolic compounds: the anomeric carbons of *O*-glycosidic HTs appear at δ 90−100 and the rest of the signals of the sugars usually at δ 60−80 (Yoshida et al. 1984; Hatano et al. 1988a), while the anomeric carbons of *C*-glycosidic HTs appear clearly at lower ppm values, at δ ~ 70, than the corresponding resonances of *O*-glycosides (Hatano et al. 1988b).

Sugar moieties consist mainly of linear chains of coupled spins and are therefore suited to spin correlation methods, such as COSY and TOCSY (Agrawal 1992). Especially, the 1D-TOCSY technique is an ideal tool for the separation of the proton signals, which are in the same spin network, from the rest of the proton resonances of the ^{1}H NMR spectrum (Bross-Walch et al. 2005). It is important to observe the resonances of carbohydrate moieties separately, since the coupling constants are related to the stereochemistry of the pyranosyl ring. In pyranosides, the six-membered ring usually takes a chair conformation allowing the classification of the ring protons as axial or equatorial. The vicinal proton−proton coupling constant depends mainly on the dihedral angle of the vicinal protons and follows the Karplus−Conroy curve that gives small coupling constants for equatorial−equatorial and axial−equatorial couplings ($^{3}J_{ee}$ ~ $^{3}J_{ae}$ ~ 2 to 4 Hz) and large coupling constant for axial−axial couplings ($^{3}J_{aa}$ ~ 8 to 10 Hz) (Agrawal 1992).

The general rules for the NMR assignment and reference data of different classes of phenolic compounds are reported in the literature. For example, databases exist for HTs (Yoshida et al. 1984; Hatano et al. 1988a, 1988b), PAs (Kolodziej 1992; Vdovin et al. 1997), flavonoids (Agrawal 1989), and lignans (Ayres and Loike 1990). Although the

characterization of phenolic compounds by NMR methods is usually straightforward, the NMR spectra of compounds that possess conformational isomerism may be difficult to assign due to the broadening or multiplication of the resonances. For instance, PAs may have hindered rotational isomerism about the interflavanoid bond(s) and conformational isomerism about the heterocyclic rings. The conformation of the heterocyclic ring oscillates between states where the 2-aryl substituent is in a pseudoequatorial or pseudoaxial position (Tarascou et al. 2006). The number and ratio of rotamers depend on the structure and number of flavanol subunits, the type and position of the interflavanoid bond(s), the temperature, and the solvent (Hatano and Hemingway 1997; Khan et al. 1997). For PC dimers, two rotamers, called extended and compact, are recognized and for PC trimers four rotamers are possible (two rotamers for both interflavanoid bonds) (Tarascou et al. 2007). PC dimers that have a catechin as an upper unit seem to have higher rotation barrier and slower exchange rate between the rotamers (in acetone at room temperature (r.t.)) than PC dimers having epicatechin as an upper unit. Therefore, separate resonances for both rotamers are observed when catechin is the upper unit, while averaged and broadened resonances are yielded when epicatechin is the upper unit (Tarascou et al. 2006). Broadening and multiplication of resonances may be avoided by derivatization and temperature elevation (Hellström et al. 2007).

2.3.3. CD spectroscopy

An optically active compound rotates the plane of linearly polarized light at a wavelength in which the chromophore of a molecule absorbs. Linearly polarized light may be decomposed to left and right circularly polarized waves and an optically active compound absorbs these lights differentially. The transmitted light is elliptically polarized and the difference in the absorption coefficient of the circular polarized waves is called circular dichroism (CD) (Koslowski et al. 2000; Slade et al. 2005). The electronic circular dichroism (ECD) measurement of an optically active compound yields a value and a sign as a function of wavelength characterizing the optical transition, and contains information about the absolute configuration or conformation of the compound (Kuball and Höfer 2000).

Common chromophores in natural compounds are an aromatic ring and a carbonyl group. The absorption bands of aromatic π–π^* transitions lie in the UV range of 200−290 nm and the n–π^* transitions of some carbonyl groups between 280 and 340 nm and the absorption range will further extend due to conjugation. Aryl and carbonyl groups are achiral chromophores and therefore the chirality has to be induced by an association with a chiral center. The observable CD activity of a compound depends on the mutual location of the chromophore and the chiral center. The assignment of the absolute configuration of a

compound from CD data may be obtained from sector and chirality rules and excitation coupling models (Smith 1998). Utilization of these models requires that the conformation of a molecule is known (Purdie 1994). The CD spectrum of conformationally mobile compounds is composed of the population-weighted contributions of the Cotton effects (CEs) of all rotameric species present (Verbit and Heffron 1968 and references therein). Therefore, CD is mostly exploited in the natural product research of rigid molecules such as steroids or flavonoids, i.e. for compounds that have ring systems. Empirically determined rules for the assignment of the absolute configurations of several types of phenolic compounds have been published, including HTs (Okuda et al. 1982), flavonoids (Slade et al. 2005), PCs (Barrett et al. 1979), diarylheptanoids (Itokawa et al. 1985), and lignans (Hulbert et al. 1981). However, the rules may not be applicable to similar types of compounds with different substituents. For example, an additional achiral substituent in an aromatic chromophore may lead to the sign inversion of a CE (Snatzke 1979). Further, the optical rotation properties of a compound may be reversed in different solvents. For example, 1,7-diaryl-5-hydroxy-3-heptanones show dextro-rotation in chloroform and levo-rotation in methanol (Ohta 1986).

3. AIMS OF THE STUDY

In this thesis, the objective was set to develop characterization methods for the phenolic compounds of the inner bark of silver birch (*Betula pendula*). The main aim was to characterize these compounds and study the quantitative changes of individual phenolics between genotypes and seasons. The fundamental topics in the original publications were:

1. Characterization of novel phenolic compounds from the inner bark of silver birch by MS and NMR techniques (Papers **I**, **II**, and **V**).
2. Characterization of oligomeric and polymeric PAs by hydrophilic interaction HPLC combined with ESI-TOF-MS (Papers **IV** and **V**)
3. Quantification of phenolics from the inner bark of silver birch (Papers **II** and **III**)
4. Clonal and seasonal variation of silver birch inner bark phenolics and induction of phenolic compounds into regrown bark after artificial wounding (Paper **III**)

4. MATERIALS AND METHODS

4.1. Plant material

Samples of silver birch inner bark (in Papers **II** and **III**) were collected from the Botanical Garden of the University of Turku between May 2009 and April 2010. The outer part of the bark was removed and the inner bark samples were enclosed in cryotubes within 2 minutes of sampling and frozen immediately in liquid nitrogen to stop enzyme activity and stored in a freezer until they were lyophilized. The sampled trees started to grow new bark at the locations from where the inner bark samples had been taken. Samples of regrown bark (Paper **III**) were collected eleven months after wounding (13 April, 2010). For the isolation and characterization of individual phenolics (Papers **I**, **II**, **IV**, and **V**), two silver birches were felled, the first in Somero, Southwest Finland (60˚34′N, 23˚24′E) in May 2006 and the second in the Botanical Garden of the University of Turku in June 2009. The felled trees were transported to the laboratory where the inner bark was separated immediately from the trunks, frozen, and lyophilized. The freeze-dried inner bark was crushed in a mortar, except the bark samples of regrown bark, which were tough and therefore ground in a mixer mill (MM 200, Retsch, Haan, Germany).

4.2. Extraction of the inner bark

Prior to the selection of the final extraction solvent, inner bark of silver birch (each sample 400 mg) was extracted (4 × 4.0 ml, for a total of 48 h) in a planar shaker (250 rpm) at r.t. with five different extraction solvents: 80% aqueous methanol, 70% aqueous acetone, methanol, acetone, and 95% aqueous ethanol. Organic solvents were evaporated from the extracts under reduced pressure at 35−40 °C. The aqueous residue was lyophilized and finally dissolved in 50% ethanol to a concentration of 20 mg/ml.

4.2.1. Large scale extraction

Three batches of crushed inner bark (each 50 g) were extracted with MeOH:H_2O (4:1, v/v) solution (each 4 × 500 ml) in a planar shaker (250 rpm) at r.t. for a total of 48 h (4 × 7−17 h). The extracts were combined and methanol was evaporated from the extract under reduced pressure at 35−40 °C. The residue was lyophilized to yield 32 g dry weight. The dry extract was dissolved in water to a concentration of 150 mg/ml and filtered through glass wool.

4.2.2. Small scale extraction

The crushed samples (20.00 ± 0.11 mg) were extracted in 1.5 ml Eppendorf tubes with MeOH:H_2O (4:1, v/v) solution (4 × 1 ml) in a planar shaker (250 rpm) at r.t. for a total of 48 h (4 × 7−17 h). Methanol was evaporated from the extracts in a vacuum concentrator at approximately 30 °C. The residues were lyophilized and dissolved in 0.5 ml of water. The samples were filtered through PTFE filters (13 mm i.d., 0.45 μm, VWR International, West Chester, Pennsylvania, U.S.) before HPLC analyses.

4.3. Fractionation and isolation of the inner bark phenolics

Birch bark extract obtained as described in Chapter 4.2.1. was partitioned into fractions by liquid−liquid extractions and column chromatography (Paper **II**). First, the crude extract was fractionated by column chromatography on Sephadex LH-20 by elution with water, aqueous ethanol (EtOH:H_2O from 1:9, v/v to 19:1, v/v), and aqueous acetone (Me_2CO:H_2O, 1:1, v/v and 7:3, v/v). After monitoring with HPLC-DAD (Chapter 4.6.), selected fractions were further fractionated and purified with semipreparative RP-HPLC yielding compounds **7**, **9**, **12**, **13**, **17**, **20**, **22**, **24**−**27**, and **29**−**36** (Table 3, Figure 5). The PA-rich fractions eluted with 40−95% aqueous ethanol and 50 and 70% aqueous acetone during Sephadex LH-20 column chromatography.

In order to isolate compounds present in small quantities, a liquid−liquid extraction step was applied prior to fractionation on a Sephadex LH-20 column. The crude extract was extracted successively with diethyl ether, ethyl acetate, and *n*-butanol. Fractions obtained with ethyl acetate and *n*-butanol extractions were purified on a Sephadex LH-20 column and by semipreparative HPLC-DAD to yield compounds **1**, **2**, **6**, **8**, and **11**. Altogether 24 compounds were isolated. All compounds could not be isolated pure. In particular, structural isomers **29** and **30**, as well as, **33** and **34** could not be separated, i.e. they coeluted as unresolved pairs. A different number of isolation and purification steps was required for different compounds. For example, compounds **22** and **31** could be isolated with over 90% purity only by successive liquid−liquid extractions with diethyl ether and ethyl acetate and column chromatography on Sephadex LH-20. In contrast, compounds **1**, **2**, and **6** required purification on semipreparative RP-HPLC after their separation by liquid−liquid extractions and Sephadex LH-20 column chromatography. Further, compound **6** could not be isolated as pure: it coeluted with an unknown compound.

Two different semipreparative RP-HPLC systems and chromatographic conditions were used. Chromatography was performed on a LiChroCART column (LiChrospher 100 RP-

18, 250 × 10 mm i.d., 10 µm, Merck Darmstadt, Germany) in both cases. The first HPLC system consisted of a Merck-Hitachi L-6200A pump, a Perkin-Elmer LC-235 diode array detector, and a Perkin-Elmer GP-100 graphics printer (Paper **I**). The eluent consisted of water with 1% (v/v) formic acid (A) and acetonitrile (B). The linear gradient elution was performed as described previously in Karonen et al. (2004a). The second system was a Waters 600E series HPLC consisting of a 600 controller, a Delta 600 pump, a 2998 diode array detector, and a fraction collector III (Papers **II** and **V**). The solvents used were water with 1% (v/v) formic acid (A) and methanol (B). The elution profile was 0–15 min, 0–16% (v/v) B in A (linear gradient); 15–20 min, 16% B in A (isocratic); 20–45 min, 16–35% B in A (linear gradient); 45–65 min, 35–80% B in A (linear gradient); and 65–80 min 80% B in A (isocratic). The flow rate was 5 ml/min and the detection wavelength was 280 nm. The injection volume was 1.0 ml.

4.4. Radical scavenging assay

Antioxidant activities of the extracts were determined with the DPPH (1,1-diphenyl-2-picrylhydrazyl) radical scavenging assay (a modification of previous methods, e.g. Blois 1958; Molyneux 2004) in a 96-well plate reader (Multiskan Ascent, Thermo Electron Corporation). An aliquot of 20 µl of each extract with six different concentrations in 7:3 EtOH:H_2O (v/v) was added to a 96-well plate with 280 µl of 0.25 mM solution of DPPH in ethanol. The final concentrations of extracts in the reaction mixtures were 1.3, 3.3, 6.7, 13.3, 33.3, 66.7, and 133.3 µg/ml. The initial absorbance (time point 0 minutes) was measured at 520 nm. The mixtures were left to stand in the dark for 10 min, shaken for 10 s, and then the absorbance was measured again. The standing, blending and measurement were repeated eight times at ten minutes intervals. The lowest absorbance value (the highest % inhibition) of nine measurements was selected. The lowest absorbance value was in each case the last measured absorbance, i.e. at time point of 90 minutes. 1 M pentagalloyl glucose (PGG) was used as a positive control (100% inhibition), and 7:3 EtOH:H_2O (v/v) (solvent) was used as a negative control (0% inhibition). The analyses were performed with four technical replicates for each sample and with six replicates for standards. The radical scavenging activity was calculated from the following equation:

$$\text{Inhibition (\%)} = \left\{1 - \left[\frac{A(sample) - A(PGG)}{A(solvent) - A(PGG)}\right]\right\} \times 100$$

The % inhibition was plotted against the concentration of extract and the IC_{50} value (the concentration of the sample required for inhibiting the formation of DPPH radical by 50%) was read from this curve.

4.5. Acid−butanol assay

Contents of PAs in the extracts were determined by using modifications of the acid−butanol assay reported in Ossipova et al. (2001). The extracts were dissolved in 7:3 EtOH:H_2O (v/v) to a mass concentration of 2 mg/ml. A 400 µl aliquot of extract was combined with 3.0 ml of 9:1 BuOH:HCl (v/v), shaken for 10 s in a test tube and placed in 95 °C for 2h. Test tubes were allowed to cool down for 45 min and the absorbance was measured in a 96-well plate reader at 550 nm. The PAs were quantified using a PA fraction of mountain birch leaves as a standard (Karonen et al. 2006). All measurements were performed with three replicates.

4.6. HPLC-DAD analysis

The analytical system consisted of a Dionex Corporation (Sunnyvale, CA, U.S.) UltiMate 3000 series: an LPG-3400A pump, a WPS-3000SL analytical autosampler, and a PDA-3000 photodiode array detector. Chromatographic separation was performed on a Waters (Milford, Massachusetts, U.S.) XBridge™ C18 column (100 × 2.1 mm i.d., 3.5 µm). The binary mobile phase consisted of water with 1% (v/v) formic acid (A) and acetonitrile (B). The elution profile was 0–25 min, 0–16% (v/v) B in A (linear gradient); 25–35 min, 16% B in A (isocratic); 35–55 min, 16–28% B in A (linear gradient); 55–63 min, 28–70% B in A (linear gradient); and 63–73 min 70% B in A (isocratic). The flow rate was 0.3 ml/min and the detection wavelength was 280 nm. The injection volume was 5 µl.

4.7. HPLC-MS analysis

The RP-HPLC-MS analysis was performed using an Agilent Technologies 1200 series HPLC system (Waldbronn, Germany) connected to a high-resolution (HR) Bruker Daltonics micrOTOF$_Q$ mass spectrometer (Bremen, Germany) via an ESI source. The HPLC consisted of a diode array detector, a pump, an autosampler, and a thermostatic column oven. The HPLC system and the mass spectrometer were controlled by HyStar software (version 3.2, Bruker BioSpin, Rheinstetten, Germany) and Compass micrOTOF

control software (Bruker Daltonics), respectively. The spectra were recorded in negative ionization mode. The endplate voltage was set to −500 V and the capillary voltage to +4000 V. Nebulizer gas (N_2) pressure was 1.6 bar. The flow rate of the drying gas (N_2) was 8 l/min and the gas was heated to 200 °C. The spectra were acquired in a mass range of *m*/*z* 100−3000. Calibration with 5 mM sodium formate was used at the end of each analysis. The RP-HPLC-MS analyses were conducted on the same column and in the same chromatographic conditions as the analytical HPLC-DAD analysis (Chapter 4.6.), except that the eluent A was replaced by water with 0.1% (v/v) formic acid (Papers **II** and **III**).

The hydrophilic interaction liquid chromatography (HILIC) –MS analyses were done using a Phenomenex Luna HILIC column (250 × 4.6 mm i.d., 5 µm, cross-linked diol) with SecurityGuard at 30 °C (Papers **IV** and **V**). Two solvents were used: water with 1% (v/v) formic acid (A) and acetonitrile (B). The elution profile was 0–40 min, 95–35% (v/v) B in A (linear gradient); 40–45 min, 35–95% B in A (linear gradient); and 45–75 min 95% B in A (isocratic). The flow rate was 0.8 ml/min and it was reduced to approximately 0.27 ml/min by splitting before the introduction into the ion source. Chromatograms were recorded at 190–950 nm. The injection volume was 50 µl.

4.8. FAB-MS

HR fast atom bombardment (FAB) mass spectra in Paper **I** were obtained by a VG ZABSpec mass spectrometer (VG Analytical, Manchester, U.K.). The spectra were recorded in positive ionization mode with glycerol as a matrix.

4.9. NMR spectroscopy

NMR spectra were recorded on Bruker Avance 400 and 500 spectrometers operating at 400.13 MHz and 500.13 MHz for ^{1}H and 100.61 MHz and 125.77 MHz for ^{13}C, respectively. Spectrometers were equipped with a BBI or BBO-5mm-Zgrad probe. Samples were dissolved mainly in CD_3OD but D_2O was also used as a solvent in experiments reported in Papers **IV** and **V**. Spectra were recorded on a non-spinning sample in 5 mm NMR tubes at 25 °C. Proton and carbon spectra were referenced to an internal TMS standard at 0.00 ppm or to a solvent signal (Gottlieb et al. 1997). The spectra were processed by TopSpin 1.3 software.

Parameters employed varied among the compounds. As an example, for compound **1**, the parameters with the Bruker 500 spectrometer and BBI probe were as follows. ^{1}H NMR

spectrum was acquired with single-pulse excitation, 30° flip angle (P1 6.9 μs for 90° pulse and PL1 1.5 dB), acquisition time of 4.1 s, pulse repetition time of 5.1 s, 8 transients and spectral width of 8 kHz consisting of 64 k data points (digital resolution 0.12 Hz/pt). No apodisation was applied prior to Fourier transformation. The ^{13}C NMR proton-decoupled spectrum was acquired with single-pulse excitation, 45° flip angle (P1 12.6 μs for 90° pulse and PL1 –2 dB), Waltz16 decoupling sequence with 90 μs decoupling pulse, acquisition time of 1.1 s, pulse repetition time of 3.1 s, 15000 transients and with the spectral width of 30 kHz consisting of 64 k data points (digital resolution 0.46 Hz/pt). 1 Hz exponential weighting was applied prior to Fourier transformation.

The gradient selected DQF-COSY spectrum was acquired with the cosygpmfqf pulse program (pulse programs refer to original ones installed by Bruker), with the spectral width of 6.7 × 6.7 kHz, 1024 × 128 data points, 4 transients and processed with zero-filling (×1, ×8) and non-shifted sine weighting applied in both dimensions prior to Fourier transformation. The gradient selected NOESY spectrum was acquired with the noesygpph pulse program, with the spectral width of 5.1 × 5.1 kHz, mixing time of 0.3 s, 1024 × 128 data points, 10 transients and processed with zero-filling (×1, ×8) and shifted (SSB 2) qsine weighting applied in both dimensions prior to Fourier transformation. The gradient selected multiplicity edited ^{1}H–^{13}C HSQC spectrum was acquired with the hsqcedetgpsisp2 pulse program, with the spectral width of 6.7 × 27.7 kHz, 1024 × 256 data points, 2 transients, 145 Hz one-bond coupling constant and processed with zero-filling (×1, ×4) and shifted (SSB 2) qsine weighting applied in both dimensions prior to Fourier transformation. The gradient selected ^{1}H–^{13}C HMBC spectrum was acquired with the hmbcgplpndqf pulse program, with the spectral width of 6.5 × 27.9 kHz, 1024 × 128 data points, 6 transients, 10 Hz long-range coupling constant and processed with zero-filling (×2, ×8) and non-shifted sine weighting applied in both dimensions prior to Fourier transformation. The 1D TOCSY spectrum was acquired with the selmlgp.2 pulse program using Gaus1.1000 shaped pulse (P12 60000 μs and SP2 66.58 dB), with the spectral width of 10 kHz consisting of 32 k data points (digital resolution 0.31 Hz/pt), 32 transients and spinlock time 0.08 s.

4.10. CD spectroscopy

The ECD spectra were recorded with a Chirascan CD Spectrometer (Applied Photophysics, Leatherhead, U.K.). The spectrometer was controlled by Chirascan Pro-Data software (Applied Photophysics). The samples were dissolved in water or in a few drops of methanol and diluted with water (Paper **II**) or in methanol (Paper **V**) and placed in a 1 cm

cuvette. The spectra were scanned from 200 nm to 400 nm at r.t. The data were handled by Applied Photophysics Pro-data Viewer (version 4.2.0). The background was subtracted from the spectra and the spectra were smoothened.

4.11. Computational methods

Computational methods were applied as reference purposes for the interpretation of ECD spectra of compounds **6**, **7**, **9**, and **17**. The preferred conformations of the compounds were searched using usage directed search method in HyperChem 7.5 software (Hypercube Inc.). Geometry optimization of the conformers of compounds **6**, **7**, **9**, and **17** were obtained using density functional theory (DFT) with the Becke's three-parameter Lee−Yang−Parr functional (B3LYP) and 6-311G(d,p) basis set in a gas phase (except for compound **9**, which was optimized in a water phase). The geometry optimization was followed by ECD spectra calculations using hybrid meta density functional with double nonlocal exchange (M06-2X) and 6-311++G(d,p) basis set with H_2O as solvent (IEFPCM solvent model). All calculations were done with Gaussian 09W revision A.02 software (Frisch et al. 2009).

5. RESULTS AND DISCUSSION

5.1. Extraction of the phenolic compounds

Several solvents were tested for the extraction of phenolics from inner bark: 80% aqueous methanol, 70% aqueous acetone, methanol, acetone, and 95% aqueous ethanol. 80% aqueous methanol was chosen for the extraction because it extracted the largest amount of phenolics, and in addition it extracted PAs almost as well as 70% aqueous acetone. Furthermore, the extract obtained with 80% aqueous methanol had the lowest inhibition concentration against free radicals (Table 2).

Table 2. The content of phenolics and proanthocyanidins (PAs) in the different extracts of inner bark and their radical scavenging activities (RSA)

Extraction solvent	Content of phenolics as a chromatogram area at 280 nm	Content of PAs (mg/g)	RSA, IC_{50} (mg/ml)
80% aqueous methanol	3270	213	0.029
70% aqueous acetone	3220	222	0.042
methanol	2890	101	0.039
acetone	2880	83	0.057
95% aqueous ethanol	2680	59	0.055

The volume of extraction solvent and the amount of sample material were scaled up for the larger scale extraction but also scaled down for the quantitative analysis. The efficiencies of the extractions were monitored: The extract from each extraction step was kept separate and an additional extraction step of 24 h was applied after the conventional extraction (48 h). The small scale extraction was quantitative with four extraction steps within 48 h, but the larger scale extraction did not reach completion within 48 h. The additional extraction still extracted PAs from the matrix. However, the extraction time was kept to 48 h to avoid the possible oxidation of the compounds during longer extraction.

5.2. Characterization of the phenolic compounds

Inner bark phenolics were tentatively characterized by LC-DAD/ESI-MS (in Papers **II**, **IV**, and **V**). Some of the compounds were isolated (Chapter 4.3.) and their structures confirmed by NMR (in Papers **I**, **II**, and **V**) and CD, when applicable. All identified compounds are presented in Table 3 and Figure 5.

Table 3. The phenolic compounds identified from the inner bark of silver birch

Compound		Rt (min)	Molecular ion $[M–H]^-$	Cluster ion $[2M–H]^-$	Aglycone ion $[A–H]^-$	Other fragments	Calcld. exact mass
1	tachioside [a]	5.6	301.1	-	-	-	302.1002
2	isotachioside [a]	7.0	301.1	-	-	-	302.1002
3	gallocatechin [b]	8.8	305.1	611.1	-	-	306.0740
4	vanillic acid hexoside [b]	10.0	329.1	659.2	167.0	-	330.0951
5	procyanidin trimer	10.2	865.2	1731.4	-	-	866.2058
6	3-β-glucopyranosyloxy-2-hydroxy-1-(4-hydroxy-3-methoxy-phenyl)-propan-1-one [a]	11.4	373.1	-		193.1	374.1213
7	syringic acid 4-β-glucopyranoside [a]	11.9	359.1	719.2	197.0	-	360.1056
8	procyanidin dimer (B3) [a]	14.0	577.1	1155.3	-	287.1, 289.1, 407.1, 425.1, 451.1	578.1424
9	*trans*-3-*O*-*p*-coumaroyl quinic acid [a]	14.3	337.1	675.2	-	-	338.1002
10	procyanidin dimer	14.5	577.1	1155.3	-	287.1, 289.1, 407.1, 425.1, 451.1	578.1424
11	procyanidin dimer xylopyranoside [a]	14.8	709.2	-	577.1	287.1, 289.1, 557.1, 583.1	709.1774
12	(+)-catechin 7-*O*-β-D-xylopyranoside [a]	15.0	421.1	843.2	289.1	-	422.1213
13	(+)-catechin [a]	15.3	289.1	579.1	-	245.1	290.0790
14	procyanidin dimer xylopyranoside	16.4	709.2	-	577.1	287.1, 289.1, 557.1, 583.1	709.1774
15	sinapic acid hexoside [b]	17.0	385.1	771.2	223.1	-	386.1213
16	procyanidin trimer	17.2	865.2	1731.4	-	-	866.2058
17	3-β-glucopyranosyloxy-1-(4-hydroxyphenyl)-butanone [a]	18.5	341.1	683.3	-	-	342.1315
18	procyanidin dimer	18.7	577.1	-	-	287.1, 289.1, 407.1, 425.1, 451.1	578.1424
19	epicatechin pentoside [b]	20.1	421.1	843.2	289.1	-	422.1213
20	epicatechin [a]	20.1	289.1	579.1	-	-	290.0790
21	procyanidin dimer xylopyranoside	21.1	709.2	1419.4	577.1	287.1, 289.1, 557.1, 583.1	709.1774
22	rhododendrin [a]	22.1	327.1	655.3	-	-	328.1522
23	(2*R*)-4-(4-hydroxy-phenyl)-2-butanol 2-*O*-α-L-arabinofuranosyl-(1→6)-β-D-glucopyranoside [b]	22.4	459.2	919.4	-	-	460.1945

Compound		Rt (min)	Molecular ion $[M–H]^-$	Cluster ion $[2M–H]^-$	Aglycone ion $[A–H]^-$	Other fragments	Calcld. exact mass
24	(2*R*)-4-(4-hydroxyphenyl)-2-butanol 2-*O*-β-D-apiofuranosyl-(1→6)-β-D-glucopyranoside [a]	23.4	459.2	919.4	-	-	460.1945
25	lyoniside [a]	27.4	551.2	1103.4	-	-	552.2207
26	nudiposide [a]	27.9	551.2	1103.4	-	-	552.2207
27	7-{3*R*-[(4-hydroxyphenyl)butyl] β-glucopyranosid-*O*-6-yl} 4-*O*-β-glucopyranosyl-vanillin [a]	29.6	639.2	1279.5	477.2	-	640.2367
28	(–)-isolariciresinol 3α-*O*-β-D-xylopyranoside [b]	30.8	491.2	983.4	-	-	492.1995
29	(5*S*)-5-hydroxy-1,7-bis(4-hydroxyphenyl)-3-heptanone 5-*O*-β-D-apiofuranosyl-(1→6)-β-D-glucopyranoside [a]	38.6	607.2	1215.5	475.2	-	608.2469
30	(5*S*)-5-hydroxy-1,7-bis(4-hydroxyphenyl)-3-heptanone 5-*O*-β-D-apiofuranosyl-(1→2)-β-D-glucopyranoside [a]	38.6	607.2	1215.5	475.2	-	608.2469
31	platyphylloside [a]	39.0	475.2	951.4	-	295.1	476.2046
32	(3*R*)-1,7-bis(4-hydroxyphenyl)-3-heptanol 3-*O*-[2,6-bis-*O*-(β-D-apiofuranosyl)-β-D-glucopyranoside] [a]	52.9	725.3	1451.6	-	-	726.3099
33	aceroside VIII [a]	54.1	593.3	1187.5	-	-	594.2676
34	1,7-bis(4-hydroxyphenyl)-3-heptanol 3-*O*-β-apiofuranosyl-(1→2)-β-glucopyranoside [a]	54.1	593.3	1187.5	-	-	594.2676
35	aceroside VII [a]	55.3	461.2	923.4	-	-	462.2254
36	(*E*)-1,7-bis(4-hydroxyphenyl)hept-4-en-3-one [a]	62.0	295.1	591.3	-	-	296.1412

[a] The structure was confirmed by NMR, [b] Tentative identification based only on UV and MS data

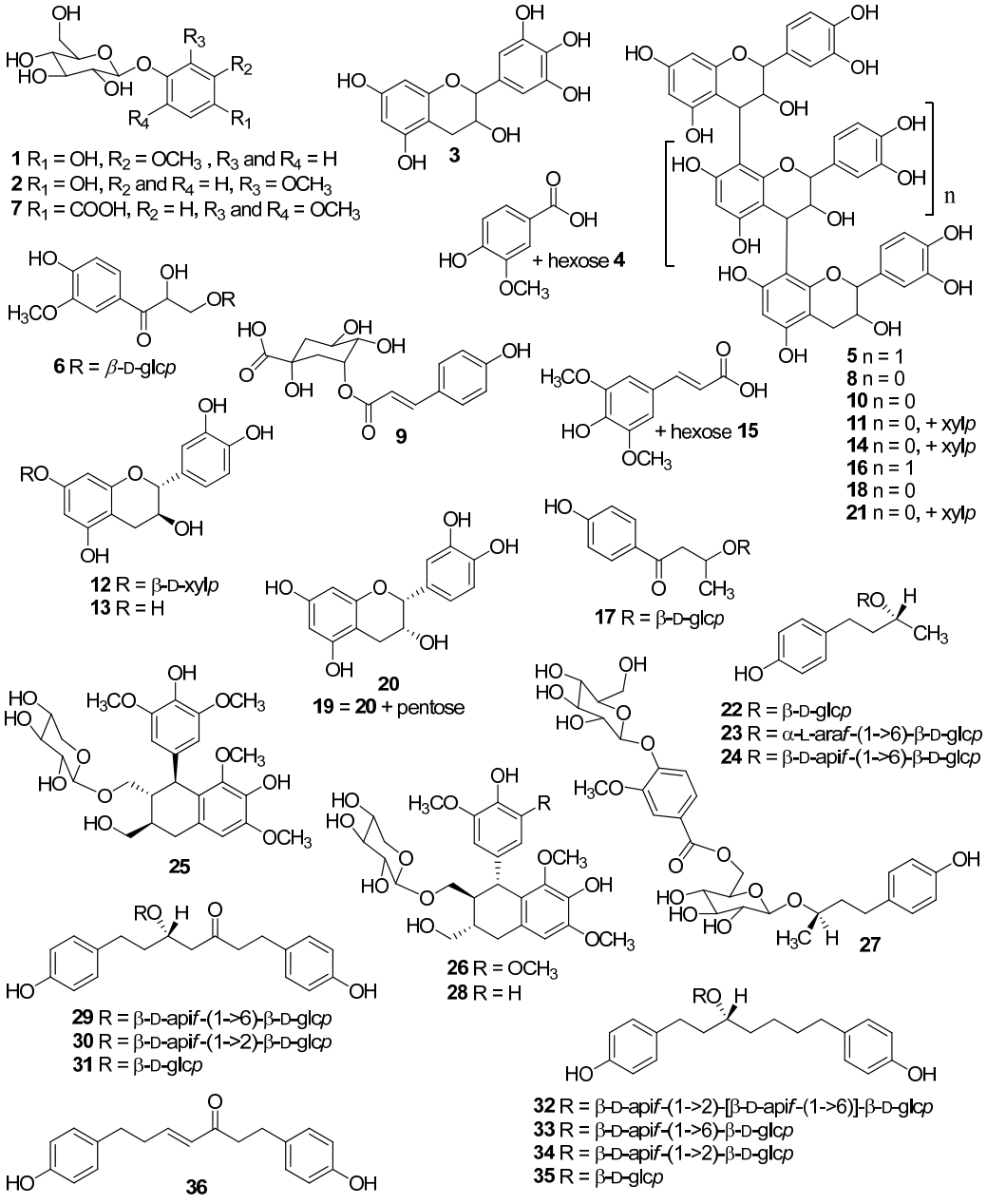

Figure 5. The structures of phenolic compounds identified from the inner bark of silver birch.

5.2.1. RP-HPLC-DAD/ESI-MS analysis

Chromatographic behavior

Phenolics eluted within 62 minutes in the following order: simple phenolics (Rt 5−10 min), phenolic acids (Rt 11−15 min), PC dimers and trimers (Rt 10−20 min), flavanols (Rt 8−21 min), arylbutanoids (Rt 18−30 min), lignans (Rt 27−31 min), and diarylheptanoids (Rt 38−62 min). In addition, PC polymers and oligomers (higher than trimers) eluted with a retention time of 18−38 min as an unresolved hump. Within flavanols, the elution order was gallocatechin (**3**, Rt 8.8 min), catechin xyloside (**12**, Rt 15.0 min), catechin (**13**, Rt 15.3 min), epicatechin glycoside (**19**, Rt 20.1 min), and epicatechin (**20**, Rt 20.1 min). This is in accordance with the relative elution order of flavanols in RP chromatography reported by Santos-Buelga et al. (2003): "1) Gallocatechins are more polar and elute earlier than corresponding catechins, and 2) flavanols with 2*R*,3*S* stereochemistry elute earlier than the corresponding 2*R*,3*R* compounds". For oligomeric PAs, the elution order is influenced by the stereochemistry of the terminal unit, type and position of interflavanoid linkages, and presence of substantial moieties, such as acylated galloyl units (Santos-Buelga et al. 2003). In this study, several PC dimers were detected but only two of them, catechin−catechin (B3, **8**, Rt 14.0 min) and its xyloside (**11**, Rt 14.8 min), were unambiguously determined by NMR.

Within diarylheptanoids and arylbutanoids, the presence of a carbonyl group in the aryl chain increased the polarity of the compound and therefore platyphylloside (**31**) and its glycosides eluted prior to aceroside VII (**35**) and its glycosides. The presence of sugar substituents had variable effects on the retention. The introduction of apiose(s) on the glucosyl of a diarylheptanoid glucoside decreased the retention time. The opposite retention behavior was observed for arylbutanoids, while the retention times of flavanols and their xylosides overlapped. Despite the long total time of elution, not all of the compounds could be resolved (Paper **II**). For example, structural isomers **29** and **30** coeluted, as did structural isomers **33** and **34**.

Online UV spectroscopy

UV spectral characteristics of the inner bark phenolics did not allow their easy preliminary identification. Inner bark phenolic compounds have an absorption maximum at a wavelength of around 280 nm (Figure 6). This is because they have the same chromophore, a benzene ring. Small alterations to the position of the wavelength maximum were observed due to different auxochromes, such as hydroxyls, methoxyls, and

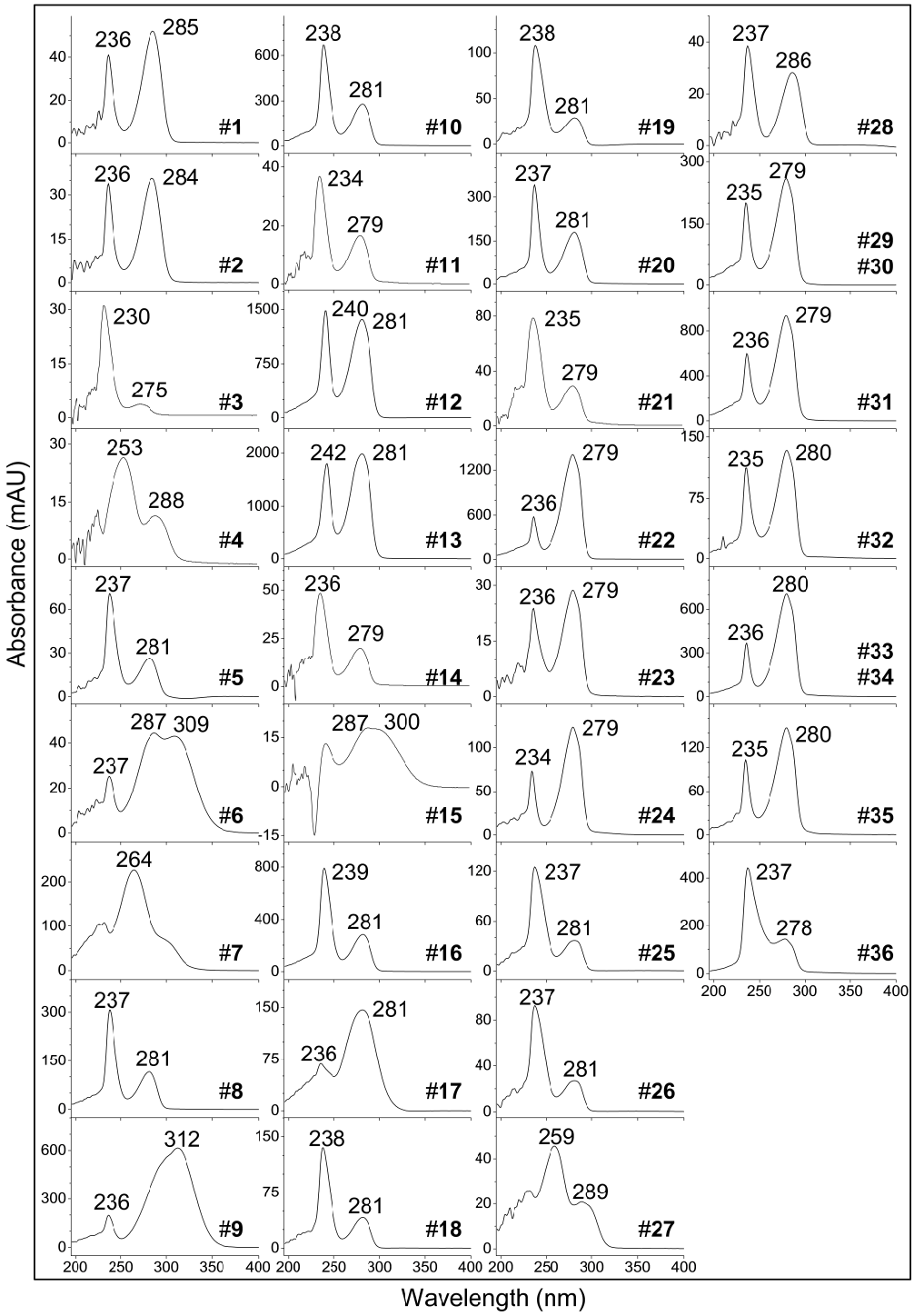

Figure 6. UV spectra of phenolic compounds in the inner bark of silver birch. Spectra were obtained by HPLC-DAD with 1% aqueous formic acid and acetonitrile as eluents. The numbers refer to compounds listed in Table 3.

sugar groups (Waterman and Mole 1994), due to changes in solvent composition during HPLC separation (Santos-Buelga et al. 2003), and interference of partly coeluting compounds. Only compounds **4**, **6**, **7**, **9**, **15**, and **27** had distinct UV spectra. Compounds **4**, **7**, **9**, **15**, and **27** were derivatives of hydroxycinnamic and hydroxyl benzoic acids. Cinnamic and phenolic acids usually have two absorption bands at 250−330 nm (Waterman and Mole 1994) due to the larger chromophores via conjugated double bonds. Similarly compound **6** has a different chromophore resulting from the presence of a carbonyl group and therefore it has a distinct UV spectrum (Figure 6).

Online HR-ESI-MS analysis

The crude extract and some of the fractions were subjected to HPLC-HR-ESI-MS analysis. Accurate mass values were obtained online by utilizing a HR TOF analyzer and ESI source. For example, the accurate mass value measured online for compound **17** from a crude extract was 342.1303, while the accurate mass for isolated compound **17** measured by FAB-sector-MS was 342.1314. The calculated accurate mass of **17** is 342.1315 and the errors of different methods were –3.5 and –0.3 ppm, respectively. The most intensive signal in the mass spectra of studied phenolics was the deprotonated molecule $[M–H]^-$, except for the compound **27** and PCs higher than trimers. In addition, clustered, multiply charged, and/or fragment ions (e.g. $[2M–H]^-$, $[M–2H]^{2–}$, and $[M–gly–H]^-$, respectively) were detected, except in spectra of compounds **1** and **2**. Fragment ions most often involved the cleavage of the glycosyl unit. The loss of 162.05 Da corresponded to the cleavage of the glucosyl moiety in compounds **7** and **27,** and the cleavage of an undefined hexose in compounds **4** and **15**. The loss of 132.04 Da corresponded to the cleavage of a xylosyl or apiosyl moiety in compounds **12, 29** and **30**, and **11**. For compounds **6** and **31**, a loss of 180.06 Da was observed and it corresponded to the loss of glucose and water. For PC dimers and PC dimer xylosides, fragmentations through retro-Diels−Alder (RDA) mechanism, heterocyclic ring fission (HRF), and quinone methide (QM) cleavage were observed (Figure 4; Gu et al. 2003; Karonen 2007). RDA fragmentation provided ions at *m/z* 425.1 and *m/z* 407.1 for PC dimers and at *m/z* 557.1 for PC dimer xylosides without subsequent water elimination. A product of HRF fragmentation was observed at *m/z* 451.1 for PC dimers and at *m/z* 583.1 for PC dimer xylosides. QM cleavage produced fragments ions at *m/z* 287.1 and *m/z* 289.1 for both PC dimers and PC dimer xylosides (after the fragmentation of xylose). However, the fragment signals of PC dimer xylosides were very weak and they partly overlapped with PC aglycones. Online ESI-MS did not reveal whether the attachment site of the xylose unit was on the terminal or extension unit. PC trimers fragmented through QM cleavage to ions at *m/z* 577.1 and 287.1 (cleavage of the upper interflavanoid bond) and ions at *m/z* 575.1 and 289.1 (cleavage of the lower

interflavanoid bond). Other fragment ions of trimers were very weak or absent. It is likely that more fragmentations could be observed for PC trimers and PC dimer xylosides, if they were isolated and analyzed separately by the direct infusion ESI-TOF-MS (see e.g. the fragmentation of PC dimer xyloside in Paper **V**).

5.2.2. Hydrophilic interaction HPLC-ESI-MS analysis

Elution of PAs

PA oligomers and polymers higher than tetramers exist as a chromatographically unseparated hump in the RP-HPLC chromatograms of plant extracts (Santos-Buelga et al. 2003). Traditionally, the oligomeric PAs have been analyzed by normal-phase (NP) HPLC. A HILIC-MS method was developed as an alternative to NP chromatography in order to enhance the analysis of PAs. The fraction eluted with 50% aqueous acetone on Sephadex LH-20 column chromatography was first used as a PA-rich fraction in HILIC-ESI-TOF-MS analyses. At first acetonitrile and aqueous methanol were tested as eluents according to Kelm et al. (2006). However, aqueous methanol was not able to elute higher oligo- and polymers and therefore it was replaced by more polar solvent; water. The linear elution was started with acetonitrile/0.1% aqueous formic acid (95:5). The concentration of 0.1% aqueous formic acid was increased to nearly 100% but all of the PAs did not elute out of the column in a reasonable time. Therefore, the gradient was performed to obtain acetonitrile/0.1% aqueous formic acid (35:65) in 40 min. Following this, the linear gradient was turned towards the starting point to reach acetonitrile/0.1% aqueous formic acid (95:5) in 5 min. In this way, PAs with high DP were forced to elute out of the column as a small hump at the end of the chromatogram (Figure 7a).

Characterization of PC aglycones

The PAs were identified based on their singly ($[M–H]^-$) or multiply charged molecular ions ($[M–2H]^{2-}$, $[M–3H]^{3-}$, or $[M–4H]^{4-}$). The fact that PAs form multiply charged ions in ESI is highly advantageous, since multiply charged ions expand the analyzable mass range. To properly exploit this phenomenon, it is very important to use a HR mass analyzer, such as TOF, which can resolve PAs with close mass-to-charge ratio (Gu et al. 2003). For example, B-type PCs with the DP of 8, 12, and 16 form doubly, triply, and fourfold charged ions, respectively, and these ions exist at *m/z* 1152.25, 1151.92, and 1151.75 (calculated values, Figure 8). Further, A-type PCs with one additional ether bond with the DP of 8, 12, and 16 form doubly, triply and fourfold charged ions, respectively, at *m/z* 1151.25. All of these ions can be resolved with HR mass analyzer due to the isotopic patterns and accurate mass values obtained.

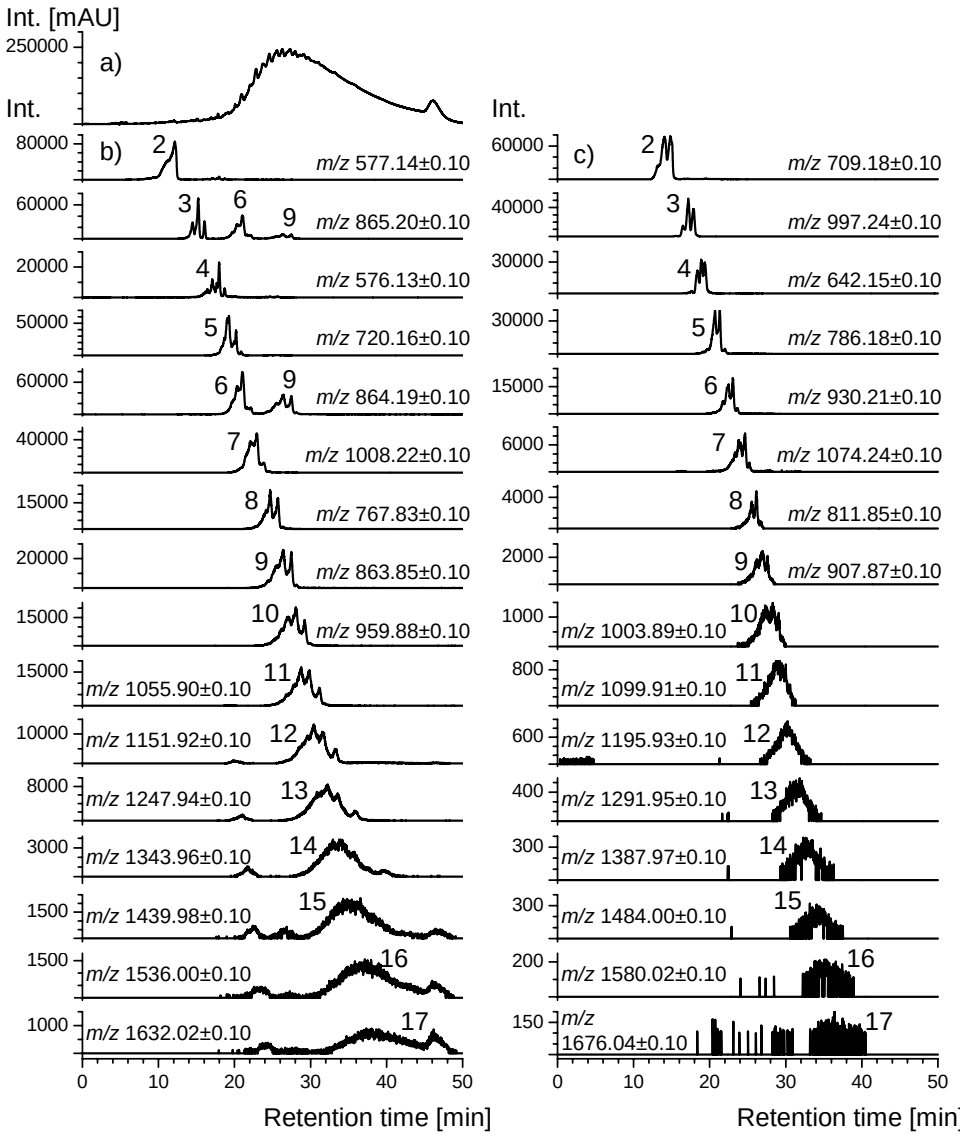

Figure 7. a) A UV-Vis chromatogram of a procyanidin (PC) −rich fraction at 190−950 nm. b) Extracted ion chromatograms of PC aglycones, obtained from the PC-rich fraction. c) Extracted ion chromatograms of PC monoxylosides, obtained from three different PC fractions. The labels 2–17 indicate the degree of polymerization. The isotopic signals of higher PC aglycones are seen in the extracted ion chromatograms of *m/z* 865.20 ± 0.10 for trimers and *m/z* 864.19 ± 0.10 for hexamers.

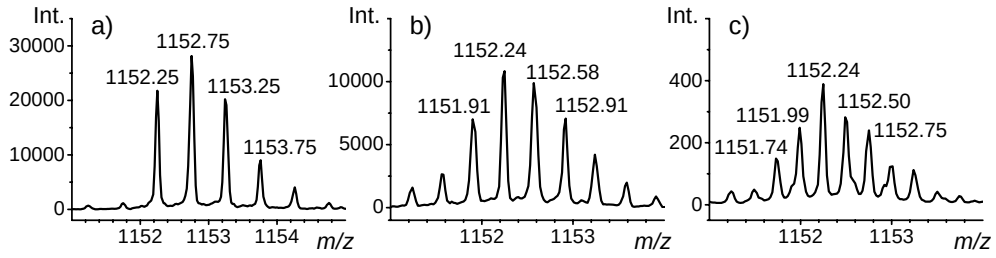

Figure 8. Isotopic patterns of a) $[M–2H]^{2–}$, b) $[M–3H]^{3–}$, and c) $[M–4H]^{4–}$ ions of procyanidin octamer, dodecamer, and hexadecamer, respectively. Spectra were obtained from a procyanidin-rich fraction after separation in a hydrophilic interaction column.

The PA-rich fractions eluted with 40−95% aqueous ethanol and 50 and 70% aqueous acetone on Sephadex LH-20 column chromatography were subjected to HILIC-ESI-TOF-MS analysis. The fractions contained mainly PC aglycones. The dominant ions detected for PC dimers and trimers were singly charged, those for PC tetra- to octamers were doubly charged, and those for PC nonamers to octadecamers were triply charged. Fourfold charged ions were observed for the rest of the polymers. PC aglycones were detected up to the DP of 22 and they were all B-type PCs. Although the mass spectra of PCs with high DP consistently contained small amounts of $[M–H]^–$ ions with a mass difference of 2 Da, they were thought to be due to the QM cleavage of even longer overlapping polymers (Figure 4), rather than ions of corresponding A-type PCs.

The HILIC method provided similar retention behavior for PCs as NP chromatography: the PCs eluted according to the increasing DP (Figure 7a/b). Individual peaks of PCs were detected up to dodecamers. PCs higher than dodecamers eluted still in the order of increasing DP but they were overlapping each other. PCs higher than hexadecamers eluted in the small hump in the end of chromatogram. Due to the enhanced separation, higher PC concentration, and enhanced ionization (a result of high acetonitrile content), the fragmentations of PC oligomers were better observed than in RP-ESI-MS analysis. For example, PC trimers produced singly charged ions through the RDA fragmentation at *m/z* 713.2 and 695.1, QM cleavage at *m/z* 287.1 and 577.1 (the cleavage of the upper bond), 289.1 and 575.1 (the cleavage of the lower bond), and HRF at *m/z* 739.2. RDA fragments were detected for PC oligomers up to the DP of 8, and HRF fragments from dimers to pentamers (Table 4). The small fragments of QM cleavage, such as 287.1, 289.1, 575.1, and 577.1, were constantly seen in the backgrounds of mass spectra (Karonen et al. 2004b). However, the fragmentation was minor and the intensities of the fragments decreased with the increase in DP as previously reported by Gu et al. (2003).

Table 4. Observed ions of procyanidins with different degree of polymerization by HILIC-ESI-TOF-MS

DP	Molecular ions [*m/z* (charge)]	RDA fragment ions [*m/z* (charge)]	QM fragment ions [*m/z* (charge)]	HRF fragment ions [*m/z* (charge)]
2	577.13 (−1)	425.08 (–1), 407.08 (–1)	287.06 (–1), 289.07 (–1)	451.10 (–1)
3	865.19 (–1), 432.09 (–2)	356.07 (–2), 347.07 (–2)	287.06 (–1), 577.13 (–1), 289.07 (–1), 575.12 (–1)	739.17 (–1)
4	576.13 (–2), 1153.25 (–1)	500.10 (–2), 491.10 (–2)	287.06 (–1), 865.18 w (–1), 289.07 (–1), 863.18 (–1)	513.11 (–2)
5	720.16 (–2), 1441.32 (–1)	644.13 (–2), 635.13 (–2)	287.06 (–1), 576.13 w (–2), 289.07 (–1), 575.12 (–2)	657.15 w (–2)
6	864.19 (–2), 1729.38 (–1)	788.17 (–2)	287.06 (–1), 720.16 w (–2), 289.07 (–1), 719.15 (–2)	nd
7	1008.22 (–2), 671.81 (–3)	621.13 (–3)	287.06 w (–1), 864.19 w (–2), 289.07 (–1), 863.18 (–2)	nd
8	767.83 (–3), 1152.25 (–2)	717.15 (–3)	287.06 w (–1), 1008.22 w (–2), 289.07 (–1), 1007.21 (–2)	nd

RDA = retro-Diels−Alder, QM = quinone methide, HRF = heterocyclic ring fission, w = weak, nd = not detected

Characterization of PC glycosides

In addition to PC aglycones, PC-rich fractions contained glycosylated PCs: a series of PC glycosides containing 132.04 Da higher molecular mass than the corresponding PC aglycones. Based on the presence of the PC dimer xylopyranoside and a previously reported catechin xylopyranoside in the birch bark (Šmite et al. 1995), the oligomeric and polymeric PC pentosides were thought to be larger analogues of these. PC xylosides with the DP of 3 or higher were identified based on MS data. The PC xylosides were observed from dimers to heptadecamers and they were all monoxylosides. PC xylosides eluted in the order of increasing degree of polymerization with similar retention times as the corresponding aglycones (Figure 7). The dominant ions detected for PC xyloside dimers and trimers were singly charged, for PC tetra- to heptamers doubly charged, and for PC octamers to heptadecamers triply charged. Fourfold charged ions were not observed. Fragmentation was observed only for the dimers. The lack of fragmentation of the other PC oligomers was probably due to the low concentration of PC xylosides in comparison to the PC aglycones. PC xylosides were found in the same fractions as PC aglycones. However, their concentration decreased in the very last fractions compared with PC aglycones.

5.2.3. NMR spectroscopy

Altogether 20 compounds and 2 compound pairs were isolated. These 24 compounds were characterized by NMR (Tables 5−13). The assignment of proton and carbon signals was achieved by a set of NMR experiments, such as DQF-COSY, NOESY, 1D-TOCSY, HSQC, and HMBC. The exchanging hydroxyl protons were not detected in any sample due to the CD_3OD solvent.

The ^{1}H NMR spectrum of **1** displayed three signals in the aromatic region (δ 6.60−6.81), six signals in the aliphatic region (δ 3.40−4.80) (including one under the solvent signal at δ 4.80), and one threefold singlet at δ 3.83 corresponding to a methoxy group (Table 5, Figure 9). The coupling constants of the aromatic signals indicated one *ortho*-coupled (*J* = 8.6 Hz, H5), one meta-coupled (*J* = 2.7 Hz, H2), and one *meta*- and *ortho*-coupled (*J* = 2.7 and 8.6 Hz, H6) proton. The signals in the aliphatic region belonged to one spin system, i.e. hexose sugar, which was easily recognized in the 1D-TOCSY and COSY spectra. In addition, 1D-TOCSY spectrum revealed the anomeric proton signal (δ 4.80, $H1_{glc}$) under the solvent resonance. The coupling constant of the anomeric proton (*J* = 7.6 Hz) and other vicinal protons of the pyranose ring (*J* = 8.5−9.2 Hz) indicated diaxial couplings for these protons. Therefore, the aliphatic signals were determined to arise from the β-glucopyranose unit. The ^{13}C NMR spectrum of **1** showed 13 signals. All non-quaternary carbons were assigned from HSQC correlations. The methoxy protons (δ 3.83) had an HMBC correlation to an aromatic carbon at δ 149.2. This carbon was the only one of the three quaternary carbons that did not have an HMBC correlation from H6, and was therefore assigned to C3. The anomeric proton of the β-glucopyranose unit (δ 4.80) had an HMBC correlation to an aromatic carbon at δ 152.5. Further, this carbon was assigned to C1 due to the NOESY correlation between the anomeric proton and the aromatic protons at δ 6.60 and 6.81 (H6 and H2, respectively).

Compound **2** was a regioisomer of **1** and the assignment of its proton and carbon signals was similar to that of **1** (Table 5, Figure 9). Compounds **1** and **2** were established as tachioside and isotachioside. The structure of **7** was very similar to **1** and **2**. The difference was that in **7**, the benzene ring contained two chemically equivalent methoxyl groups and one carboxyl group and the β-glucopyranosyl unit as substituents. The assignment of the locations of the substituents was straightforward with the aid of HMBC and compound **7** was identified as syringic acid 4-β-glucoside (Table 5, Figure 9).

Table 5. ^{1}H and ^{13}C NMR data for compounds **1**, **2**, and **7** in CD_3OD at 25 °C

	Tachioside (**1**)		Isotachioside (**2**)		Syringic acid 4-β-glucoside (**7**)	
Pos.	^{1}H (multip.; *J*/Hz)	^{13}C	^{1}H (multip.; *J*/Hz)	^{13}C	^{1}H (multip.; *J*/Hz)	^{13}C
1	-	152.5	-	141.1	-	127.7
2	6.81 (d; 2.7)	103.8	-	152.0	7.38 (s br)	108.4
3	-	149.2	6.47 (d; 2.8)	101.8	-	153.7
4	-	142.5	-	154.9	-	139.4
5	6.74 (d; 8.6)	116.1	6.30 (dd; 2.8, 8.7)	107.6	-	153.7
6	6.60 (dd; 2.7, 8.6)	109.9	7.02 (d; 8.7)	120.5	7.38 (s br)	108.4
O$\underline{C}H_3$[a]	3.83 (s)	56.6	3.81 (s)	56.5	3.92 (s)	57.2
4-$\underline{C}$OOH					-	169.9
glc1	4.80 (d; 7.6)	103.4	4.70 (d; 7.7)	104.3	5.10 (d; 7.5)	104.1
glc2	3.46 [b]	74.6	3.44 [c]	75.1	3.56 (dd br; 7.5, 8.8)	75.1
glc3	3.50 (dd; 8.5, 9.2)	77.5	3.43 [c]	77.8	3.51 [d]	77.2
glc4	3.40 (dd; 8.8, 9.2)	71.2	3.38 (t br; 9.1)	71.4	3.50 [d]	70.6
glc5	3.45 (m) [b]	77.8	3.33 (m)	78.1	3.29 (m)	77.8
glc6	3.71 (dd; 5.8, –12.2)	62.2	3.69 (dd; 5.4, –12.0)	62.6	3.72 (dd; 4.5, –12.2)	61.7
	3.90 (dd; 2.1, –12.2)		3.86 (dd; 2.2, –12.0)		3.78 (dd; 2.0, –12.2)	

[a] 3-OCH_3 for **1**, 2-OCH_3 for **2**, and 2-OCH_3 and 6-OCH_3 for **7**, [b–d] signals with the same superscript are overlapping

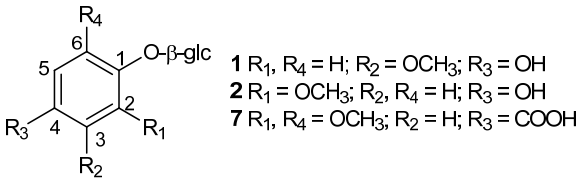

Figure 9. The structures and numbering of compounds **1**, **2**, and **7**.

The proton and carbon signals of **6** were assigned as described in Paper **III**. Compound **6** was identified as 3-β-glucopyranosyloxy-2-hydroxy-1-(4-hydroxy-3-methoxyphenyl)-propan-1-one (Table 6, Figure 10). Compound **9** contained a phenyl propenoic acid moiety which was assigned as *p*-coumaric acid. The coumaric acid existed in a *trans* form as indicated by the large coupling constant (J = 15.9 Hz) between the two protons of the propenoic tail (Table 6, Figure 10). The coumaric acid was conjugated with a quinic acid. The relative stereochemistry of the quinic acid moiety was deducted from the coupling constants of the vicinal protons (see e.g. Pauli et al 1999; Clifford 2003). Finally, the HMBC correlation from the proton at δ 5.34 ($H3_q$) to the carbon at δ 169.0 (H1) indicated the conjugation site and the compound was identified as *trans*-3-*O*-*p*-coumaroyl quinic acid.

Compounds **13** and **20** showed both 15 ^{13}C NMR and 9 ^{1}H NMR resonances. The compounds were assigned to flavanol-type structures (Table 7, Figure 11). The main distinctive NMR spectral feature of these stereoisomers was the coupling constant between protons H2 and H3. In compound **13**, these protons were assigned to be *trans* to each other

Table 6. ^{1}H and ^{13}C NMR data for compounds **6** and **9** in CD_3OD at 25 °C

	6			**9**	
Pos.	^{1}H (multip.; *J*/Hz)	^{13}C	Pos.	^{1}H (multip.; *J*/Hz)	^{13}C
1	-	197.5	1	-	169.0
2	5.30 (dd; 3.7, 5.0)	72.2	2	6.37 (d; 15.9)	115.9
3	3.94 (dd; 3.7, –11.0)	72.1	3	7.65 (d; 15.9)	146.4
	4.11 (dd; 5.0, –11.0)		1’	-	127.4
1’	-	126.7	2’	7.46 (d; 8.6)	131.1
2’	7.57 (d; 2.0)	111.1	3’	6.80 (d; 8.6)	116.8
3’	-	147.8	4’	-	161.1
4’	-	152.4	5’	6.80 (d; 8.6)	116.8
5’	6.88 (d; 8.3)	114.5	6’	7.46 (d; 8.6)	131.1
6’	7.61 (dd; 2.0, 8.3)	123.8	q1	-	75.5
3’-	3.91 (s)	55.1	q2	2.16 [b]	36.8
glc1	4.30 (d; 7.8)	103.5		2.18 [b]	
glc2	3.17 (dd; 7.8, 9.3)	73.6	q3	5.36 (m)	73.0
glc3	3.34 (t; 9.3)	76.4	q4	3.67 (dd; 3.2, 8.1)	74.6
glc4	3.25 [a]	70.1	q5	4.13 (m)	68.6
glc5	3.25 (m) [a]	76.6	q6	1.95 (dd; 9.3, –13.6)	41.1
glc6	3.61 (m)	61.2		2.12 (dd; 3.8, –13.6)	
	3.81 (m)		q7	-	178.9

[a, b] signals with the same superscript are overlapping

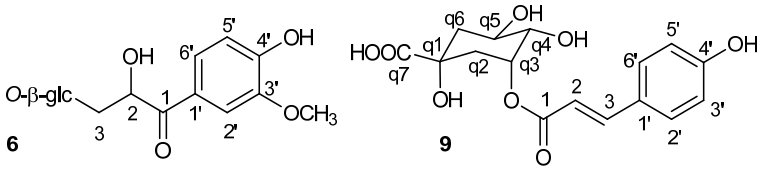

Figure 10. The structures and numbering of compounds **6** and **9**.

according to rather large coupling constant at H2 (*J* = 7.4 Hz), while in compound **20**, the protons were *cis*-orientated indicated by the unresolved coupling, i.e. a broad singlet, at H2. Compounds **13** and **20** were identified as catechin and epicatechin, respectively. The ^{1}H NMR spectrum of compound **12** contained a similar resonance set as compound **13** along with six additional aliphatic signals, of which one was a typical anomeric signal of a sugar moiety (Table 7, Figure 11). The sugar moiety was assigned as β-xylopyranose according to the large coupling constants between the methine protons. An HMBC correlation from the anomeric proton (δ 4.77) to the C7 at δ 158.4 revealed the attachment site of the xylopyranose unit to C7. The glycosylation site was also indicated by the change of the chemical shifts of H6 and H8 towards the higher frequency compared with the corresponding chemical shifts of the compound **13**.

Table 7. ^{1}H and ^{13}C NMR data for compounds **12**, **13**, and **20** in CD_3OD at 25 °C

	Catechin xylopyranoside (**12**)		Catechin (**13**)		Epicatechin (**20**)	
Pos.	^{1}H (multip.; *J*/Hz)	^{13}C	^{1}H (multip.; *J*/Hz)	^{13}C	^{1}H (multip.; *J*/Hz)	^{13}C
2	4.60 (d; 7.4)	82.8	4.57 (d; 7.4)	82.8	4.81 (s br)	79.9
3	4.00 (m)	68.5	3.98 (m)	68.8	4.17 (m)	67.5
4	2.54 (dd; 8.0, –16.4)	28.4	2.51 (dd; 8.1, –16.2)	28.5	2.73 (dd; 2.6, –16.7)	29.3
	2.86 (dd; 5.4, –16.4)		2.85 (dd; 5.5, –16.2)		2.86 (dd; 4.4, –16.7)	
4a	-	103.7	-	100.9	-	100.1
5	-	157.5	-	157.7 [d]	-	158.0 [f]
6	6.17 (d; 2.2)	97.4	5.93 (d; 2.2) [c]	96.3	5.93 (d; 2.2) [e]	96.4 [g]
7	-	158.4	-	157.5 [d]	-	157.7
8	6.12 (d; 2.2)	96.9	5.86 (d; 2.2) [c]	95.5	5.91 (d; 2.2) [e]	95.9 [g]
8a	-	156.8	-	156.9	-	157.4 [f]
1’	-	132.0	-	132.2	-	132.3
2’	6.84 (d; 2.0)	115.2	6.84 (d; 1.8) [c]	115.3	6.97 (d; 1.7)	115.4
3’	-	146.2	-	146.2	-	146.0
4’	-	146.2	-	146.2	-	145.8
5’	6.77 (d; 8.1)	116.1	6.77 (d; 8.1)	116.1	6.75 (d; 8.3)	115.9
6’	6.72 (dd; 2.0, 8.1)	120.0	6.72 (dd; 1.8, 8.1) [c]	120.1	6.79 (dd; 1.7, 8.3)	119.5
xyl1	4.77 (d; 7.4)	102.8				
xyl2	3.40 [a]	74.6				
xyl3	3.41 [a]	77.7				
xyl4	3.56 (m)	71.0				
xyl5	3.31 [b]	66.8				
	3.90 (dd; 5.4, –11.5)					

[a] overlapping signals, [b] overlapping with the solvent signal, [c] broad signals, therefore the small coupling constants are estimations, [d–g] values with the same superscript may be vice versa

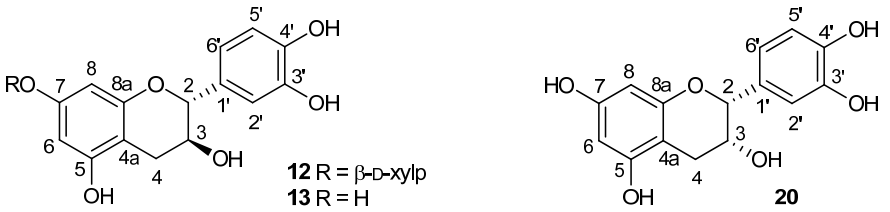

Figure 11. The structures and numbering of compounds **12**, **13**, and **20**.

The ^{1}H and ^{13}C NMR spectra of **8** showed similarities to the spectra of flavanols **13** and **20**. However, the ^{13}C NMR spectrum of **8** contained two times the number of resonances as compounds **13** and **20** and the ^{1}H NMR spectrum of **8** had 2n−2 resonances (n = number of resonances of compounds **13** and **20**), indicating that **8** was a dimer of flavanol units (Table 8, Figure 12). In addition, all resonances occurred as pairs with an intensity ratio of 2:1, indicating the existence two rotameric forms (Table 8). For the assignment of the ^{1}H and ^{13}C NMR resonances, it was easiest to start from the two protons of the C4 terminal unit. The aliphatic signals of the pyrane ring of the terminal unit were assigned by COSY and the assignment proceeded through the whole structure with the aid of HMBC and HSQC correlations and compound **8** was identified as a PC dimer consisting of two

Table 8. ^{1}H and ^{13}C NMR data for compounds **8** and **11** in CD_3OD at 25 °C

	8: major rotamer		**8**: minor rotamer		**11**: major rotamer [i]		**11**: minor rotamer [i]	
Pos.	^{1}H (multip.; *J*/Hz)	^{13}C	^{1}H (multip.; *J*/Hz)	^{13}C	^{1}H (multip.; *J*/Hz)	^{13}C	^{1}H (multip.; *J*/Hz)	^{13}C
ext 2	4.26 (d; 9.6)	83.9	4.36 [a]	84.1	4.31 (d; 9.7)	83.8	4.36 (d; 10.0)	84.3
ext 3	4.35 (dd; 7.9, 9.6) [a]	73.7	4.52 [c]	73.6	4.08 (dd; 8.7, 9.7)	74.0	4.44 (dd; 8.2, 10.0)	74.2
ext 4	4.41 (d; 7.9)	38.6	4.51 [c]	38.5	4.59 (d; 8.7)	38.6	4.58 (d; 8.2)	38.6
ext 4a	-	107.2	-	107.1	-	107.0	-	108.4
ext 5	-	157.1 [d]	-	157.3−157.4 [g]	-	157.1	-	158.0
ext 6	5.89 (d; 2.5) [b]	97.3 [e]	5.84 (d; 2.4) [f]	97.5 [h]	5.87 (d; 2.4)	97.5	5.83 (d; 2.4)	97.8
ext 7	-	157.1	-	157.3−157.4	-	157.1	-	157.7
ext 8	5.79 (d; 2.5) [b]	96.8 [e]	5.81 (d; 2.4) [f]	96.2 [h]	5.74 (d; 2.4)	96.9	5.88 (d; 2.4)	95.5
ext 8a	-	158.6 [d]	-	158.6 [g]	-	158.6	-	158.7
ext 1’	-	132.6	-	132.4	-	132.4	-	132.3
ext 2’	6.74 (d; 2.0)	116.3	6.96 (d; 2.0)	115.9	6.74 (d; 2.0)	116.3	6.96 (d; 2.3)	116.3
ext 3’	-	145.5−146.1	-	145.5−146.4	-	145.4−146.5	-	145.4−146.5
ext 4’	-	145.5−146.1	-	145.5−146.4	-	145.4−146.5	-	145.4−146.5
ext 5’	6.67−6.68 (d; 8.2)	116.1−116.3	6.76−6.77 (d; 8.1)	116.1−116.3	6.69 (d; 8.2)	116.2	6.77 (d; 7.6)	116.2
ext 6’	6.47 (dd; 2.0, 8.2)	120.6	6.82−6.83 (dd; 2.0, 8.1)	121.0	6.55 (dd; 2.0, 8.2)	120.7	6.82 (dd; 2.3, 7.6)	121.1
ter 2	4.54 (d; 7.4) [c]	82.4	4.75 (d; 7.4)	82.9	4.44 (d; 7.7)	82.7	4.73 (d; 7.6)	82.9
ter 3	3.80 (m)	68.9	4.07 (m)	68.5	3.72 (m)	69.0	4.07 (m)	68.6
ter 4	2.49 (dd; 8.1, –16.3)	28.8	2.58 (dd; 7.7, –16.2)	28.5	2.50 (dd; 8.5, –16.5)	29.2	2.60 (dd; 8.0, –16.4)	28.7
	2.76 (dd; 5.6, –16.3)		2.82 (dd; 5.5, –16.2)		2.81 (dd; 5.6, –16.5)		2.86 (dd; 5.4, –16.4)	
ter 4a	-	102.2	-	100.5	-	105.1	-	102.9
ter 5	-	155.6	-	155.8	-	155.8	-	155.5
ter 6	6.07 (s)	96.0	5.94 (s)	97.5	6.36 (s)	97.2	6.14 (s)	97.2
ter 7	-	155.6	-	155.8	-	157.0	-	155.0
ter 8	-	108.2	-	108.3	-	112.4	-	111.2
ter 8a	-	154.9	-	155.0	-	154.6	-	155.5
ter 1’	-	131.8	-	132.1	-	131.7	-	132.3
ter 2’	6.59 (d; 2.0)	115.7	6.96 (d; 2.0)	115.3	6.54 (d; 1.9)	115.7	6.96 (d; 2.2)	115.3
ter 3’	-	145.5−146.1	-	145.5−146.4	-	145.4−146.5	-	145.4−146.5
ter 4'	-	145.5−146.1	-	145.5−146.4	-	145.4−146.5	-	145.4−146.5
ter 5'	6.67−6.68 (d; 8.2)	116.1−116.3	6.76−6.77 (d; 8.1)	116.1−116.3	6.68 (d; 8.2)	116.3	6.76 (d; 7.4)	116.2
ter 6'	6.25 (dd; 2.0, 8.2)	119.9	6.82−6.83 (dd; 2.0, 8.1)	120.2	6.20 (dd; 1.9, 8.2)	119.9	6.83 (dd; 2.2, 7.4)	120.3

[a, c] signals with same superscript are overlapping, [b, d−h] values with same superscript may be vice versa, [i] only the data for the aglycone of **11** is presented here, for full characterization see Paper **V**

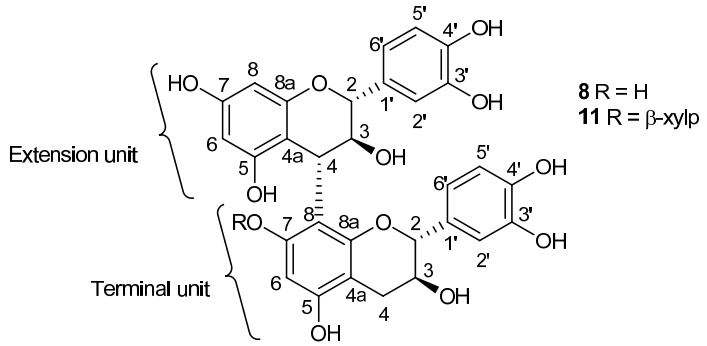

Figure 12. The structures and numbering of compounds **8** and **11**.

catechin units linked by a 4→8 carbon−carbon bond. The assignment of proton and carbon signals of both rotamers of **11** is described in Paper **V** where **11** was identified as xylopyranoside of **8** (Table 8, Figure 12).

Aromatic hydrogens H6 and H8 of PAs and flavonoids can undergo hydrogen–deuterium exchange reactions when dissolved in protic solvents such as CD_3OD or D_2O. This is a result of a keto−enol equilibrium that occurs between hydrogens at position 6/8 and phenolic ODs (Tarascou et al. 2006). In this study, hydrogen–deuterium exchange was observed through the partial or total disappearance of the proton resonances at positions 6/8 for catechin (**13**), epicatechin (**20**), and PC dimer (**8**) after a long term storage. The exchange was hindered in the catechin xylopyranoside (**12**) and in the terminal unit of PC dimer xylopyranoside (**11**), due to the inhibition of keto−enol tautomerism by the xylose substituent.

Compounds **17**, **22**, **24**, and **27** were characterized as arylbutanoid glucosides. The ^{1}H NMR spectrum of compound **22** showed a *para*-substituted aromatic ring (twofold doublets at δ 6.67 and δ 7.03), and one butyl and β-glucopyranosyl substituent (nine aliphatic resonances at δ 1.28−4.45, which were assigned by 1D-TOCSY) (Table 9, Figure 13). The substituents were located with the aid of HMBC correlations and compound **22** was characterized as rhododendrin. Compounds **17**, **24**, and **27** were derivatives of rhododendrin. Compound **17** was identified as the oxidation product of rhododendrin and compound **27** as the conjugate of rhododendrin and glucovanillin. Their NMR assignments are presented in Paper **I**. Compound **24** was identified as an apiose conjugate of rhododendrin (Table 9, Figure 13).

Table 9. ^{1}H and ^{13}C NMR data for compounds **17**, **22**, **24**, and **27** in CD_3OD at 25 °C

	17		Rhododendrin (**22**)		Rhododendrin apioside (**24**)		**27** [c]	
Pos.	^{1}H (multip.; *J*/Hz)	^{13}C	^{1}H (multip.; *J*/Hz)	^{13}C	^{1}H (multip.; *J*/Hz)	^{13}C	^{1}H (multip.; *J*/Hz)	^{13}C
1	1.28 (d; 6.4)	20.7	1.20 (d; 6.2)	19.9	1.18 (d; 6.0)	20.2	1.17 (d; 6.2)	20.3
2	4.45 (m; 6.1, 6.3, 6.4)	73.5	3.90 (m)	75.1	3.84 (m)	75.3	3.81 (m; 4.2, 6.2, 7.8)	75.6
3	2.93 (dd; 6.3, –16.0)	47.2	1.68 (m)	40.6	1.67 (m)	40.7	1.64 (m; 4.2, 6.8, 9.6, –13.9)	40.6
	3.50 (dd; 6.1, –16.0)		1.86 (m)		1.84 (m)		1.76 (m; 5.3, 7.8, 9.5, –13.9)	
4	-	199.7	2.61 (m)	31.8	2.62 (m)	31.9	2.47 (m; 6.8, 9.5, –13.9)	31.8
							2.55 (m; 5.3, 9.6, –13.9)	
1’	-	130.5	-	134.7	-	134.8	-	134.6
2’	7.91 (m; 8.8)	132.2	7.03 (dd; 1.9, 8.5)	130.4	7.04 (m; 8.1)	130.5	6.91 (m; 8.4)	130.4
3’	6.84 (m; 8.8)	116.3	6.67 (dd; 1.9, 8.5)	116.0	6.69 (m; 8.1)	116.1	6.58 (m; 8.4)	116.0
4’	-	164.0	-	156.2	-	156.2	-	156.2
5’	6.84 (m; 8.8)	116.3	6.67 (dd; 1.9, 8.5)	116.0	6.69 (m; 8.1)	116.1	6.58 (m; 8.4)	116.0
6’	7.91 (m; 8.8)	132.2	7.03 (dd; 1.9, 8.5)	130.4	7.04 (m; 8.1)	130.5	6.91 (m; 8.4)	130.4
glc1	4.37 (d; 7.8)	103.0	4.33 (d; 7.8)	102.3	4.31 (d; 7.9)	102.4	4.36 (d; 7.8)	102.7
glc2	3.10 (dd; 7.8, 9.3)	75.1	3.18 (dd; 7.8, 8.8)	75.1	3.18 (t; 7.9)	75.1	3.22 (dd; 7.8, 9.3)	75.2
glc3	3.32 (dd; 9.0, 9.3)	78.1	3.36 (t; 8.8)	78.2	3.36 [b]	76.7	3.40 (dd; 9.1, 9.3)	78.1
glc4	3.24 (dd; 9.0, 9.9)	71.6	3.32 [a]	71.7	3.35 [b]	71.6	3.42 (dd;9.1, 9.3)	72.0
glc5	3.18 (m; 2.5, 5.6, 9.9)	77.7	3.25 (m)	77.8	3.35 [b]	78.1	3.57 (m; 2.3, 6.1, 9.3)	75.3
glc6	3.56 (dd; 5.6, –12.0)	62.7	3.70 (dd; 5.5, –11.8)	62.8	3.64 (dd; 4.0, –10.9)	68.4	4.48 (dd; 6.1, –11.8)	65.1
	3.67 (dd; 2.5, –12.0)		3.87 (dd; 2.4, –11.8)		3.99 (dd br; 1.4, –10.9)		4.66 (dd; 2.3, –11.8)	
api1					5.02 (d; 1.9)	110.9		
api2					3.91 (d; 1.9)	78.0		
api3					-	80.6		
api4					3.75 (d; –9.7)	75.0		
					3.94 (d; –9.7)			
api5					3.55 (d; –11.5)	65.7		
					3.58 (d; –11.5)			

[a] overlapping with the solvent signal, [b] overlapping signals, [c] only the data for arylbutanoid glucoside part of the compound **27** is presented here, for full characterization see Paper **I**

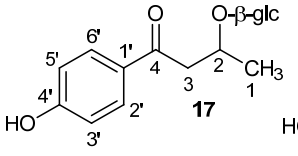

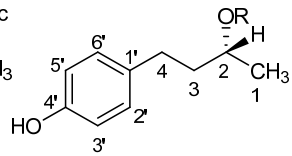

22 R = β-D-glcp
24 R = β-D-apif-(1–>6)-β-D-glcp
27 R = 4-O-β-glcp-3-methoxybenzoate-(7–>6)-β-glcp

Figure 13. The structures and numbering of compounds **17**, **22**, **24**, and **27**.

Table 10. ^{1}H and ^{13}C NMR data for compounds **25** and **26** in CD_3OD at 25 °C

	Lyoniside (**25**)		Nudiposide (**26**)	
Pos.	^{1}H (multip.; *J*/Hz)	^{13}C	^{1}H (multip.; *J*/Hz)	^{13}C
1	-	139.5	-	139.7
2	6.42 (s)	106.9	6.41 (s)	107.0
3	-	149.1	-	149.0
4	-	134.5	-	134.5
5	-	149.1	-	149.0
6	6.42 (s)	106.9	6.41 (s)	107.0
7	4.38 (d; 6.5)	43.1	4.22 (d; 7.1)	43.4
8	2.05 (m)	46.8	2.02 (m)	46.9
9	3.42 (dd; 3.9, –9.6)	71.0	3.58 (dd; 4.7, –10.2)	71.1
	3.84 (dd; 5.3, –9.6)		3.81 (dd; 4.7, –10.2)	
3-OCH_3	3.74 (s)	56.9	3.74 (s)	56.8
5-OCH_3	3.74 (s)	56.9	3.74 (s)	56.8
1’	-	126.5	-	126.4
2’	-	130.2	-	130.2
3’	-	147.7	-	147.6
4’	-	138.9	-	138.9
5’	-	148.7	-	148.7
6’	6.57 (s)	107.8	6.57 (s)	107.8
7’	2.63 (dd; 11.5, –15.0)	34.0	2.68 [a]	34.1
	2.71 (dd; 4.5, –15.0)		2.69 [a]	
8’	1.70 (m)	40.5	1.71 (m)	40.7
9’	3.55 (dd; 6.4, –10.8)	66.1	3.62 [b]	66.1
	3.65 (dd; 4.2, –10.8)		3.62 [b]	
3’-OCH_3	3.32 (s)	60.0	3.30 (s)	60.0
5’-OCH_3	3.85 (s)	56.6	3.85 (s)	56.6
xyl1	4.22 (d; 7.6)	105.6	4.09 (d; 7.6)	105.1
xyl2	3.22 (dd; 7.6; 9.0)	75.0	3.19 (dd; 7.6, 9.1)	75.0
xyl3	3.31 (t; 9.0)	78.1	3.27 (t; 9.1)	78.0
xyl4	3.47 (m)	71.3	3.49 (m)	71.3
xyl5	3.16 (dd; 10.5, –11.3)	67.0	3.13 (dd; 10.5, –11.0)	67.1
	3.83 (dd; 5.4, –11.3)		3.85 (dd; 5.3, –11.0)	

[a, b] signals with the same superscript are overlapping

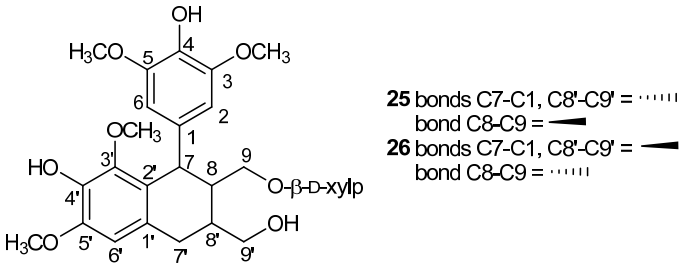

Figure 14. The structures and numbering of compounds **25** and **26**.

The relative structures of lignan glycosides, lyoniside (**25**) and nudiposide (**26**), were straightforwardly characterized from the 1D and 2D NMR data (Table 10, Figure 14). Although the aglycones of lyoniside and nudiposide are enantiomers, their D-xylosides are not and therefore small differences in the chemical shifts of anomeric protons were observed (Table 10). A comparison of the NMR data to the literature (Šmite et al. 1995) allowed compounds **25** and **26** to be identified as lyoniside and nudiposide, respectively.

All diarylheptanoids (**29**–**36**) contained two *para*-substituted aromatic rings indicated by two twofold doublet of doublets (J ~ 2 and 8.5 Hz) at ca. δ 6.7 and δ 7.0 (Tables 11–13, Figures 15 and 16). In addition, a different number of aliphatic signals was observed for these compounds according to the number of conjugated sugar moieties and state of oxidation of the heptanyl chain. All diarylheptanoids were derivatives either of platyphylloside (**31**) or aceroside VII (**35**). Platyphylloside (**31**) and its derivatives (**29**, **30**, and **36**) showed a carbonyl carbon signal (δ ~ 210) in their ^{13}C NMR spectra and were therefore easily distinguished from aceroside VII (**35**) and its conjugates (**32**, **33**, and **34**). Compounds **29** and **30**, as well as compounds **33** and **34** were isolated as pairs and analyzed with NMR as a mixture. The 1D-TOCSY experiment turned out to be a significant tool for the characterization of the sugar moieties of diarylheptanoid di- (**29**, **30**, **33**, and **34**) and trisaccharides (**32**). An example of the assignment of a diarylheptanoid structure (**34**) is given in Paper **II**.

Table 11. ^{1}H and ^{13}C NMR data for compounds **29**, **30**, and **31** in CD_3OD at 25 °C

	29		**30**		Platyphylloside (**31**)	
Pos.	^{1}H (multip.; *J*/Hz) [a]	^{13}C [a]	^{1}H (multip.; *J*/Hz) [a]	^{13}C [a]	^{1}H (multip.; *J*/Hz)	^{13}C
1	2.74 (m)	29.8	2.74 (m)	29.9	2.73 (s)	29.8
2	2.74 (m)	46.4	2.74 (m)	46.1	2.73 (s)	46.4
3	-	212.2	-	211.9	-	211.9
4	2.59 [b]	48.9 [g]	2.58 [b]	49.1 [g]	2.57 [i]	48.6
	2.81 (dd; 6.7, –16.6)		2.84 (dd; 5.8, –16.6)		2.79 (dd; 6.9, –16.6)	
5	4.13 (m)	76.4	4.20 (m)	75.0	4.16 (m)	76.2
6	1.72 (m)	38.9	1.72 (m)	38.6	1.72 (m)	38.4
	1.79 (m)		1.77 (m)		1.82 (m)	
7	2.57 (m)	31.5	2.60 (m) [b]	31.4	2.56 [i]	31.4
					2.58 [i]	
1’	-	133.3	-	133.3	-	133.2
2’	7.00−7.02 [c]	130.4	7.00−7.02 [c]	130.4	6.98−7.00 [j]	130.3
3’	6.69−6.70 [d]	116.2±0.1	6.69−6.70 [d]	116.2±0.1	6.69 [k]	116.1±0.1
4’	-	156.3±0.2	-	156.3±0.2	-	156.3±0.2
5’	6.69−6.70 [d]	116.2±0.1	6.69−6.70 [d]	116.2±0.1	6.69 [k]	116.1±0.1
6’	7.00−7.02 [c]	130.4	7.00−7.02 [c]	130.4	6.98−7.00 [j]	130.3
1’’	-	134.5	-	134.5	-	134.3
2’’	7.00−7.02 [c]	130.5	7.00−7.02 [c]	130.4	6.98−7.00 [j]	130.4
3’’	6.69−6.70 [d]	116.2±0.1	6.69−6.70 [d]	116.2±0.1	6.69 [k]	116.1±0.1
4’’	-	156.3±0.2	-	156.3±0.2	-	156.3±0.2
5’’	6.69−6.70 [d]	116.2±0.1	6.69−6.70 [d]	116.2±0.1	6.69 [k]	116.1±0.1
6’’	7.00−7.02 [c]	130.5	7.00−7.02 [c]	130.4	6.98−7.00 [j]	130.4
glc1	4.27 (d; 7.8)	103.5	4.34 (d; 7.8)	101.6	4.29 (d; 7.8)	103.4
glc2	3.16 (t; 7.8)	75.0	3.30 (dd; 7.9, 9.1)	79.4	3.16 (dd; 7.8, 8.8)	75.2
glc3	3.34−3.38 [e]	78.1	3.46 (t; 9.1)	78.4	3.37 (t; 8.8)	78
glc4	3.34−3.38 [e]	71.6	3.34 (dd; 9.1, 10.1)	71.6	3.32 [l]	71.5
glc5	3.34−3.38 [e]	76.7	3.21 (m)	78.0	3.25 (m)	77.7
glc6	3.65 (dd; 4.5, –11.0)	68.4	3.70 (dd; 5.5, –11.9)	62.7	3.71 (dd; 5.3, –11.9)	62.7
	3.99 (dd; 2.5, –11.0)		3.86 (dd; 2.2, –11.9)		3.86 (dd; 2.3, –11.9)	
api1	5.02 (d; 2.4)	110.8	5.34 (d; 1.8)	110.8		
api2	3.92 (d; 2.4)	78.0	3.95 (d; 1.8) [g]	78.0		
api3	-	80.6	-	80.6		
api4	3.74 [f]	75.0	3.74 [f]	75.2		
	3.94 [g]		4.03 (d; –9.6)			
api5	3.57 (d; –10.9)	65.7	3.61 [h]	65.9		
	3.58 (d; –10.9)		3.61 [h]			

[a] δ and *J* values were determined from a mixture of **29** and **30**, [b–k] signals with the same superscript are overlapping, [l] overlapping with the solvent signal

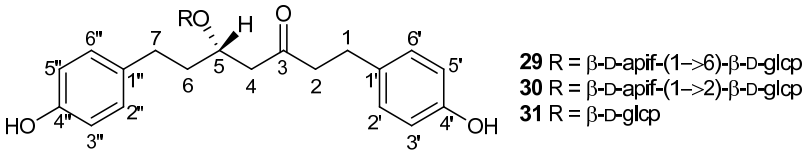

Figure 15. The structures and numbering of compounds **29**, **30**, and **31**.

Table 12. ^{1}H and ^{13}C NMR data for compounds **32**, **33**, and **34** in CD_3OD at 25 °C

	32		**33**		**34**	
Pos.	^{1}H (multip.; *J*/Hz)	^{13}C	^{1}H (multip.; *J*/Hz) [d]	^{13}C [d]	^{1}H (multip.; *J*/Hz) [d]	^{13}C [d]
1	2.59 (m)	31.7	2.59 (m)	31.7	2.59 (m)	31.6
2	1.73 (m)	38.3	1.75 (m)	38.3	1.75 (m)	38.1
3	3.65 (m)	79.4	3.66 (m)	80.0	3.70 (m)	79.2
4	1.60 (m)	35.0	1.60 (m)	35.0	1.55 (m)	34.7
5	1.35 (m)	25.8	1.36 (m)	25.7	1.36 (m)	25.7
6	1.53 (m)	33.1	1.54 (m)	33.1	1.54 (m)	33.1
7	2.50 (t; 7.5)	36.0	2.50 (m)	36.0	2.50 (m)	36.0
1’	-	134.9 [b]	-	134.8	-	134.9
2’	7.02 (dd; 2.0, 8.5)	130.6	6.96−7.02 [e]	130.4±0.2	7.01 (m)	130.5
3’	6.68 (dd; 1.7, 8.5)	116.1	6.67−6.68 [f]	116.0±0.1	6.67−6.69 (m)	116.0±0.1
4’	-	156.3	-	156.2	-	156.2
5’	6.68 (dd; 1.7, 8.5)	116.1	6.67−6.68 [f]	116.0±0.1	6.67−6.69 (m)	116.0±0.1
6’	7.02 (dd; 2.0, 8.5)	130.6	6.96−7.02 [e]	130.4±0.2	7.01 (m)	130.5
1’’	-	135.0 [b]	-	134.9	-	134.9
2’’	7.02 (dd; 2.0, 8.5)	130.4	6.96−7.02 [e]	130.4±0.2	6.97 (m)	130.4
3’’	6.68 (dd; 1.7, 8.5)	116.1	6.67−6.68 [f]	116.0±0.1	6.67−6.69 (m)	116.0±0.1
4’’	-	156.3	-	156.2	-	156.2
5’’	6.68 (dd; 1.7, 8.5)	116.1	6.67−6.68 [f]	116.0±0.1	6.67−6.69 (m)	116.0±0.1
6’’	7.02 (dd; 2.0, 8.5)	130.4	6.96−7.02 [e]	130.4±0.2	6.97 (m)	130.4
glc1	4.32 (d; 7.8)	102.0	4.27 (d; 7.8)	103.5	4.35 (d; 7.8)	101.9
glc2	3.35 [a]	79.0	3.18 (dd; 7.8, 9.0)	75.3	3.35 (dd; 7.8, 9.1)	78.9
glc3	3.46 (t; 9.1)	78.8	3.32−3.36 [g]	78.2	3.47 (t; 9.1)	78.8
glc4	3.33 [a]	71.7	3.32−3.36 [g]	71.6	3.32 (dd; 9.1, 9.7)	71.8
glc5	3.32 [a]	76.5	3.32−3.36 [g]	76.7	3.20 (ddd; 2.5, 5.6, 9.7)	77.7
glc6	3.62 (dd; 4.9, –11.1)	68.4	3.64 (dd; 4.2, –10.9)	68.4	3.69 (dd; 5.6, –11.8)	62.8
	3.97 (dd; 1.5, –11.1)		3.99 (dd; 1.5, –10.9)		3.85 (dd; 2.5, –11.8)	
api1	5.40 (d; 1.6)	110.8			5.41 (d; 1.6)	110.8
api2	3.94 (d; 1.6)	78.3			3.95 (d; 1.6)	78.3
api3	-	80.8			-	80.8
api4	3.74 (d; –9.6)	75.5			3.74 (d; –9.5)	75.4
	4.05 (d; –9.6)				4.05 (d; –9.6)	
api5	3.59 (d; –11.5)	66.3			3.59 (d; –11.4)	66.3
	3.63 (d; –11.5)				3.63 (d; –11.4)	
api’1	5.00 (d; 2.2)	110.9	5.01 (d; 2.3)	110.9		
api’2	3.90 (d; 2.2)	78.1	3.90 (d; 2.3)	78.1		
api’3	-	80.6 [c]	-	80.6		
api’4	3.72 (d; –9.6)	75.1	3.73 (d; –9.7)	75.1		
	3.91 (d; –9.6)		3.92 (d; –9.7)			
api’5	3.53 (d; –11.4)	65.8	3.53 (d; –11.5)	65.8		
	3.57 (d; –11.4)		3.57 (d; –11.5)			

[a, e–h] signals with the same superscript are overlapping, [b, c] values with the same superscript may be vice versa, [d] δ and *J* values were determined from a mixture of **33** and **34**

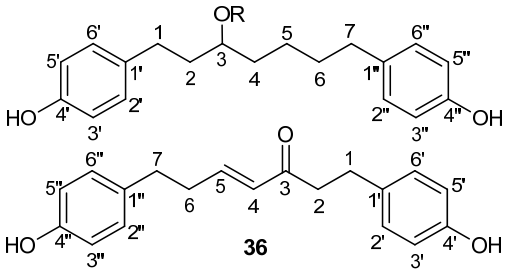

32 R = β-D-apif-(1–>2)-[β-D-apif-(1–>6)]-β-D-glcp
bond C3-O= ''''''
33 R = β-D-apif-(1–>6)-β-D-glcp
bond C3-O= ''''''
34 R = β-apif-(1–>2)-β-glcp
35 R = β-D-glcp
bond C3-O= ''''''

Figure 16. The structures and numbering of compounds **32**, **33**, **34**, and **35**.

Table 13. ^{1}H and ^{13}C NMR data for compounds **35** and **36** in CD_3OD at 25 °C

	Aceroside VII **(35)**		**36**	
Pos.	^{1}H (multip.; *J*/Hz)	^{13}C	^{1}H (multip.; *J*/Hz)	^{13}C
1	2.60 (m)	31.6	2.77 (m)	30.7
2	1.77 (m)	38.1	2.80 (m)	42.8
3	3.70 (m)	79.8	-	202.9
4	1.58 (m)	34.8	6.06 (d; 15.9)	131.7
5	1.38 (m)	25.6	6.87 (ddd; 6.9, 13.9, 15.9)	149.3
6	1.54 (m)	33.1	2.47 (m)	35.8
7	2.49 (t; 7.5)	36.0	2.67 (t; 7.5)	34.6
1’	-	134.8	-	133.1−133.2
2’	7.01 (dd; 1.9, 8.4)	130.5	6.98 (dd; 2.0, 8.2)	130.4
3’	6.67 (dd; 2.2, 8.4)	116.1	6.67−6.69 (dd; 2.0, 8.2)	116.2
4’	-	156.2	-	156.7
5’	6.67 (dd; 2.2, 8.4)	116.1	6.67−6.69 (dd; 2.0, 8.2)	116.2
6’	7.01 (dd; 1.9, 8.4)	130.5	6.98 (dd; 2.0, 8.2)	130.4
1’’	-	134.9	-	133.1−133.2
2’’	6.96 (dd; 1.9, 8.4)	130.3	6.99 (dd; 2.0, 8.2)	130.4
3’’	6.67 (dd; 2.2, 8.4)	116.1	6.67−6.69 (dd; 2.0, 8.2)	116.2
4’’	-	156.3	-	156.7
5’’	6.67 (dd; 2.2, 8.4)	116.1	6.67−6.69 (dd; 2.0, 8.2)	116.2
6’’	6.96 (dd; 1.9, 8.4)	130.3	6.99 (dd; 2.0, 8.2)	130.4
glc1	4.29 (d; 7.8)	103.4		
glc2	3.18 (dd; 7.8, 9.0)	75.4		
glc3	3.34 [h]	78.2		
glc4	3.33 [h]	71.8		
glc5	3.23 (m)	77.8		
glc6	3.70 (dd; 5.4, –11.7)	62.9		
	3.86 (dd; 2.4, –11.7)			

5.2.4. Assignment of absolute configuration

The absolute configurations of the chiral carbons of phenolics were assessed by CD spectroscopy after the relative configurations were determined by NMR spectroscopy. The signs and wavelengths of the CEs (Figure 17) were compared with the literature values of the same compound or to closely related compounds. If appropriate literature data were not available, the experimental CD spectra were compared with theoretical spectra calculated for geometry optimized structures (Chapter 4.11.). The main problem in the computational methods was the finding of all possible minimum energy conformations of the compounds,

i.e. all local minima at potential energy surface. An incomplete set of conformers in the calculation distorts the calculated CD spectrum and may lead to an incorrect conclusion about the absolute configuration. In general, the assignment of the absolute configurations of the chiral carbons of phenolic glycosides would be simplest after conversion of a compound into its aglycone and a sugar via a method like hydrolysis. However, the isolation of the hydrolysis products would demand reasonable amounts of the initial compound which sometimes is a limiting factor. Therefore, the intact molecules are discussed here.

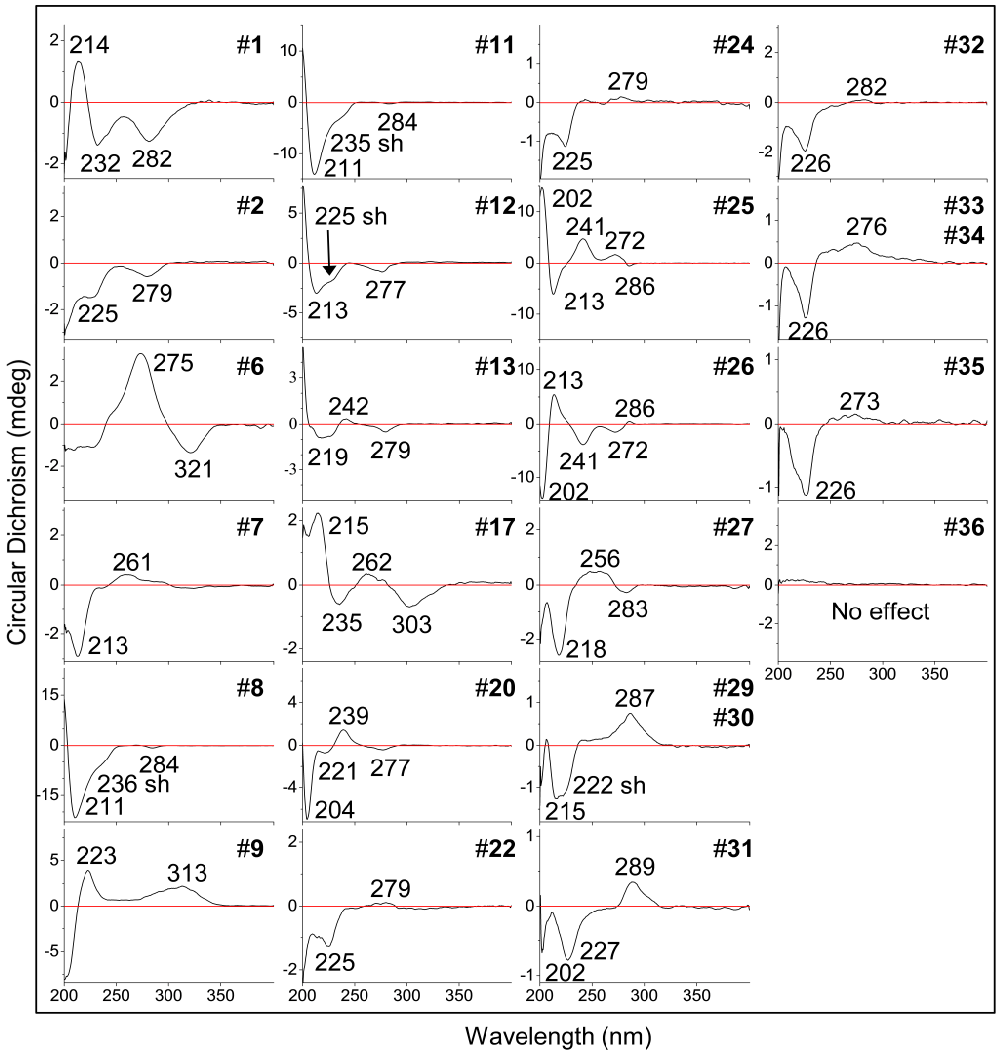

Figure 17. CD spectra of phenolic compounds in the inner bark of silver birch measured in H_2O at 22 °C.

Flavan-3-ols and PC dimers

Monomeric flavan-3-ols have absorption bands at approximately 280 nm (^1L_b transition) and 240 nm (^1L_a transition) which arise from aromatic chromophores, i.e. benzene rings A and B. Both of the absorption regions consist of two CD bands due to two aromatic chromophores (Korver and Wilkins 1971). Two separate bands are observed at low temperatures while mainly one band is observed at 25 °C (Korver and Wilkins 1971; van Rensburg et al. 1999). However, Barret et al. (1979) observed two bands or at least one band with a shoulder at r.t. for catechin, epicatechin, and several procyanidins. For the chromane chromophore, a helicity rule has been established: P/M helicity of the heterocyclic ring leads to negative/positive CD within the ^1L_b band, respectively (Slade et al. 2005 and references therein). This rule has been confirmed also for chromane derivatives that are substituted by achiral substituents at sites 2, 3, 5, and/or 7 (Antus et al. 2001). As a consequence of this, the absolute configuration of the corresponding flavan-3-ols at C2 can be deduced from the CD band of the ^1L_b region which arises from the perturbation of chiral C-ring to A-ring chromophore (the slightly longer wavelength of two bands in a case of couplet, i.e. a pair of oppositely signed maxima): 2*R* configuration exhibits a negative CD band and 2*S* configuration a positive one (Korver and Wilkins 1971). In this study, the sign of the CE of the ^1L_b transition for catechin-7-*O*-β-xylopyranoside (**12**), catechin (**13**), and epicatechin (**20**) was observed as negative (Figure 17). Therefore, with the relative configurations determined by NMR spectroscopy, the compounds **12**, **13**, and **20** were identified as (2*R*,3*S*)-catechin-7-*O*-β-xylopyranoside, (2*R*,3*S*)-catechin, and (2*R*,3*R*)-epicatechin.

Although, the absolute configuration at C3 of flavan-3-ols can be deduced from the combined data of NMR (relative configuration) and CD (absolute configuration at C2) spectra, it has been suggested that the absolute configuration at C3 could be assessed from the sign of the CE at about 240 nm (^1L_a band). However, opposite signs of CEs of ^1L_a band are observed for flavan-3-ols and derivatized flavan-3-ols: the positive ^1L_a CD band is said to correspond to a 3*R* absolute configuration by Rinaldo et al. (2010), while van Rensburg et al. (1999) have postulated that the positive CE at around 240 nm indicates a 3*S* absolute configuration except for compounds that lack A-ring hydroxylation. In the latter study, the CD spectra of flavan-3-ols were determined as their permethylaryl ether acetates. Also Barret et al. (1979) have determined alterations on the sign of the ^1L_a band of catechin derivatives. The sign inversion may be due to the change of conformation in the heterocyclic ring. The substituents seem to have higher impact on the ^1L_a CD band than the ^1L_b band.

The main PC dimers have hindered rotation about the interflavanoid bond and therefore they have preferred rotamers (Barret et al. 1979; Hatano and Hemingway 1997). The absolute configuration at C4 in PC dimers can be assessed from a strong CE at a wavelength around 210 nm. The PC dimer B3 (**8**) (with two catechin subunits and a C4−C8 interflavanoid bond) showed a strong negative CE at 211 nm and was deduced to have 4*S* configuration (Barret et al. 1979). Similarly, the PC dimer B3 xyloside (**11**) (with two catechin subunits, a C4−C8 interflavanoid bond, and a 7-*O*-β-xylopyranosyl substituent in the terminal unit) had a negative CE at 211 nm and was assessed to have a 4*S* configuration, by assuming that the sugar substituent does not alter the conformation of the PC. In conjunction with the 2,3-*trans*-3,4-*trans* relative configurations determined by NMR for **8** and **11**, the absolute configuration of 2*R*,3*S*,4*S* on the extension unit was verified for both **8** and **11**. Further, the negative sign of the CE of the ^1L_b transition for **8** and **11**, were consistent with literature data (Barret et al. 1979) and therefore the absolute configuration of the terminal unit was determined as 2*R*,3*S* for **8** and **11**.

Lignans

Aryl tetralin lignans generally have three CD bands at wavelengths at *ca.* 280 nm (^1L_b), 240 nm and 210 nm (^1L_a). The CD band of the lowest and highest wavelengths is usually observed as couplets (Hulbert et al. 1981). Aryl tetralin lignans can be classified according to the relative configuration of the aryl and alkyl substituents of the heterocyclic ring. The negative CE at the longer wavelength part of the couplet of the ^1L_b transition, approximately at 285 nm, reflects a 7-β-aryl configuration, and the corresponding positive CE reflects a 7-α-aryl configuration. However, substituents in the fused aryl ring may alter the CD maximum wavelength and magnitude, because the substituents may change the conformation of the heterocyclic ring and the torsion angle of 7-aryl group (Hulbert et al. 1981).

Two cyclolignans were isolated from birch bark. Compound **25** showed a negative CE at 286 nm indicating a 7-β-aryl configuration, while compound **26** had a positive CE at 286 nm reflecting a 7-α-aryl configuration. Further, all of the observed CEs of **25** and **26** were in accordance with the literature (Ogawa and Ogihara 1976; Hulbert et al. 1981). Hence, **25** was identified as lyoniside [(7'β,8β,8'α)-3,3',5,5'-tetramethoxy-9'-(β-xylopyranosyl-oxy)-2,7'-cyclolignane-4,4',9-triol] and **26** as nudiposide [(7'α,8α,8'β)-3,3',5,5'-tetramethoxy-9'-(β-xylopyranosyloxy)-2,7'-cyclolignane-4,4',9-triol]. These compounds have been previously identified from inner bark by Šmite et al. (1995).

Diarylheptanoids

For 1,7-diaryl-5-hydroxy-3-heptanones, the CE associated with the carbonyl n–π* transition at about 300 nm is empirically shown to be related to the stereochemistry of the hydroxyl group at C5: a negative CE at around 300 nm reflects 5*S*-configuration, while a positive CE corresponds to 5*R*-configuration (Itokawa et al. 1985). However, this applies only to CD measurements in chloroform and similar apolar solvents. Reversal of the CE at around 300 nm is obtained in polar solvents such as methanol (Ohta 1986). The changes of the conformation of the compounds and therefore the signs of the CEs are associated with the formation (apolar solvent) and breaking (polar solvent) of the intramolecular hydrogen bond and with the solvational effect (polar solvent) (Ohta 1986).

Platyphylloside (**31**) was previously identified from the inner bark of silver birch and its absolute configuration was determined by the comparison of its optical rotation with an authentic sample (Šmite et al. 1993). Originally, the absolute configuration at C5 was determined to be *S* by ^{13}C NMR spectroscopy by applying a glycosidation shift rule (Ohta et al. 1985 and references therein). In this study, the CD spectra of platyphylloside were measured both in water and chloroform to see whether the sign of the CE varies, because the above mentioned empirical rule for 1,7-diaryl-5-hydroxy-3-heptanones (Itokawa et al. 1985) was tested only for 5-hydroxy compounds. In chloroform, the CE at 284 nm was negative and reflected, according to the rule, 5*S* configuration which is consistent with the known conformation for platyphylloside (Figure 18). In water, a reversal of the sign was observed for the CE. Therefore, it can be deduced that the glucose unit at C5 does not alter dramatically the conformations of the aglycone and the empirical rule applies also to platyphylloside.

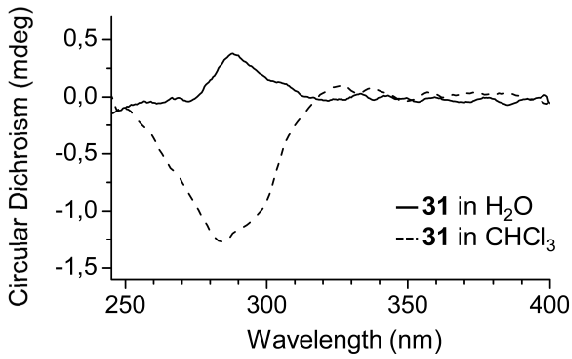

Figure 18. CD spectra of platyphylloside in water (solid line) and chloroform (dashed line).

Platyphylloside apiosides (**29** and **30**) were previously isolated from the inner bark of silver birch and identified as having 5*S* configuration (Šmite et al. 1993). In this study, **29** and **30** were isolated as a mixture. The CD spectrum of the mixture was measured in water and it resembled that of platyphylloside and was therefore in line with 5*S* configurations for both **29** and **30** (Figure 17). However, the compounds could not be isolated as pure compounds and therefore their absolute configuration at C5 could not be unambiguously determined by CD.

Compounds **32**−**35** are mono-, di-, and trisaccharides of 1,7-diaryl-heptan-3-ols. Their chiral centers lie far away from their chromophores. The nearest chiral carbon (C3) is three bonds away from the benzene chromophore. It is known that the chiral perturbation of the benzene ring by a chiral center can exceed three bonds (Ohta 1986; Christensen and Jaroszewski 2001). However, the benzene chirality rule cannot be utilized to assign the absolute configuration at C3 of **32**−**35** because the rule is formulated for chiral centers contiguous or homocontiguous to the benzene ring (Smith 1998). Therefore their absolute configurations at C3 could not be determined by CD. Šmite et al. (1993) have previously isolated compounds **32**, **33**, and **35** from the inner bark of silver birch and determined 3*R* configuration for each.

Arylbutanoids and other monoaryl compounds

In this study, the CD spectra of four arylbutanoids, **17**, **22**, **24**, and **27**, were measured. Similarly as in diarylheptanoids **32**−**35**, the chiral center C2 is three bonds away from the benzene chromophore and therefore the benzene chirality rule cannot be utilized. Compounds **22** and **24** have been previously characterized from the inner bark of silver birch to be rhododendrin and its apioside, respectively, i.e. they both have a 2*R* configuration (Šmite et al. 1993). Compound **27** was deduced to have also an *R* configuration at C2 by comparing its ^{1}H and ^{13}C NMR chemical shifts with those reported in the literature for rhododendrin and its epimer epirhododendrin (Pan and Lundgren 1994).

The chemical shifts of compound **17** could not be compared with the chemical shifts of rhododendrin and epirhododendrin because of the carbonyl group at C4. In conformationally mobile systems, the measured CD spectrum consists of the contributions of all conformational forms present (Verbit and Heffron 1968). Therefore, the ten most stable conformations of **17** with 2*R* configuration were selected for geometry optimization and CD calculations (glucose was assumed to be D-glucose) (Figure 19). The signs of the

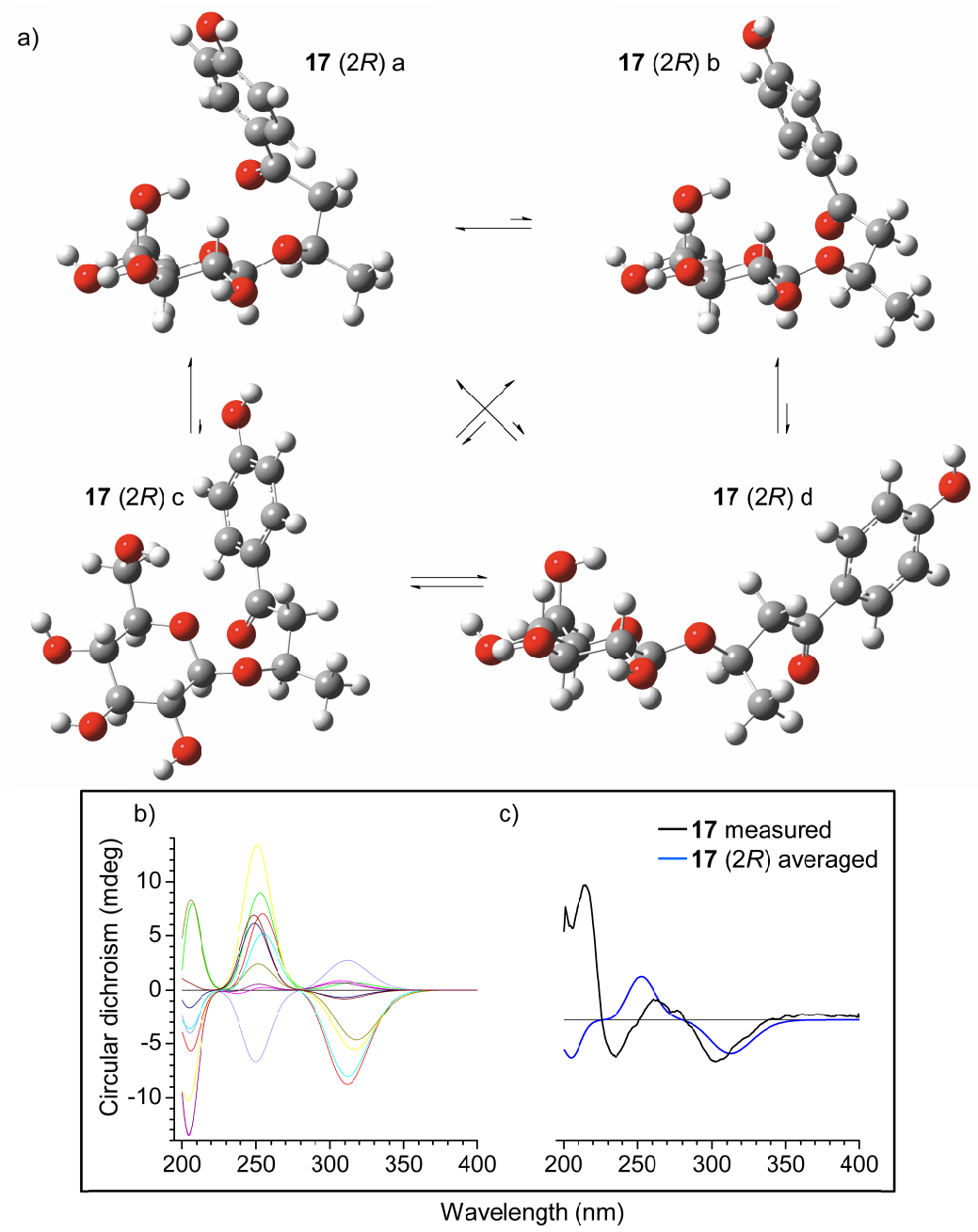

Figure 19. a) The geometry optimized structures for four of the most stable conformers of compound **17** with 2*R* stereochemistry in a gas phase (B3LYP/6-311G(d,p)). b) The calculated CD spectra (M06-2X/6-311++G(d,p)) of ten conformations of **17** and c) their population-weighted spectrum in relation to the minimum energy difference of the rotamers (blue line) together with the measured CD spectrum of **17** (black line).

CEs of different conformations varied greatly (Figure 19b). However, the signs of the CEs at ca. 310 and 260 nm in a population-weight-averaged spectrum of the rotamers matched well with the measured spectrum of **17**. The measured negative CE at about 310 nm is probably due to a carbonyl n–π* transition and matches well with the corresponding CE of the calculated 2*R* stereoisomer. Therefore, compound **17** probably has a 2*R* absolute configuration although the CEs of shorter wavelengths (< 250 nm) did not match very well.

As for compound **17**, the experimental CD spectrum of compound **6** was compared with the calculated CD spectra of **6** with 2*R* and 2*S* absolute configurations (glucose was assumed to be D-glucose). Both of the epimers were observed to have two energetically close rotameric conformations. Therefore, the geometry optimization was performed for both rotamers (Figure 20). The experimental CD spectrum of **6** was compared with the averaged spectrum (population-weighted spectrum of the rotamers; 33% **6**(2*S*)a, 67% **6**(2*S*)b; 84% **6**(2*R*)a, 16% **6**(2*R*)b) of both epimers (Figure 20). The calculated average CD spectrum of **6** with a 2*S* absolute configuration matched well with the experimental CD spectrum of **6** and compound **6** was deduced to have a 2*S* absolute configuration.

Compounds **1**, **2**, **7**, and **9** have chiral centers only in their sugar or quinic acid moieties. Compounds **1** and **2** have been previously isolated from the inner bark of silver birch and they have been characterized via enzymatic hydrolysis to have the D-glucopyranose sugar group (Šmite et al. 1995). Compound **7** was presumed to have also D-glucopyranose sugar, since D-glucose is more common than L-glucose in nature. Therefore, the geometry optimization was performed for 15 conformers of **7** with D-glucopyranose. Seven minimum energy structures of 15 optimized structures were selected for CD calculations (Figure 21). The experimental CD spectrum of **7** was compared with the population-weight-averaged spectrum of seven conformers (Figure 21c). The calculated average CD spectrum of **7** resembled the experimental CD spectrum of **7** and therefore the sugar unit of **7** was probably D-glucopyranose.

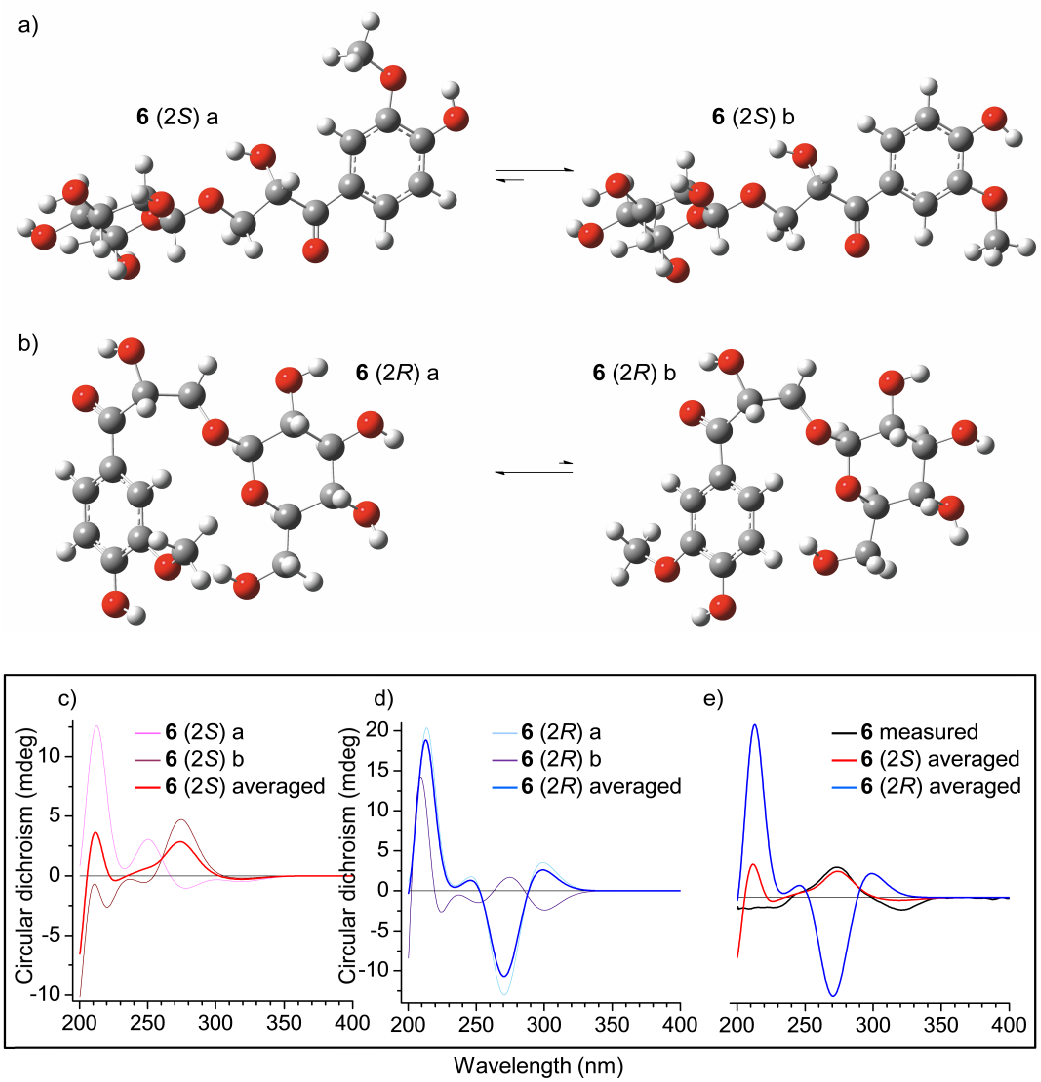

Figure 20. The geometry optimized structures of two rotameric forms of compound **6** a) with 2*S* stereochemistry and b) with 2*R* stereochemistry (each calculated in a gas phase, B3LYP/6-311G(d,p)). Calculated CD spectra (M06-2X/6-311++G(d,p)) of the rotameric forms of 6 with c) 2*S* stereochemistry and d) 2*R* stereochemistry and the averaged spectrum of both epimers in relation to the minimum energy difference of the rotamers (33% **6**(2*S*)a, 67% **6**(2*S*)b; 84% **6**(2*R*)a, 16% **6**(2*R*)b) e) together with the measured CD spectrum of **6.**

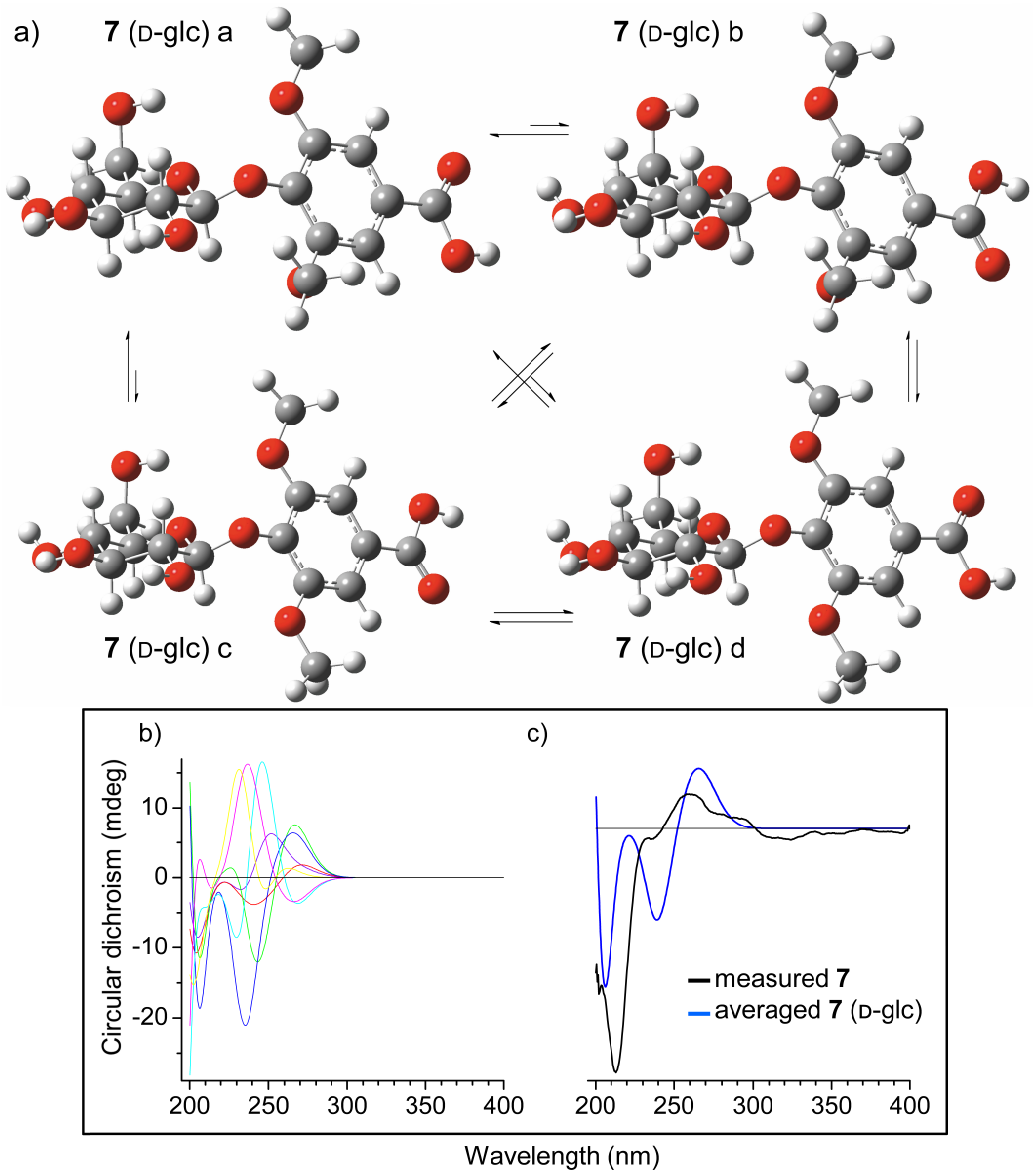

Figure 21. a) The geometry optimized structures for four of the most stable conformers of compound **7** with D-glucopyranose stereochemistry in a gas phase (B3LYP/6-311G(d,p)). b) The calculated CD spectra (M06-2X/6-311++G(d,p)) of seven conformations of **7** and c) their population-weight-averaged spectrum (blue line) together with the measured CD spectrum of **7** (black line).

Compound **9** has chiral centers only in its quinic acid moiety. Quinic acid is thought to naturally occur only as the (−)-enantiomer (Pauli et al. 1999). Therefore, the geometry optimization was performed for five conformers of **9** containing (−)-quinic acid. Two

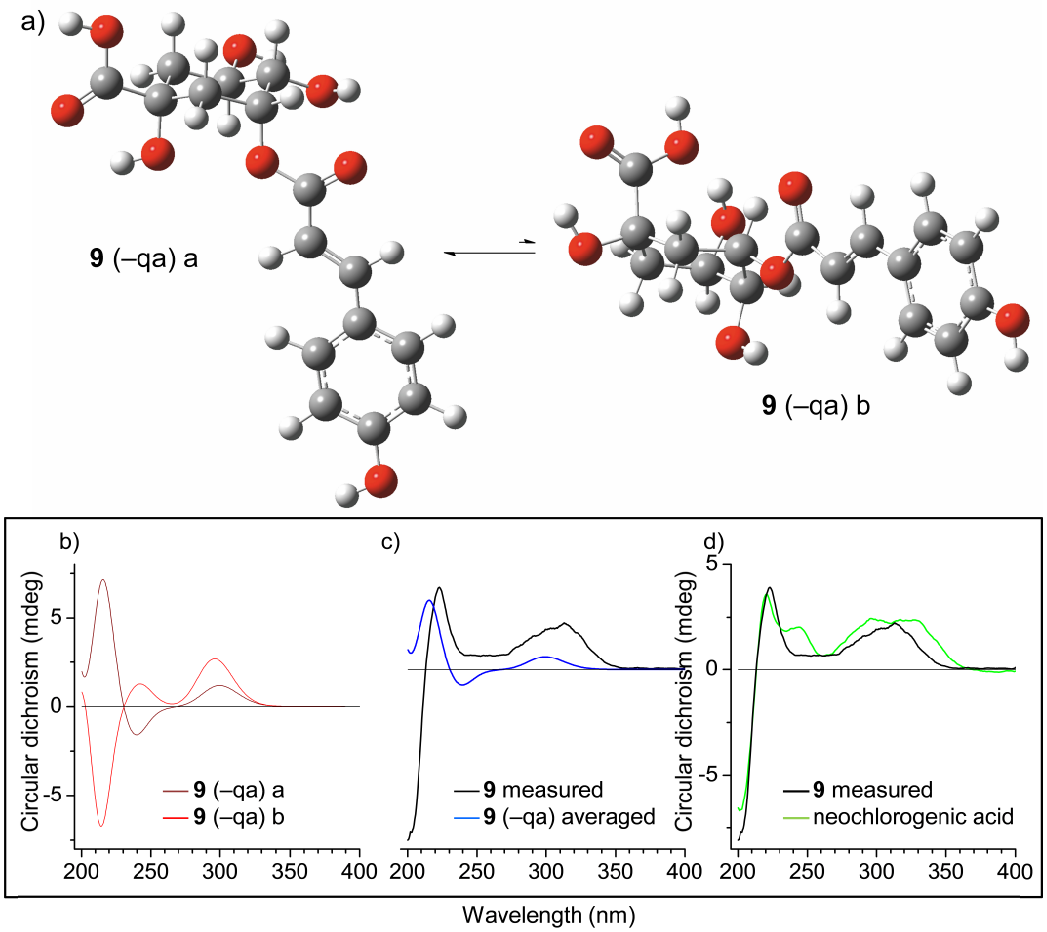

Figure 22. a) The geometry optimized structures for two of the most stable conformers of compound **9** containing (−)-quinic acid in a water phase (B3LYP/6-311G(d,p)). b) The calculated CD spectra (M06-2X/6-311++G(d,p)) of two conformations of **9** and c) their population-weight-averaged spectrum (blue line) together with the measured CD spectrum of **9** (black line). d) The CD spectrum of commercially available neochlorogenic acid (green line) together with the measured CD spectrum of **9** (black line).

minimum energy structures (two chair conformations of the (−)-quinic acid moiety) of five optimized structures were selected for CD calculations (Figure 22). Unlike the other compounds, the optimization of the structures of the conformers was performed in a water phase, since the CD spectrum obtained from the gas phase optimized structures did not resemble the measured CD spectrum of **9**. The experimental CD spectrum of **9** was compared with the population-weight-averaged spectrum of two conformers (Figure 22c). The calculated averaged CD spectrum of **9** containing (−)-quinic acid moiety resembled the experimental CD spectrum of **9**. For further confirmation that the measured CD

spectrum of compound **9** was correct and that the compound had not been partially cleaved prior the CD measurement, its CD spectrum was compared with a CD spectrum of a very similar kind of compound that was commercially available, 3-*O*-caffeoyl quinic acid (neochlorogenic acid). The calculated population-weight-averaged CD spectrum of **9** and the measured CD spectrum of neochlorogenic acid resembled the experimental CD spectrum of **9** and therefore its quinic acid moiety was determined to be the (−)-enantiomer.

5.3. Quantification and seasonal variation

Quantitative analysis was performed by HPLC-DAD at 280 nm. However, the quantification of individual inner bark phenolics by HPLC-DAD was complicated because of the large number of phenolics that could not be fully separated. Further, the similar UV absorption wavelengths of the compounds did not allow their quantification with specific UV wavelengths. Therefore, only 12 individual compounds (**7**, **8**, **14**, **16**, **22**−**26**, **31**, **32**, and **35**) and four chromatographically unresolved compound pairs (**9** and **10**; **12** and **13**; **29** and **30**; **33** and **34**) were quantified.

Table 14. The mean contents of the quantified compounds in inner bark at six sampling dates (n = 21)

Compound	Mean content ± SE (mg/g)					
	7 May 2009	2 July 2009	7 September 2009	11 January 2010	23 March 2010	13 April 2010
7	0.34 ± 0.03	0.32 ± 0.03	0.29 ± 0.02	0.32 ± 0.02	0.32 ± 0.02	0.31 ± 0.02
8	0.67 ± 0.05	0.79 ± 0.08	0.78 ± 0.03	0.82 ± 0.08	0.73 ± 0.06	0.57 ± 0.04
9, **10**	3.17 ± 0.12	3.17 ± 0.15	2.82 ± 0.11	3.25 ± 0.18	3.08 ± 0.15	2.84 ± 0.10
12, **13**	9.9 ± 0.7	10.1 ± 0.9	9.1 ± 0.7	9.8 ± 0.8	9.6 ± 0.8	8.9 ± 0.7
14	0.17 ± 0.02	0.19 ± 0.03	0.20 ± 0.02	0.21 ± 0.03	0.17 ± 0.02	0.16 ± 0.02
16	1.98 ± 0.07	2.04 ± 0.11	1.96 ± 0.04	2.17 ± 0.13	2.08 ± 0.08	1.87 ± 0.07
22	16.4 ± 0.5	15.5 ± 0.6	15.1 ± 0.7	16.6 ± 0.8	16.5 ± 0.8	15.8 ± 0.6
23	2.20 ± 0.09	2.27 ± 0.16	2.53 ± 0.11	2.38 ± 0.13	2.03 ± 0.11	2.13 ± 0.13
24	6.3 ± 0.4	6.5 ± 0.4	6.6 ± 0.4	6.7 ±0.4	6.1 ± 0.3	6.2 ± 0.4
25	0.46 ± 0.03	0.45 ± 0.02	0.45 ± 0.03	0.51 ± 0.03	0.45 ± 0.03	0.46 ± 0.03
26	0.33 ± 0.01	0.33 ± 0.01	0.36 ± 0.02	0.38 ± 0.02	0.36 ± 0.01	0.36 ± 0.01
29, **30**	2.15 ± 0.06	2.11 ± 0.11	1.91 ± 0.07	2.11 ± 0.08	1.89 ± 0.06	1.87 ± 0.06
31	52 ± 3	50 ± 4	48 ± 4	51 ± 3	49 ± 3	48 ± 3
32	0.98 ± 0.06	0.98 ± 0.06	0.88 ± 0.04	0.98 ± 0.06	0.98 ± 0.05	1.00 ± 0.05
33, **34**	5.3 ± 0.6	5.4 ± 0.6	5.7 ± 0.6	5.4 ± 0.5	5.1 ± 0.5	5.7 ± 0.6
35	1.68 ± 0.18	1.71 ± 0.19	1.69 ± 0.20	1.74 ± 0.16	1.74 ± 0.18	1.87 ± 0.21
Sum total	104	102	98	100	104	99

The amounts of the main inner bark phenolics were influenced by season and genotype (Paper **III)**. Compounds **24** and **35** were the only compounds that did not show statistically significant seasonal variation in their concentrations. Despite the statistical significance, the seasonal variation was small and the inner bark contained a high concentration of phenolics throughout the year. The overall content of the quantified compounds varied from 99 mg/g to 104 mg /g among the sampling dates (Table 14).

Among clones, significant variation in the quantity of phenolics was found for the majority of the compounds; only compounds **8**, **22**, **26**, and the mixture of **9** and **10** did not exhibit genotypic variation. For example, the content of the main component, platyphylloside (**31**) had high variation among clones, varying from 39 mg/g to 67 mg/g. The overall content of the quantified compounds varied from 86 mg/g to 127 mg /g among the clones (see Table 1 in Paper **III**).

5.4. Induction of phenolics by wounding

Qualitative differences in the phenolic content among seasons or genotypes were not observed. Instead, the phenolic content of the regrown tissue that was formed after the sampling was distinct from the inner bark. The new compounds **A**−**E** were categorized as ETs. The UV spectra of compounds **A** (at least two isomers), **B**, and **C** resembled the UV spectra of ETs containing merely HHDP groups attached to the glucose core, i.e. the spectra were lacking the valley between 230 and 270 nm (Figure 23) (Moilanen et al. 2013). The UV spectra of compounds **D** (two isomers) and **E** showed a small valley at around 250 nm, which indicated the existence of both HHDP and galloyl groups in these ETs. However, the UV spectra of **D** and **E** were partially distorted due to the low concentration of the compounds. Compound **F** had a typical ellagic acid like UV spectrum (Figure 23) (Moilanen et al. 2013). These compounds were identified based on their retention times and mass spectral data (Table 15 and Paper **III**). The exact positions of HHDP and galloyl groups in compounds **A** (at least two isomers), **B**, and **D** (two isomers) could not be determined. Compounds **C** and **E** had a free anomeric hydroxyl group since in the chromatograms their peaks appeared as doublets (in a 1:1 ratio) corresponding to two anomers. Compounds **C** and **E** were tentatively identified as pedunculagin and tellimagrandin I, respectively (Table 15, Figure 24).

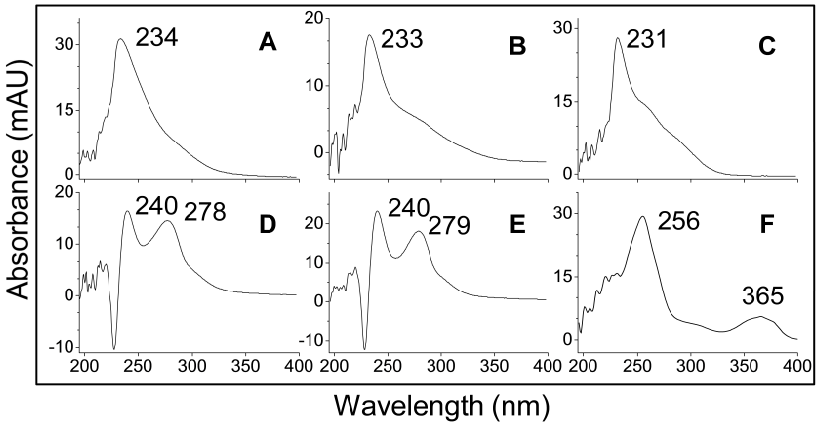

Figure 23. UV spectra of phenolic compounds in the regrown bark of silver birch. Letters in the spectra refer to Table 15. Spectra were obtained by HPLC-DAD with 1% aqueous formic acid and acetonitrile as eluents.

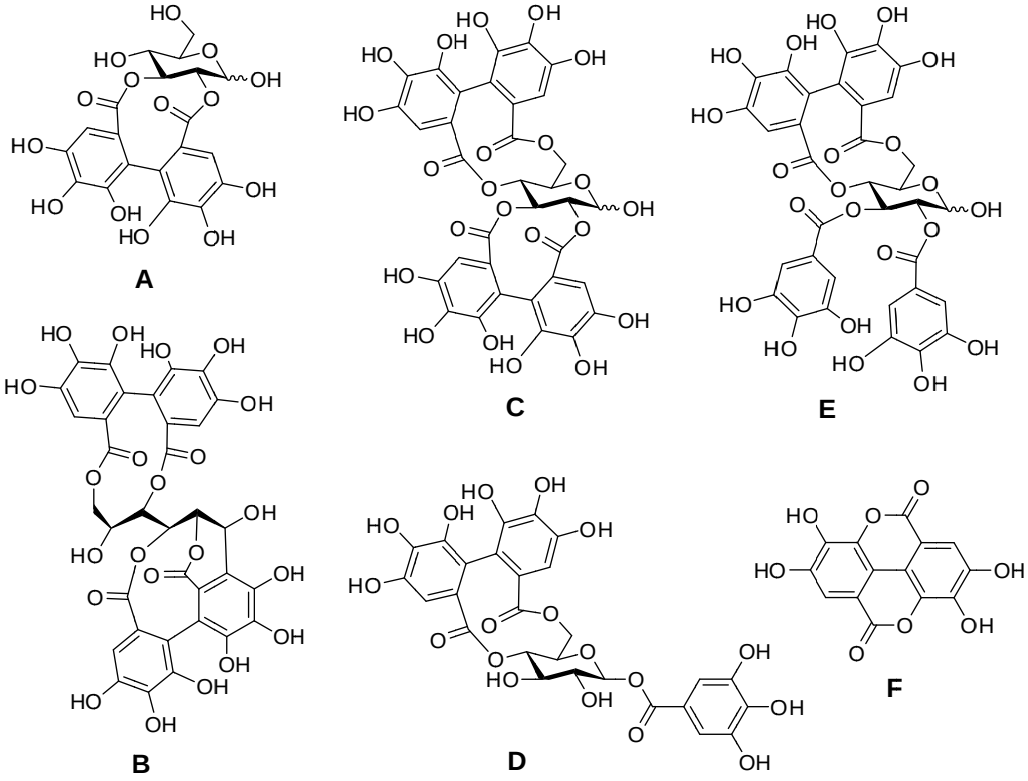

Figure 24. Structures of ellagitannins in the regrown bark of silver birch: an example of a HHDP-glucopyranose (**A**), an example of a *C*-glycosidic bis(HHDP) (**B**), pedunculagin (**C**), an example of a galloyl-HHDP-glucopyranose (**D**), tellimagrandin I (**E**), and ellagic acid (**F**).

Table 15. Ellagitannins detected in the regrown bark of silver birch and their retention times, observed ions, and exact masses

	Compound	Rt (min)	Molecular ion		Cluster ion	Calculated exact mass
			$[M–H]^–$	$[M–2H]^{2–}$	$[2M–H]^–$	
A	HHDP-glucopyranose isomers	1.3, 1.5, 1.7	481.1	-	963.1	482.0697
B	*C*-glycosidic bis(HHDP)	2.0	783.1	391.0	-	784.0759
C	pedunculagin	5.4, 10.6	783.1	391.0	-	784.0759
D	galloyl-HHDP-glucopyranose isomers	10.3, 15.5	633.1	316.0	-	634.0806
E	tellimagrandin I	13.2, 17.7	785.1	392.0	-	786.0916
F	ellagic acid	24.6	301.0	-	603.0	302.0063

6. CONCLUSIONS

The most suitable solvent for the extraction of phenolic compounds of the inner bark of silver birch was 80% aqueous methanol. A reproducible extraction of the phenolics was obtained in 48 h. Several different isolation steps were required for the purification of the various phenolic compounds. The main compounds, platyphylloside and rhododendrin, were easily isolated with over 90% purity by successive liquid−liquid extractions and column chromatography on Sephadex LH-20. Other compounds required purification at least on Sephadex LH-20 column chromatography and semipreparative RP-HPLC. PCs were isolated as a mixture by Sephadex LH-20 column chromatography.

Altogether 36 compounds were characterized by HPLC-DAD/ESI-MS. The structures of 24 compounds, including five novel compounds, were confirmed by NMR spectroscopy, and CD spectroscopy was applied for their configurational analysis. The compounds identified belonged to simple phenolics, phenolic acids, flavanols, lignans, arylbutanoids, diarylheptanoids, and PCs. Oligomeric and polymeric PCs were studied by HILIC-HR-ESI-MS. The HILIC phase and HR-ESI-MS detection allowed the analysis of PCs according to their increasing DP with high resolving power and sensitive ionization. B-type PC aglycones were detected from dimers to 22-mers and B-type PC monoxylosides from dimers to heptadecamers.

Qualitative differences in the phenolic composition among birch clones or seasons were not found. Instead, the amounts of the inner bark phenolics were influenced by genotype and season: the quantities of nine compounds and three chromatographically unresolved compound pairs correlated with the genotype and ten compounds and four compound pairs with the season. The overall content of the quantified compounds varied from 86 mg/g to 127 mg/g among the clones and from 99 mg/g to 104 mg/g among the seasons. After the manual wounding of the bark, the callus tissue was found to contain ellagitannins that were not present in the original inner bark.

This study showed that the inner bark of silver birch is a potent source for several types of phenolic compounds throughout the year. It is especially rich in diarylheptanoids and arylbutanoids, which are characteristic of only a limited number of plant species. In addition, it contains an interesting series of oligomeric and polymeric PC monoxylosides, which as such were found for the first time in nature.

REFERENCES

A.-H.-Mackerness, S. 2000. Plant responses to ultraviolet-B (UV-B: 280–320 nm) stress: What are the key regulators? *Plant Growth Regul.* 32:27–39.

Abreu, I.N., Ahnlund, M., Moritz, T., Albrectsen, B.R. 2011. UHPLC-ESI/TOFMS determination of salicylate-like phenolic glycosides in *Populus tremula* leaves. *J. Chem. Ecol.* 37:857–870.

Abu-Reidah, I.M., Arráez-Román, D., Quirantes-Piné, R., Fernández-Arroyo, S., Segura-Carretero, A., Fernández-Gutiérrez, A. 2012. HPLC-ESI-Q-TOF-MS for a comprehensive characterization of bioactive phenolic compounds in cucumber whole fruit extract. *Food Res. Int.* 46:108–117.

Agrawal, A.A., Hastings, A.P., Johnson, M.T.J., Maron, J.L., Salminen, J.-P. 2012. Insect herbivores drive real-time ecological and evolutionary change in plant populations. *Science* 338:113–116.

Agrawal, P.K. 1989. *Carbon-13 NMR of Flavonoids*. Elsevier Science Publishers B.V., Amsterdam, The Netherlands.

Agrawal, P.K. 1992. NMR spectroscopy in the structural elucidation of oligosaccharides and glycosides. *Phytochemistry* 31:3307–3330.

Allwood, J.W., Goodacre, R. 2010. An introduction to liquid chromatography–mass spectrometry instrumentation applied in plant metabolomic analyses. *Phytochem. Anal.* 21:33–47.

Andersen, Ø.M. 2007. In Roberts, K. (Ed.), *Handbook of Plant Science*, Vol. 2. John Wiley & Sons Ltd, Chichester, England, pp. 966–973.

Antus, S., Kurtán, T., Juhász, L., Kiss, L., Hollósi, M., Májer, Z.S. 2001. Chiroptical properties of 2,3-dihydrobenzo[b]furan and chromane chromophores in naturally occurring O-heterocycles. *Chirality* 13:493–506.

Archetti, M. 2009. Phylogenetic analysis reveals a scattered distribution of autumn colours. *Ann. Bot.* 103:703–713.

Archetti, M., Döring, T.F., Hagen, S.B., Hughes, N.M., Leather, S.R., Lee, D.W., Lev-Yadun, S., Manetas, Y., Ougham, H.J., Schaberg, P.G., Thomas, H. 2009. Unravelling the evolution of autumn colours: an interdisciplinary approach. *Trends Ecol. Evol.* 24:166–173.

Atkinson, M.D. 1992. *Betula pendula* Roth (*B.verrucosa* Ehrh.) and *B. pubescens* Ehrh. *J. Ecol.* 80:837–870.

Ayres, M.P., Clausen, T.P., MacLean, S.F. Jr., Redman, A.M., Reichardt, P.B. 1997. Diversity of structure and antiherbivore activity in condensed tannins. *Ecology* 78:1696–1712.

Ayres, D.C., Loike, J.D. 1990. *Lignans: Chemical, Biological and Clinical Properties*. Cambridge University Press, Cambridge, U.K.

Barnes, J.S., Nguyen, H.P., Shen, S., Schug, K.A. 2009. General method for extraction of blueberry anthocyanins and identification using high performance liquid chromatography-electrospray ionization-ion trap-time of flight-mass spectrometry. *J. Chromatogr. A* 1216:4728–4735.

Barrett, M.W., Klyne, W., Scopes, P.M., Fletcher, A.C., Porter, L.J., Haslam, E. 1979. Plant proanthocyanidins. Part 6. Chiroptical studies. Part 95. Circular dichroism of procyanidins. *J. Chem. Soc. Perkin Trans. 1* 2375–2377.

Blois, M.S. 1958. Antioxidant determinations by the use of a stable free radical. *Nature* 181:1199–1200.

Brewer, E., Henion, J. 1998. Atmospheric pressure ionization LC/MS/MS techniques for drug disposition studies. *J. Pharm. Sci.* 87:395–402.

Bross-Walch, N., Kühn, T., Moskau, D., Zerbe, O. 2005. Strategies and tools for structure determination of natural products using modern methods of NMR spectroscopy. *Chem. Biodivers*. 2:147–177.

Cádiz-Gurrea, M.L., Férnandez-Arroyo, S., Joven, J., Segura-Carretero, A. 2013. Comprehensive characterization by UHPLC-ESI-Q-TOF-MS from an *Eryngium bourgatii* extract and their antioxidant and anti-inflammatory activities. *Food Res. Int.* 50:197–204.

Cerovic, Z.G., Ounis, A., Cartelat, A., Latouche, G., Goulas, Y., Meyer, S., Moya, I. 2002. The use of chlorophyll fluorescence excitation spectra for the non-destructive *in situ* assessment of UV-absorbing compounds in leaves. *Plant Cell Environ.* 25:1663–1676.

Chalker-Scott, L., Krahmer, R.L. 1989. Microscopic studies of tannin formation and distribution in plant tissues. In Hemingway, R.W., Karchesy, J.J. (Eds.), *Chemistry and Significance of Condensed Tannins*. Plenum Press, New York, U.S., pp. 345–368.

Christensen, J., Jaroszewski, J.W. 2001. Natural glycosides containing allopyranose from the passion fruit plant and circular dichroism of benzaldehyde cyanohydrin glycosides. *Org. Lett.* 3:2193–2195.

Claridge, T.D.W. 1999. *High-Resolution NMR Techniques in Organic Chemistry*. Elsevier Science Ltd, Oxford, U.K.

Clausen, T.P., Provenza, F.D., Burritt, E.A., Reichardt, P.B., Bryant, J.P. 1990. Ecological implications of condensed tannin structure: a case study. *J. Chem. Ecol.* 16:2381–2392.

Clifford, M.N. 2003. The analysis and characterization of chlorogenic acids and other cinnamates. In Santos-Buelga, C., Williamson, G. (Eds.), *Methods in Polyphenol Analysis*. The Royal Society of Chemistry, Cambridge, U.K., pp. 314–337.

Clifford, M.N., Johnston, K.L., Knight, S., Kuhnert, N. 2003. Hierarchical scheme for LC-MS^n identification of chlorogenic acids. *J. Agric. Food Chem.* 51:2900–2911.

Clifford, M.N., Knight, S., Kuhnert, N. 2005. Discriminating between the six isomers of dicaffeoylquinic acid by LC-MS^n. *J. Agric. Food Chem.* 53:3821–3832.

Cuyckens, F., Claeys, M. 2004. Mass spectrometry in the structural analysis of flavonoids. *J. Mass Spectrom.* 39:1–15.

de la Rosa, T.M., Julkunen-Tiitto, R., Lehto, T., Aphalo, P.J. 2001. Secondary metabolites and nutrient concentrations in silver birch seedlings under five levels of daily UV-B exposure and two relative nutrient addition rates. *New Phytol.* 150:121–131.

Ekman, R. 1983. The suberin monomers and triterpenoids from the outer bark of *Betula verrucosa* Ehrh. *Holzforschung* 37:205–211.

Ekman, R., Sjöholm, R. 1983. Betulinol 3-caffeate in outer bark of *Betula verrucosa* Ehrh. *Finn. Chem. Lett.* 5:134–136.

Feucht, W., Treutter, D., Dithmar, H., Polster, J. 2008. Microspore development of three coniferous species: affinity of nuclei for flavonoids. *Tree Physiol*. 28:1783–1791.

Feucht, W., Treutter, D., Polster, J. 2012. Flavanols in nuclei of tree species: facts and possible functions. *Trees* 26:1413–1425.

Figueiredo, P., George, F., Tatsuzawa, F., Toki, K., Saito, N., Brouillard, R. 1999. New features of intramolecular copigmentation by acylated anthocyanins. *Phytochemistry* 51:125–132.

Frisch, M.J., Trucks, G.W., Schlegel, H.B., Scuseria, G.E., Robb, M.A., Cheeseman, J.R., Scalmani, G., Barone, V., Mennucci, B., Petersson, G.A., Nakatsuji, H., Caricato, M., Li, X., Hratchian, H.P., Izmaylov, A.F., Bloino, J., Zheng, G., Sonnenberg, J.L., Hada, M., Ehara, M., Toyota, K., Fukuda, R., Hasegawa, J., Ishida, M., Nakajima, T., Honda, Y., Kitao, O., Nakai, H., Vreven, T., Montgomery, J.A. Jr., Peralta, J.E., Ogliaro, F., Bearpark, M., Heyd, J.J., Brothers, E., Kudin, K.N., Staroverov, V.N., Kobayashi, R., Normand, J., Raghavachari, K., Rendell, A., Burant, J.C., Iyengar, S.S., Tomasi, J., Cossi, M., Rega, N., Millam, N.J., Klene, M., Knox, J.E., Cross, J.B., Bakken, V., Adamo, C., Jaramillo, J., Gomperts, R., Stratmann, R.E., Yazyev, O., Austin, A.J., Cammi, R., Pomelli, C., Ochterski, J.W., Martin, R.L., Morokuma, K., Zakrzewski, V.G., Voth, G.A., Salvador, P., Dannenberg, J.J., Dapprich, S., Daniels, A.D., Farkas, Ö., Foresman, J.B., Ortiz, J.V., Cioslowski, J., Fox, D.J. 2009. Gaussian, Inc., Wallingford, CT, U.S..

Gottlieb, H.E., Kotlyar, V., Nudelman, A. 1997. NMR chemical shifts of common laboratory solvents as trace impurities. *J. Org. Chem.* 62:7512–7515.

Grundhöfer, P., Niemetz, R., Schilling, G., Gross, G.G. 2001. Biosynthesis and subcellular distribution of hydrolyzable tannins. *Phytochemistry* 57:915–927.

Gu, L., Kelm, M.A., Hammerstone, J.F., Zhang, Z., Beecher, G., Holden, J., Haytowitz, D., Prior, R.L. 2003. Liquid chromatographic/electrospray ionization mass spectrometric studies of proanthocyanidins in foods. *J. Mass Spectrom.* 38:1272–1280.

Guyot, S., Marnet, N., Drilleau, J.-F. 2001. Thiolysis–HPLC characterization of apple procyanidins covering a large range of polymerization states. *J. Agric. Food Chem.* 49:14–20.

Hagerman, A.E., Butler, L.G. 1981. The specificity of proanthocyanidin-protein interactions. *J. Biol. Chem.* 256:4494–4497.

Haslam, E. 2007. Vegetable tannins – lessons of a phytochemical lifetime. *Phytochemistry* 68:2713–2721.

Harborne, J.B. 1982. *Introduction to Ecological Biochemistry*. Academic Press, London, U.K.

Harborne, J.B. 2007. Secondary metabolites: attracting pollinators. In Roberts, K. (Ed.), *Handbook of Plant Science*, Vol. 2. John Wiley & Sons Ltd, Chichester, England, pp. 1050–1054.

Hatano, T., Hemingway, R.W. 1997. Conformational isomerism of phenolic procyanidins: preferred conformations in organic solvents and water. *J. Chem. Soc. Perkin Trans. 2* 1035–1043.

Hatano, T., Yoshida, T., Shingu, T., Okuda, T. 1988a. ^{13}C nuclear magnetic resonance spectra of hydrolyzable tannins. II. Tannins forming anomer mixtures. *Chem. Pharm. Bull.* 36:2925–2933.

Hatano, T., Yoshida, T., Shingu, T., Okuda, T. 1988b. ^{13}C nuclear magnetic resonance spectra of hydrolyzable tannins. III. Tannins having $^{1}C_4$ glucose and C-glucosidic linkage. *Chem. Pharm. Bull.* 36:3849–3856.

Hellström, J., Sinkkonen, J., Karonen, M., Mattila, P. 2007. Isolation and structure elucidation of procyanidin oligomers from saskatoon berries (*Amelanchier alnifolia*). *J. Agric. Food Chem.* 55:157–164.

Hemingway, R.W. 1989. Biflavonoids and proanthocyanidins. In Rowe, J.W. (Ed.), *Natural Products of Woody Plants I*. Springer-Verlag, Berlin, Germany, pp. 571–651.

Hendry, G.A.F., Houghton, J.D., Brown, S.B. 1987. The degradation of chlorophyll – a biological enigma. *New Phytol.* 107:255–302.

Herderich, M., Richling, E., Roscher, R., Schneider, C., Schwab, W., Humpf, H.-U., Schreier, P. 1997. Application of atmospheric pressure ionization HPLC-MS-MS for the analysis of natural products. *Chromatographia* 45:127–132.

Hiltunen, E., Pakkanen, T.T., Alvila L. 2004. Phenolic extractives from wood of birch (*Betula pendula*). *Holzforschung* 58:326–329.

Hiltunen, E., Pakkanen, T.T., Alvila L. 2006. Phenolic compounds in silver birch (*Betula pendula* Roth) wood. *Holzforschung* 60:519–527.

Hulbert, P.B., Klyne, W., Scopes, P.M. 1981. Chiroptical studies. Part 100. Lignans. *J. Chem. Res. (M)* 2:401–449.

Hutzler, P., Fischbach, R., Heller, W., Jungblut, T.P., Reuber, S., Schmitz, R., Veit, M., Weissenböck, G., Schnitzler, J.-P. 1998. Tissue localization of phenolic compounds in plants by confocal laser scanning microscopy. *J. Exp. Bot.* 49:953–965.

Hättenschwiler, S., Vitousek, P.M. 2000. The role of polyphenols in terrestrial ecosystem nutrient cycling. *Tree* 15:238–243.

Itokawa, H., Morita, H., Midorikawa, I., Aiyama, R., Morita, M. 1985. Diarylheptanoids from the rhizome of *Alpinia officinarum* Hance. *Chem. Pharm. Bull.* 33:4889–4893.

Jaganath, I.B., Crozier, A. 2010. Dietary flavonoids and phenolic compounds. In Fraga, C.G. (Ed.), *Plant Phenolics and Human Health: Biochemistry, Nutrition, and Pharmacology*. John Wiley & Sons, Inc., Hoboken, U.S., pp. 1–49.

Jaiswal, R., Jayasinghe, L., Kuhnert, N. 2012. Identification and characterization of proanthocyanidins of 16 members of the *Rhododendron* genus (*Ericaceae*) by tandem LC-MS. *J. Mass Spectrom.* 47:502–515.

Kanerva, S., Kitunen, V., Loponen, J., Smolander, A. 2008. Phenolic compounds and terpenes in soil organic horizon layers under silver birch, Norway spruce and Scots pine. *Biol. Fertil. Soils* 44:547–556.

Karonen, M. 2007. *Plant Proanthocyanidins: Characterization and Quantification by Degradation Methods, HPLC-DAD/ESI-MS and NMR*. Ph.D. dissertation, University of Turku, Turku, Finland.

Karonen, M., Hämäläinen, M., Nieminen, R., Klika, K.D., Loponen, J., Ovcharenko, V.V., Moilanen, E., Pihlaja, K. 2004a. Phenolic extractives from the bark of *Pinus sylvestris* L. and their effects on inflammatory mediators nitric oxide and prostaglandin E2. *J. Agric. Food Chem*. 52:7532–7540.

Karonen, M., Loponen, J., Ossipov, V., Pihlaja, K. 2004b. Analysis of procyanidins in pine bark with reversed-phase and normal-phase high-performance liquid chromatography–electrospray ionization mass spectrometry. *Anal. Chim. Acta* 522:105–112.

Karonen, M., Ossipov, V., Sinkkonen, J., Loponen, J., Haukioja, E., Pihlaja, K. 2006. Quantitative analysis of polymeric proanthocyanidins in birch leaves with normal-phase HPLC. *Phytochem. Anal.* 17:149–156.

Keinänen, M., Julkunen-Tiitto, R. 1998. High-performance liquid chromatographic determination of flavonoids in *Betula pendula* and *Betula pubescens* leaves. *J. Chromatogr. A* 793:370–377.

Kelm, M.A., Johnson, J.C., Robbins, R.J., Hammerstone, J.F., Schmitz, H.H. 2006. High-performance liquid chromatography separation and purification of cacao (*Theobroma cacao* L.) procyanidins according to degree of polymerization using a diol stationary phase. *J. Agric. Food Chem.* 54:1571–1576.

Keserü, G.M., Nógrádi, M. 1995. The chemistry of natural diarylheptanoids. *Stud. Nat. Prod. Chem.* 17:357–394.

Khan, M.L., Haslam, E., Williamson M.P. 1997. Structure and conformation of the procyanidin B-2 dimer. *Magn. Reson. Chem.* 35:854–858.

Kind, T., Fiehn, O. 2010. Advances in structure elucidation of small molecules using mass spectrometry. *Bioanal. Rev.* 2:23–60.

Koes, R.E., Quattrocchio, F., Mol, J.N.M. 1994. The flavonoid biosynthetic pathway in plants: function and evolution. *BioEssays* 16:123–132.

Koivikko, R. 2008. *Brown Algal Phlorotannins: Improving and Applying Chemical Methods*. Ph.D. dissertation, University of Turku, Turku, Finland.

Kolodziej, H. 1989. Procyanidins from medicinal birch: bonding patterns and sequence of units in triflavanoids of mixed stereochemistry. *Phytochemistry* 28:3487–3492.

Kolodziej, H. 1992. ^{1}H NMR spectral studies of procyanidin derivatives: diagnostic ^{1}H NMR parameters applicable to the structural elucidation of oligomeric procyanidins. In Hemingway, R.W., Laks, P.E. (Eds.), *Plant Polyphenols.* Plenum Press, New York, U.S., pp. 295–319.

Korver, O., Wilkins, C.K. 1971. Circular dichroism spectra of flavanols. *Tetrahedron* 27:5459–5465.

Koslowski, A., Sreerama, N., Woody, R.W. 2000. Theoretical approach to electronic optical activity. In Berova, N., Nakanishi, K., Woody, R.W (Eds.), *Circular Dichroism: Principles and Applications*. Wiley-VCH, Inc., New York, U.S., pp. 55–95.

Kostina, E., Wulff, A., Julkunen-Tiitto, R. 2001. Growth, structure, stomatal responses and secondary metabolites of birch seedlings (*Betula pendula*) under elevated UV-B radiation in the field. *Trees* 15:483–491.

Kraus, T.E.C., Dahlgren, R.A., Zasoski, R.J. 2003. Tannins in nutrient dynamics of forest ecosystems – a review. *Plant Soil* 256:41–66.

Kuball, H.-G., Höfer, T. 2000. Circular dichroism of oriented molecules. In Berova, N., Nakanishi, K., Woody, R.W (Eds.), *Circular Dichroism: Principles and Applications*. Wiley-VCH, Inc., New York, U.S., pp. 133–158.

Kähkönen, M.P., Hopia, A.I., Vuorela, H.J., Rauha, J.-P., Pihlaja, K., Kujala, T.S., Heinonen, M. 1999. Antioxidant activity of plant extracts containing phenolic compounds. *J. Agric. Food Chem*. 47:3954–3962.

Lahtinen, M., Lempa, K., Salminen, J.-P., Pihlaja, K. 2006. HPLC analysis of leaf surface flavonoids for the preliminary classification of birch species. *Phytochem. Anal.* 17: 197–203.

Laitinen, J., Julkunen-Tiitto, R., Rousi, M., Heinonen, J., Tahvanainen, J. 2005b. Ontogeny and environment as determinants of the secondary chemistry of three species of white birch. *J. Chem. Ecol.* 31:2243–2262.

Laitinen, M.-L., Julkunen-Tiitto, R., Tahvanainen, J., Heinonen, J., Rousi, M. 2005a. Variation in birch (*Betula pendula*) shoot secondary chemistry due to genotype, environment, and ontogeny. *J. Chem. Ecol.* 31:697–717.

Lattanzio, V., Cardinali, A., Linsalata, V. 2012. Plant phenolics: a biochemical and physiological perspective. In Cheynier, V., Sarni-Manchado, P., Quideau, S. (Eds.), *Recent Advances in Polyphenol Research*, Vol. 3. Wiley-Blackwell, Chichester, U.K., pp. 1–39.

Lavola, A., Julkunen-Tiitto, R., Aphalo, P., de la Rosa, T., Lehto, T. 1997. The effect of u.v.-B radiation on u.v.-absorbing secondary metabolites in birch seedlings grown under simulated forest soil conditions. *New Phytol.* 137:617–621.

Lazarus, S.A., Kelm, M.A., Wächter, G.A., Hammerstone, J.F., Schmitz, H.H. 2003. Analysis and purification of proanthocyanidin oligomers. In Santos-Buelga, C., Williamson, G.

(Eds.), *Methods in Polyphenol Analysis*. The Royal Society of Chemistry, Cambridge, U.K., pp. 267–283.

Li, H.-J., Deinzer, M.L. 2007. Tandem mass spectrometry for sequencing proanthocyanidins. *Anal. Chem.* 79:1739–1748.

Li, J., Li, W.Z.M., Huang, W., Cheung, A.W.H., Bi, C.W.C., Duan, R., Guo, A.J.Y., Dong, T.T.X., Tsim, K.W.K. 2009. Quality evaluation of Rhizoma Belamcandae (*Belamcanda chinensis* (L.) DC.) by using high-performance liquid chromatography coupled with diode array detector and mass spectrometry. *J. Chromatogr. A* 1216:2071–2078.

Lundgren, L. N., Pan, H., Theander, O., Eriksson, H., Johansson, U., Svenningsson, M. 1995. Development of a new chemical method for distinguishing between *Betula pendula* and *Betula pubescens* in Sweden. *Can. J. For. Res*. 25:1097–1102.

Matthews, S., Mila, I., Scalbert, A., Donnelly, D.M.X. 1997. Extractable and non-extractable proanthocyanidins in barks. *Phytochemistry* 45:405–410.

Moilanen, J., Sinkkonen, J., Salminen, J.-P. 2013. Characterization of bioactive plant ellagitannins by chromatographic, spectroscopic and mass spectrometric methods. *Chemoecology* 23:165–179.

Molyneux, P. 2004. The use of the stable free radical diphenylpicrylhydrazyl (DPPH) for estimating antioxidant activity. *Songklanakarin J. Sci. Technol.* 26:211–219.

Mononen, K., Alvila, L., Pakkanen, T.T. 2004. Effect of growth site type, felling season, storage time and kiln drying on contents and distributions of phenolic extractives and low molar mass carbohydrates in secondary xylem of silver birch *Betula pendula*. *Holzforschung* 58:53–65.

Morales, L.O., Tegelberg, R., Brosché, M., Keinänen, M., Lindfors, A., Aphalo, P.J. 2010. Effects of solar UV-A and UV-B radiation on gene expression and phenolic accumulation in *Betula pendula* leaves. *Tree Physiol.* 30:923–934.

Moss, G.P. 2000. Nomenclature of lignans and neolignans. *Pure Appl. Chem.* 72:1493–1523.

Mustonen, E.A., Jokela, T., Saastamoinen, I., Taponen, J., Taponen, S., Saloniemi, H., Wähälä, K. 2006. High serum *S*-equol content in red clover fed ewes: the classical endocrine disruptor is a single enantiomer. *Environ. Chem. Lett.* 3:154–159.

Mutikainen, P., Walls, M., Ovaska, J., Keinänen, M., Julkunen-Tiitto, R., Vapaavuori, E. 2000. Herbivore resistance in *Betula pendula*: effect of fertilization, defoliation, and plant genotype. *Ecology* 81:49–65.

Myburg, A.A., Sederoff, R.R. 2007. Xylem structure and function. In Roberts, K. (Ed.), *Handbook of Plant Science*, Vol. 2. John Wiley & Sons Ltd, Chichester, England, pp. 859–867.

Mämmelä, P. 2001. Phenolics in selected European hardwood species by liquid chromatography–electrospray ionisation mass spectrometry. *Analyst* 126:1535–1538.

Newsham, K.K., Robinson, S.A. 2009. Responses of plants in polar regions to UVB exposure: a meta-analysis. *Glob. Change Biol.* 15:2574–2589.

Northup, R.R., Yu, Z., Dahlgren, R.A., Vogt, K.A. 1995. Polyphenol control of nitrogen release from pine litter. *Nature* 377:227–229.

Ogawa, M., Ogihara, Y. 1976. Studies on the constituents of *Enkianthus nudipes*. V. A new lignan xyloside from the stems. *Chem. Pharm. Bull.* 24:2102–2105.

Ohta, S. 1986. The solvent effects on the optical rotatory properties of 1,7-diaryl-5-hydroxy-3-heptanones and related compounds. *Bull. Chem. Soc. Jpn.* 59:1181–1188.

Ohta, S., Koyama, M., Aoki, T., Suga, T. 1985. Absolute configuration of platyphylloside and (–)-centrolobol. *Bull. Chem. Soc. Jpn.* 58:2423–2424.

Oksanen, E., Manninen, S., Vapaavuori, E., Holopainen, T. 2009. Near-ambient ozone concentrations reduce the vigor of *Betula* and *Populus* species in Finland. *Ambio* 38:413–417.

Okuda, T., Yoshida, T., Hatano, T., Koga, T., Toh, N., Kuriyama, K. 1982. Circular dichroism of hydrolysable tannins - I – ellagitannins and gallotannins. *Tetrahedron Lett.* 23:3937–3940.

Ossipov, V., Nurmi, K., Loponen, J., Haukioja, E., Pihlaja, K. 1996. High-performance liquid chromatographic separation and identification of phenolic compounds from leaves of *Betula pubescens* and *Betula pendula*. *J. Chromatogr. A* 721:59–68.

Ossipova, S., Ossipov, V., Haukioja, E., Loponen, J., Pihlaja, K. 2001. Proanthocyanidins of mountain birch leaves: quantification and properties. *Phytochem. Anal.* 12:128–133.

Pan H., Lundgren L.N. 1994. Rhododendrol glycosides and phenyl glucoside esters from inner bark of *Betula pubescens*. *Phytochemistry* 36:79–83.

Pauli, G.F., Kuczkowiak, U., Nahrstedt, A. 1999. Solvent effects in the structure dereplication of caffeoyl quinic acids. *Magn. Reson. Chem.* 37:827–836.

Peng, J.-B., Jia, H.-M., Liu, Y.-T., Zhang, H.-W., Dong, S., Zou, Z.-M. 2011. Qualitative and quantitative characterization of chemical constituents in Xin-Ke-Shu preparations by liquid chromatography coupled with a LTQ Orbitrap mass spectrometer. *J. Pharm. Biomed. Anal.* 55:984–995.

Pérez-Magariño, S., Revilla, I., González-SanJosé, M.L., Beltrán, S. 1999. Various applications of liquid chromatography–mass spectrometry to the analysis of phenolic compounds. *J. Chromatogr. A* 847:75–81.

Pietarinen, S.P., Willför, S.M., Sjöholm, R.E., Holmbom, B.R. 2005. Bioactive phenolic substances in important tree species. Part 3: Knots and stemwood of *Acacia crassicarpa* and *A. mangium*. *Holzforschung* 59:94–101.

Pietarinen, S.P., Willför, S.M., Vikström, F.A., Holmbom, B.R. 2006. Aspen knots, a rich source of flavonoids. *J. Wood Chem. Technol.* 26:245–258.

Pinto, P.C.R.O., Sousa, A.F., Silvestre, A.J.D., Neto, C.P., Gandini, A., Eckerman C., Holmbom, B. 2009. *Quercus suber* and *Betula pendula* outer barks as renewable sources of oleochemicals: a comparative study. *Ind. Crops Prod.* 29:126–132.

Porter, L.J. 1989a. Tannins. In Dey, P.M., Harborne, J.B. (Eds.), *Methods in Plant Biochemistry*, Vol. 1. Academic Press, London, U.K., pp. 389–419.

Porter, L.J. 1989b. Condensed tannins. In Rowe, J.W. (Ed.), *Natural Products of Woody Plants I*. Springer-Verlag, Berlin, Germany, pp. 651–690.

Purdie, N. 1994. Analytical applications of CD to the forensic, pharmaceutical, clinical, and food sciences. In Purdie, N., Brittain, H.G. (Eds.), *Analytical Applications of Circular Dichroism*. Elsevier Science B.V., Amsterdam, The Netherlands, pp. 241–278.

Ralph, J., Brunow, G., Boerjan, W. 2007. Lignins. In Roberts, K. (Ed.), *Handbook of Plant Science*, Vol. 2. John Wiley & Sons Ltd, Chichester, England, pp. 1123–1132.

Rauha, J.-P., Vuorela, H., Kostiainen, R. 2001. Effect of eluent on the ionization efficiency of flavonoids by ion spray, atmospheric pressure chemical ionization, and atmospheric pressure photoionization mass spectrometry. *J. Mass Spectrom.* 36:1269–1280.

Raulo, J. 1981. *Koivukirja*. Gummerus, Jyväskylä, Finland.

Rausher, M.D. 2006. The evolution of flavonoids and their genes. In Grotewold, E. (Ed.), *The Science of Flavonoids.* Springer Science, New York, U.S., pp. 175–211.

Ren, Q., Wu, C., Ren, Y., Zhang, J. 2013. Characterization and identification of the chemical constituents from tartary buckwheat (*Fagopyrum tataricum* Gaertn) by high performance liquid chromatography/photodiode array detector/linear ion trap FTICR hybrid mass spectrometry. *Food Chem.* 136:1377–1389.

Rinaldo, D., Batista, J.M. Jr., Rodrigues, J., Benfatti, A.C., Rodrigues, C.M., Dos Santos, L.C., Furlan, M., Vilegas, W. 2010. Determination of catechin diastereomers from the leaves of *Byrsonima* species using chiral HPLC-PAD-CD. *Chirality* 22:726–733.

Rivas-Gonzalo, J.C. 2003. Analysis of anthocyanins. In Santos-Buelga, C., Williamson, G. (Eds.), *Methods in Polyphenol Analysis*. The Royal Society of Chemistry, Cambridge, U.K., pp. 338–358.

Robbins, C.T., Hagerman, A.E., Austin, P.J., McArthur, C., Hanley, T.A. 1991. Variation in mammalian physiological responses to a condensed tannin and its ecological implications. *J. Mammal.* 72:480–486.

Ruiz, A., Mardones, C., Vergara, C., Hermosín-Gutiérrez, I., von Baer, D., Hinrichsen, P., Rodriguez, R., Arribillaga, D., Dominguez, E. 2013. Analysis of hydroxycinnamic acids derivatives in calafate (*Berberis microphylla* G. Forst) berries by liquid chromatography with photodiode array and mass spectrometry detection. *J. Chromatogr. A* 1281:38–45.

Salminen, J.-P., Ossipov, V., Pihlaja, K. 2002. Distribution of hydrolysable tannins in the foliage of Finnish birch species. *Z. Naturforsch.* 57c:248–256.

Santos-Buelga, C., García-Viguera, C., Tomás-Barberán, F.A. 2003. On-line identification of flavonoids by HPLC coupled to diode array detection. In Santos-Buelga, C., Williamson, G. (Eds.), *Methods in Polyphenol Analysis*. The Royal Society of Chemistry, Cambridge, U.K., pp. 92–127.

Scalbert, A. 1991. Antimicrobial properties of tannins. *Phytochemistry* 30:3875–3883.

Schulz, A., Thompson, G.A. 2007. Phloem structure and function. In Roberts, K. (Ed.), *Handbook of Plant Science*, Vol. 2. John Wiley & Sons Ltd, Chichester, England, pp. 870–879.

Simirgiotis, M.J., Schmeda-Hirschmann, G., Bórques, J., Kennelly, E.J. 2013. The *Passiflora tripartita* (banana passion) fruit: a source of bioactive flavonoid C-glycosides isolated by HSCCC and characterized by HPLC-DAD-ESI/MS/MS. *Molecules* 18:1672–1692.

Sinkkonen, A., Somerkoski, E., Paaso, U., Holopainen, J.K., Rousi, M., Mikola, J. 2012. Genotypic variation in yellow autumn leaf colours explains aphid load in silver birch. *New Phytol.* 195:461–469.

Sinkkonen, J., Liimatainen, J., Karonen, M., Pihlaja, K. 2005. A new dihydroflavonol from *Pinus sylvestris* L. *Magn. Reson. Chem.* 43:348–349.

Slade, D., Ferreira, D., Marais, J.P.J. 2005. Circular dichroism, a powerful tool for the assessment of absolute configuration of flavonoids. *Phytochemistry* 66:2177–2215.

Šmite, E., Lundgren, L.N., Andersson, R. 1993. Arylbutanoid and diarylheptanoid glycosides from inner bark of *Betula pendula*. *Phytochemistry* 32:365–369.

Šmite, E., Pan, H., Lundgren, L.N. 1995. Lignan glycosides from inner bark of *Betula pendula*. *Phytochemistry* 40:341–343.

Smith, H.E. 1998. Chiroptical properties of the benzene chromophore. A method for the determination of the absolute configurations of benzene compounds by application of the benzene sector and benzene chirality rules. *Chem. Rev.* 98:1709–1740.

Smolander, A., Loponen, J., Suominen, K., Kitunen, V. 2005. Organic matter characteristics and C and N transformations in the humus layer under two tree species, *Betula pendula* and *Picea abies*. *Soil Biol. Biochem.* 37:1309–1318.

Snatzke, G. 1979. Semiempirical rules in circular dichroism of natural products. *Pure Appl. Chem.* 51:769–785.

Snyder, J., Breuning, R., Derguini, F., Nakanishi, K. 1989. Fractionation and proof of structure of natural products. In Rowe, J.W. (Ed.), *Natural Products of Woody Plants I.* Springer-Verlag, Berlin, Germany, pp. 27–124.

Strack, D. 1997. Phenolic metabolism. In Dey, P.M., Harborne, J.B. (Eds.), *Plant Biochemistry*. Academic Press, London, U.K., pp. 387–416.

Sumner, L.W., Paiva, N.L., Dixon, R.A., Geno, P.W. 1996. High-performance liquid chromatography/continuous-flow liquid secondary ion mass spectrometry of flavonoid glycosides in leguminous plant extracts. *J. Mass Spectrom.* 31:472–485.

Sun, W., Miller, J.M. 2003. Tandem mass spectrometry of the B-type procyanidins in wine and B-type dehydrodicatechins in an autoxidation mixture of (+)-catechin and (-)-epicatechin. *J. Mass Spectrom.* 38:438–446.

Sunnerheim, K., Palo, R.T., Theander, O., Knutsson, P.-G. 1988. Chemical defense in birch. Platyphylloside: a phenol from *Betula pendula* inhibiting digestibility. *J. Chem. Ecol.* 14:549–560.

Sunnerheim, K., Bratt, K. 2004. Identification of centrolobol as the platyphylloside metabolite responsible for the observed effect on in vitro digestibility of hay. *J. Agric. Food Chem.* 52:5869–5872.

Sunnerheim-Sjöberg, K., Knutsson, P.-G. 1995. Platyphylloside: metabolism and digestibility reduction *in vitro*. *J. Chem. Ecol.* 21:1339–1348.

Suominen, K., Kitunen, V., Smolander, A. 2003. Characteristics of dissolved organic matter and phenolic compounds in forest soils under silver birch (*Betula pendula*), Norway spruce (*Picea abies*) and Scots pine (*Pinus sylvestris*). *Eur. J. Soil Sci.*54:287–293.

Sutela, S., Niemi, K., Edesi, J., Laakso, T., Saranpää, P., Vuosku, J., Mäkelä, R., Tiimonen, H., Chiang, V.L., Koskimäki, J., Suorsa, M., Julkunen-Tiitto, R., Häggman, H. 2009. Phenolic compounds in ectomycorrhizal interaction of lignin modified silver birch. *BMC Plant Biol.* 9:124–139.

Swain, T., Bate-Smith, E.C. 1962. Flavonoid compounds. In Florkin, M., Mason, H.S. (Eds.), *Comparative Biochemistry,* Vol. III. Academic Press, New York, U.S., pp. 755–809.

Swatsitang, P., Tucker, G., Robards, K., Jardine, D. 2000. Isolation and identification of phenolic compounds in *Citrus sinensis*. *Anal. Chim. Acta* 417:231–240.

Tarascou, I., Barathieu, K., Simon, C., Ducasse, M.-A., André, Y., Fouquet, E., Dufourc, E.J., de Freitas, V., Laguerre, M., Pianet, I. 2006. A 3D structural and conformational study of procyanidin dimers in water and hydro-alcoholic media as viewed by NMR and molecular modeling. *Magn. Reson. Chem.* 44:868–880.

Tarascou, I., Ducasse, M.-A., Dufourc, E.J., Moskau, D., Fouquet, E., Laguerre, M., Pianet, I. 2007. Structural and conformational analysis of two native procyanidin trimers. *Magn. Reson. Chem.* 45:157–166.

Taiz, L., Zeiger, E. 1998. *Plant Physiology*. Sinauer Associates Inc., Massachusetts, U.S.

Tegelberg, R., Julkunen-Tiitto, R., Aphalo, P.J. 2001. The effects of long term elevated UV-B on the growth and phenolics of field-grown silver birch (*Betula pendula*). *Glob. Change Biol.* 7:839–848.

Tegelberg, R., Aphalo, P.J., Julkunen-Tiitto, R. 2002. Effects of long-term, elevated ultraviolet-B radiation on phytochemicals in the bark of silver birch (*Betula pendula*). *Tree Physiol.* 22:1257–1263.

Thomson, B.A. 1998. Atmospheric pressure ionization and liquid chromatography/mass spectrometry – together at last. *J. Am. Soc. Mass Spectrom.* 9:187–193.

Tibe, O., Meagher, L.P., Fraser, K., Harding, D.R.K. 2011. Condensed tannins and flavonoids from the forage legume sulla (*Hedysarum coronarium*). *J. Agric. Food Chem.* 59:9402–9409.

Touriño, S., Fuguet, E., Jáuregui, O., Saura-Calixto, F., Cascante, M., Torres, J.L. 2008. High-resolution liquid chromatography/electrospray ionization time-of-flight mass spectrometry combined with liquid chromatography/electrospray ionization tandem mass spectrometry to identify polyphenols from grape antioxidant dietary fiber. *Rapid Commun. Mass Spectrom.* 22:3489–3500.

Triebwasser, D.J., Tharayil, N., Preston, C.M., Gerard, P.D. 2012. The susceptibility of soil enzymes to inhibition by leaf litter tannins is dependent on the tannin chemistry, enzyme class and vegetation history. *New Phytol.* 196:1122–1132.

Valkama, E., Salminen, J.-P., Koricheva, J., Pihlaja, K. 2003. Comparative analysis of leaf trichome structure and composition of epicuticular flavonoids in Finnish birch species. *Ann. Bot.* 91:643–655.

Valkama, E., Salminen, J.-P., Koricheva, J., Pihlaja, K. 2004. Changes in leaf trichomes and epicuticular flavonoids during leaf development in three birch taxa. *Ann. Bot.* 94:233–242.

van Rensburg, H., Steynberg, P.J., Burger, J.F.W., van Heerden, P.S., Ferreira, D. 1999. Circular dichroic properties of flavan-3-ols. *J. Chem. Res. (S)* 7:450–451.

van der Hooft, J.J.J., Akermi, M., Ünlü, F.Y., Mihaleva, V., Roldan, V.G., Bino, R.J., de Vos, R.C.H., Vervoort, J. 2012. Structural annotation and elucidation of conjugated phenolic compounds in black, green, and white tea extracts. *J. Agric. Food Chem.* 60:8841–8850.

Vdovin, A.D., Kuliev., Z.A., Abdullaev, N.D. 1997. ^{1}H and ^{13}C NMR spectroscopy in the study of flavan-3-ols, proanthocyanidins, and their derivatives III. ^{13}C NMR spectroscopy of flavan-3-ols and proanthocyanidins. *Chem. Nat. Compd.* 33:417–437.

Verbit, L., Heffron, P.J. 1968. Optically active aromatic chromophores – IV: circular dichroism studies of some open-chain systems. *Tetrahedron* 24:1231–1236.

Vukics, V., Guttman, A. 2010. Structural characterization of flavonoid glycosides by multi-stage mass spectrometry. *Mass Spectrom. Rev.* 29:1–16.

Waterman, P.G., Mole, S. 1994. *Analysis of Phenolic Plant Metabolites*. Blackwell Scientific Publications, Oxford, U.K.

Willför, S.M., Ahotupa, M.O., Hemming, J.E., Reunanen, M.H.T., Eklund, P.C., Sjöholm, R.E., Eckerman, C.S.E., Pohjamo, S.P., Holmbom, B.R. 2003c. Antioxidant activity of knotwood extractives and phenolic compounds of selected tree species. *J. Agric. Food Chem.* 51:7600–7606.

Willför, S., Hemming, J., Reunanen, M., Eckerman, C., Holmbom, B. 2003a. Lignans and lipophilic extractives in Norway spruce knots and stemwood. *Holzforschung* 57:27–36.

Willför, S., Hemming, J., Reunanen, M., Holmbom, B. 2003b. Phenolic and lipophilic extractives in Scots pine knots and stemwood. *Holzforschung* 57:359–372.

Willför, S., Nisula, L., Hemming, J., Reunanen, M., Holmbom, B. 2004. Bioactive phenolic substances in industrially important tree species. Part 2: Knots and stemwood of fir species. *Holzforschung* 58:650–659.

Wink, M. 2007. Secondary metabolites: deterring herbivores. In Roberts, K. (Ed.), *Handbook of Plant Science*, Vol. 2. John Wiley & Sons Ltd, Chichester, England, pp. 1071–1079.

Wolfender, J.L., Maillard, M., Hostettmann, K. 1993. Liquid chromatographic-thermospray mass spectrometric analysis of crude plant extracts containing phenolic and terpene glycosides. *J. Chromatogr.* 647:183–190.

Wu, X., Prior, R.L. 2005. Identification and characterization of anthocyanins by high-performance liquid chromatography–electrospray ionization–tandem mass spectrometry in common foods in the United States: vegetables, nuts, and grains. *J. Agric. Food Chem.* 53:3101–3113.

Wulff, A., Anttonen, S., Pellinen, R., Savonen, E.-M., Sutinen, M.-L., Heller, W., Sandermann, H. Jr., Kangasjärvi, J. 1999. Birch (*Betula pendula* Roth.) responses to high UV-B radiation. *Boreal Env. Res.* 4:77–88.

Yoshida, T., Hatano, T., Okuda, T., Memon, M.U., Shingu, T., Inoue, K. 1984. Spectral and chromatographic analyses of tannins. I. ^{13}C nuclear magnetic resonance spectra of hydrolyzable tannins. *Chem. Pharm. Bull.* 32:1790–1799.

Zhu, F., Cai, Y.-Z., Sun, M., Ke, J., Lu, D., Corke, H. 2009. Comparison of major phenolic constituents and in vitro antioxidant activity of diverse kudingcha genotypes from *Ilex kudingcha*, *Ilex cornuta*, and *Ligustrum robustum*. *J. Agric. Food Chem.* 57:6082–6089.

Zhu, F., Cai, Y.-Z., Yang, X., Ke, J., Corke, H. 2010. Anthocyanins, hydroxycinnamic acid derivatives, and antioxidant activity in roots of different Chinese purple-fleshed sweetpotato genotypes. *J. Agric. Food Chem.* 58:7588–7596.

Zucker, W.V. 1983. Tannins: does structure determine function? An ecological perspective. *Am. Nat.* 121:335–365.